# CONFORMATIONAL STUDIES OF SOME SMALL BIOLOGICAL MOLECULES AND THEIR INTERACTIONS WITH METAL IONS

A thesis submitted to

THE UNIVERSITY OF CAPE TOWN

in fulfilment of the requirements for the degree of

DOCTOR OF PHILOSOPHY

by

JILL C. RUSSELL

Department of Chemistry,

University of Cape Town,

Rondebosch, Cape,

South Africa.

March, 1976.

# A C K N O W L E D G E M E N T S

I would like to express my sincere thanks to my supervisor, Dr. G. V. Fazakerley for his invaluable guidance, encouragement and friendship during the course of this work.

I would also like to thank my colleagues, Melanie Wolfe, Graham Jackson and Graham Mortimore, for many helpful discussions.

I am indebted to the University of Cape Town and to the South African Council for Scientific and Industrial Research for financial assistance.

# A B S T R A C T

The solid Cu(II) and Co(II) complexes and complex salts of some thiamine analogues have been prepared. Their electronic spectra, I.R. spectra and Magnetic Moments are presented and discussed in terms of suggested coordination geometries for the complexes.

In addition the solution conformations of the Gd(III), Dy(III) and Ho(III) complexes of some 3',5' cyclic nucleotides were determined quantitatively using NMR line broadening and line shifting techniques. Reactions of Mn(II) with the cyclic nucleotides were used to find the preferred binding sites on the ligands also using line broadening techniques.

# C O N T E N T S

## GLOSSARY OF SYMBOLS

| | |
|---|---|
| $A/\hbar$ | hyperfine coupling constant |
| $\gamma_I$ | nuclear gyromagnetic ratio |
| $\delta$ | pseudo-contact shift |
| $E_A$ | activation energy of rotation |
| $f$ | ratio of nuclei in bound and unbound state |
| $g$ | nuclear g factor |
| $H_{loc}$ | spread of local magnetic fields |
| $I$ | nuclear spin quantum number |
| $k$ | Boltzmann's constant |
| $q$ | number of bound ligand nuclei per metal-ion |
| $r$ | metal-proton internuclear distance |
| $S$ | total electron spin |
| $T$ | absolute temperature |
| $T_1$ | longitudinal relaxation time |
| $T_2$ | transverse relaxation time |
| $T_{iM}$ | i = 1,2 relaxation rate of bound site |
| $T_{ip}$ | i = 1,2 paramagnetic contribution to the relaxation rate |
| $\tau_c$ | dipolar correlation time |
| $\tau_e$ | scalar correlation time |
| $\tau_M$ | lifetime of bound state |
| $\tau_r$ | rotational correlation time |
| $\tau_s$ | electron spin relaxation time |
| $\mu$ | nuclear magnetic moment |
| $\nu$ | I.R. spectrum absorption frequency |
| $\Delta\nu$ | line width (in Hz) at half peak height |
| $\omega_I$ | nuclear Larmor frequency |
| $\omega_s$ | electron Larmor frequency |
| $\Delta\omega_M$ | chemical shift of nucleus in bound state |

STRUCTURAL FORMULAE OF LIGANDS INVESTIGATED

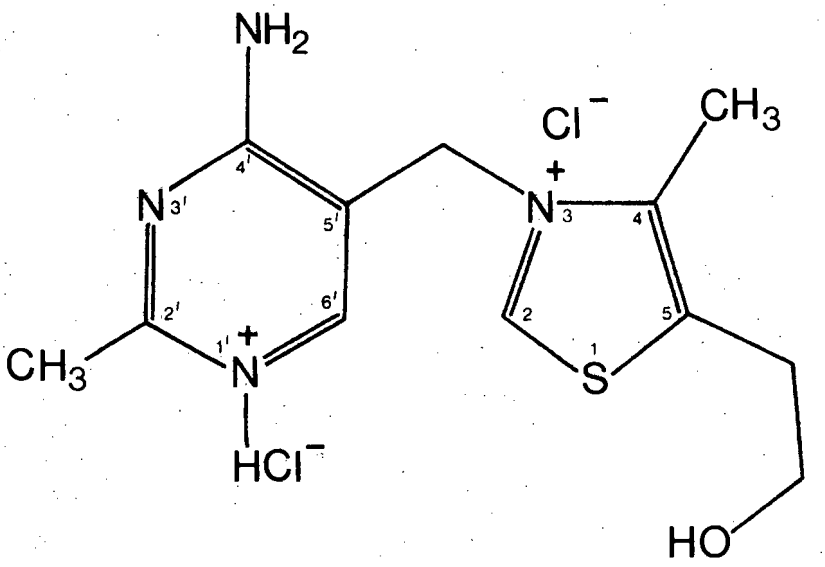

Thiamine chloride hydrochloride (= thiam Cl HCl)

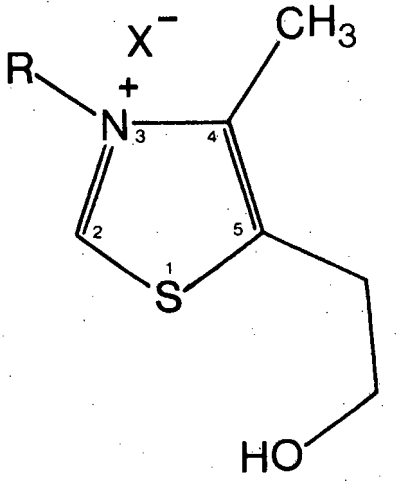

(i) R = H; X = Cl
5-(2-hydroxyethyl)-4-methyl thiazole hydrochloride (= thiaz HCl)

(ii) R = H; X = Br
5-(2-hydroxyethyl)-4-methyl thiazole hydrobromide (= thiaz HBr)

(iii) R = Me; X = Br
5-(2-hydroxyethyl)-4-methyl thiazole methylbromide (= thiaz MeBr)

5-(2-hydroxyethyl)-4-methyl thiazole

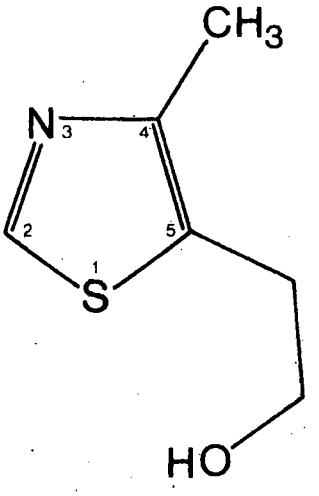

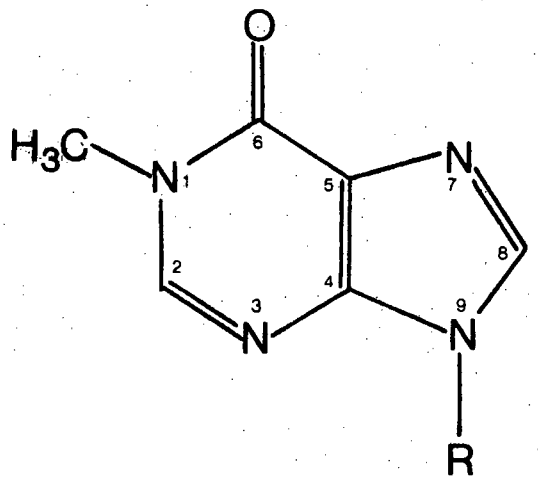

(i) R = H

1-methyl hypoxanthine

(ii) R =

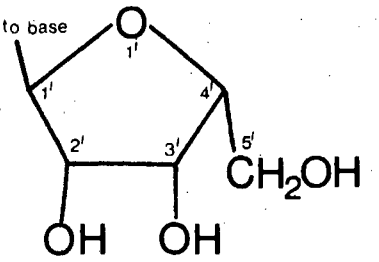

1-methyl inosine

(i) R = Me

9-methyl hypoxanthine

(ii) R =

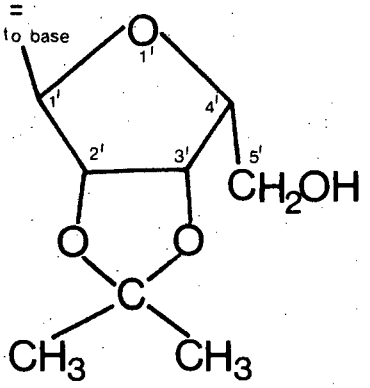

2',3'-O-isopropylidene inosine

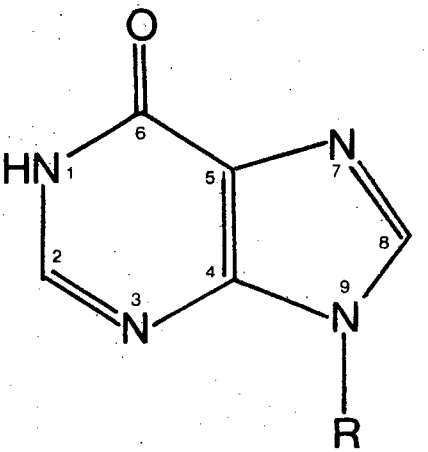

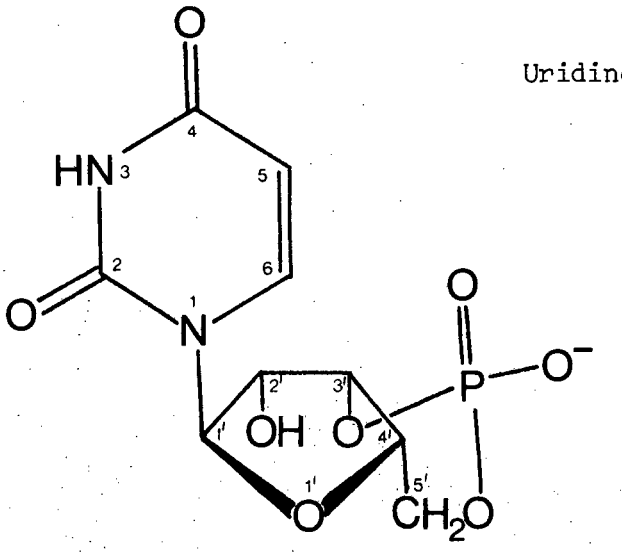

Uridine 3',5' cyclic monophosphate
(cUMP)

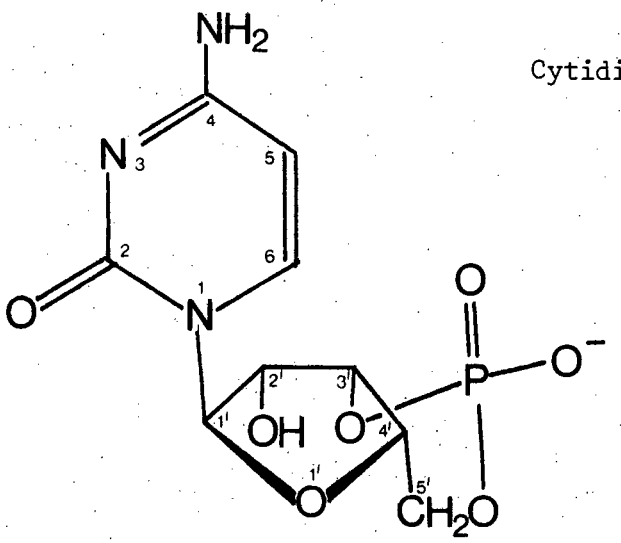

Cytidine 3',5' cyclic monophosphate
(cCMP)

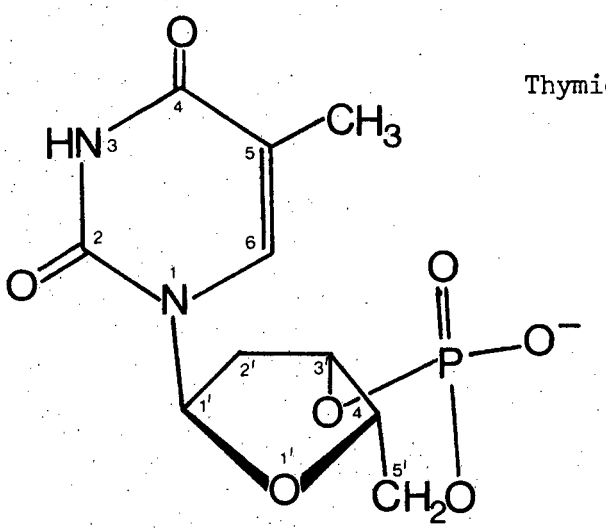

Thymidine 3',5' cyclic monophosphate
(cTMP)

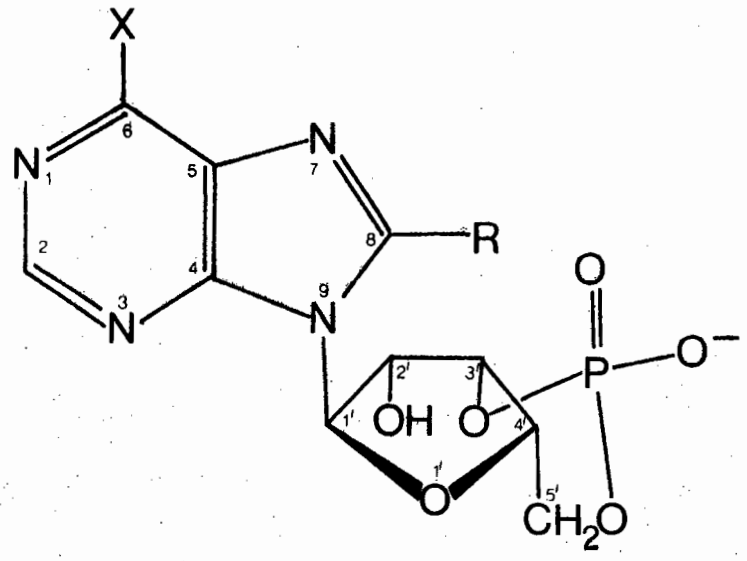

(i) X = OH; R = H

Inosine 3',5' cyclic monophosphate (cIMP)

(ii) X = Cl; R = H

6-chloropurine riboside 3',5' cyclic monophosphate

(iii) X = $NH_2$; R = SMe

8-methylthioadenosine 3',5' cyclic monophosphate

# C H A P T E R  1

## INTRODUCTION

## 1.1 Vitamin $B_1$ and its analogues

Thiamine chloride hydrochloride (Vitamin $B_1$) plays a very important role in biological functions.

It is a dietary requirement for all animals other than ruminants. Jansen in Java and later Windaus in Germany were the first to isolate the vitamin in pure form from crude rice polish extracts. Only twenty six years later, in 1936, was the full isolation, characterization, determination of structure, and synthesis completed by R. R. Williams and his colleagues. In man beriberi has long been endemic in those areas where polished rice is the staple diet. Beriberi takes two forms: the wet type which shows extensive endematous swellings of the extremities and the dry type where muscular atrophy is externally conspicuous. Lameness, ataxia, numbness of the extremities, and loss or exaggeration of patellar reflexes reveal a disturbance of the motor and sensory nerves[1]. In many cases direct administration of small quantities of thiamine will alleviate the condition. The outer layers of the seeds of plants are especially rich in thiamine. Whole-wheat bread, therefore, is an excellent source of the vitamin as are most animal tissues, pork products being especially rich.

Studies of the synthesis of thiamine by extracts of baker's yeast have revealed that the pyrimidine and thiazole moieties are formed independently[2]. The origins of the pyrimidine and thiazole moieties shown as starting materials in Fig. 1.1 have not been established.

FIGURE 1.1 Biosynthesis of Thiamine

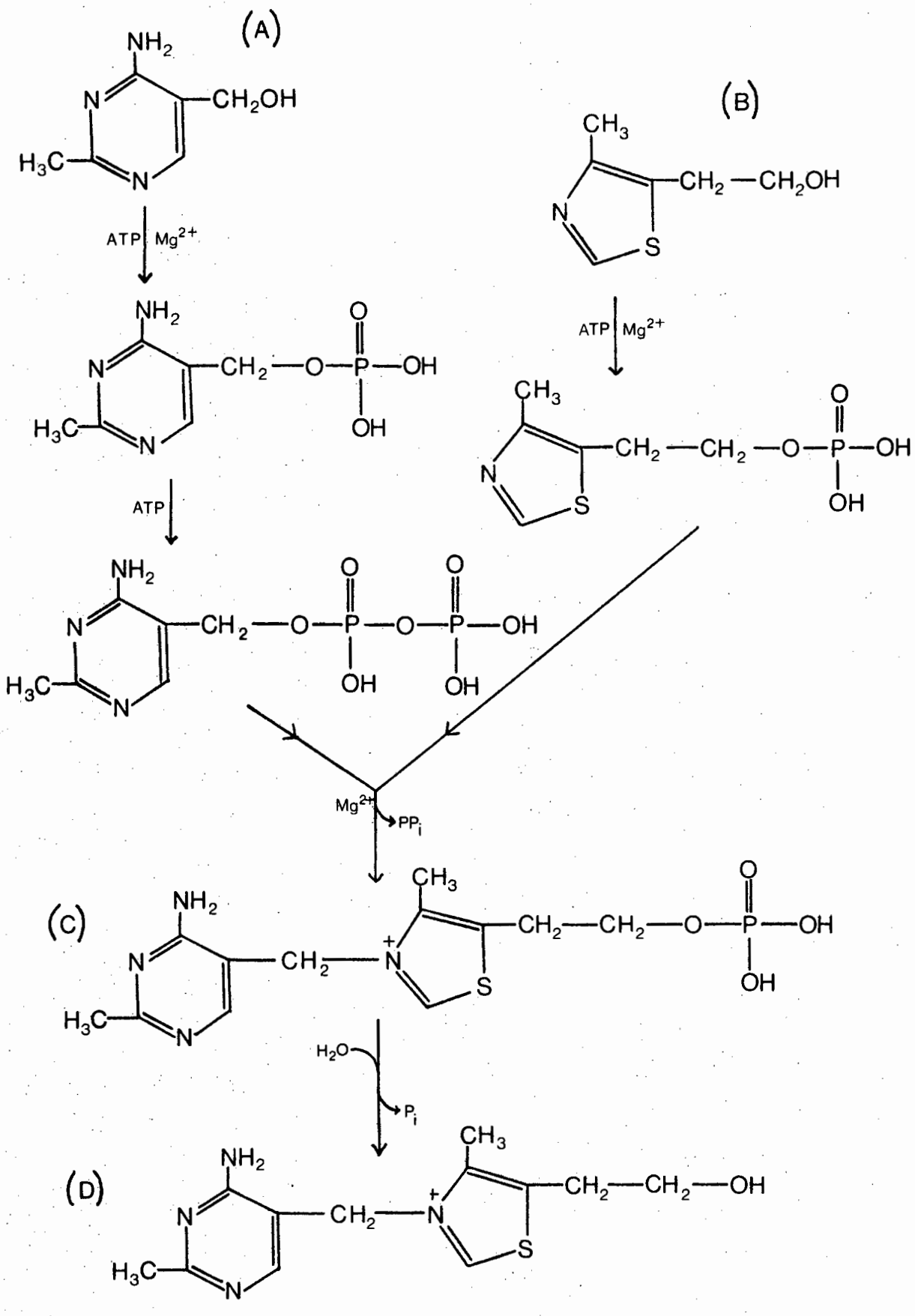


(A) 2-methyl-4-amino-5-hydroxymethyl pyrimidine.
(B) 5-(2-hydroxyethyl)-4-methyl thiazole.
(C) Thiamine phosphate.
(D) Thiamine.

It is the phosphate or the pyrophosphate of the vitamin which participates in mammalian metabolism in the following three reaction types: (a) the decarboxylation of α-keto acids to aldehydes or acyloins, (b) the decarboxylation of α-keto acids to acids (oxidative decarboxylation), and (c) the transformation of α-keto acids to acyl phosphates[3].

Thiamine pyrophosphate or cocarboxylase which is synthesised by direct transfer of the pyrophosphate group from ATP is so-called since it is the coenzyme of carboxylase in the reaction (a) above. The important step of the reaction is the ionization of the proton at the 2-position of the thiazolium ring. This 2-position must be unsubstituted for biological activity. The thiazolium system provides the high electron density required at the 2-carbon[4].

Thiazolium ligands are, therefore, good coenzyme models, though the amino group on the pyrimidine moiety is now thought to be a second reaction centre[5].

Thiamine-requiring enzymes catalyze reactions in which carbon-carbon bonds immediately adjacent to carbonyl groups are cleaved (α-type cleavage). The major carbohydrate metabolic cycles (the citric acid cycle and the fixation of carbon dioxide by photosynthesis) are absolutely dependent on thiamine since they all depend upon α-type cleavages.

The thiazole moiety of thiamine 5-(2-hydroxyethyl)-4-methyl thiazole (=thiaz) can replace thiamine as a nutrient for some bacteria[6].

Both cleavage products of thiamine have been isolated from urine of rats which have been dosed with large amounts of the vitamin. It seems, therefore, that the rat is capable of cleaving thiamine[7]. This thiazole moiety (thiaz) has been found to be biologically active in that it stimulates growth of rats with a thiamine-deficient diet[8] and it has also been identified as a component of glycerol phosphate dehydrogenase[9].

## 1.2 Cyclic Nucleotides.

Nucleotides are comprised of three major portions: the base (either purine or pyrimidine) the pentose or deoxypentose sugar, and the phosphate group. The nucleic acids which make up the deoxyribonucleic acid (DNA) and ribonucleic acid (RNA) thread-like macromolecules, are chains of nucleotides. Nucleic acids are digested in the duodenum and the liberated nucleotides are hydrolysed to give nucleosides (the base and sugar portions without the phosphate group). The purines, adenine and guanine and the pyrimidines, thymine and cytosine are found in DNA whereas in RNA uracil takes the place of thymine. The biological importance of pyrimidines is not restricted to nucleic acids. Several pyrimidine nucleotides play important roles in carbohydrate and lipid metabolism[2]. Likewise some purines are essential constituents of coenzymes and a few have shown definite anti neoplastic activity[3].

Cyclic nucleotides are less well known but are also nevertheless important constituents of biological systems. They differ from normal monophosphates since the phosphate group is attached at both C-3' and C-5' in the 3',5' cyclic monophosphates and at C-2' and C-3' in the 2',3' cyclic monophosphates. The 3',5' cyclic monophosphates are dealt with in this work. 3',5' cyclic adenosine monophosphate (cAMP) is the best known of the cyclic nucleotides and has been shown to be of great importance in the regulation of metabolism and function in a wide variety of tissues and species, and to mediate the actions of many hormones. To be more specific, it has been shown that the actions of cAMP in mammalian tissues as well as in tissues

of species in eight different invertebrate phyla are mediated through activation of tissue-specific protein kinases[10], kinases being enzymes that catalyse transfer of phosphate from ATP to an acceptor. Other cyclic nucleotides including those derived from inosine, guanosine, uridine, thymidine and cytosine (cIMP, cGMP, cUMP, cTMP and cCMP) were experimented upon. The cAMP-dependent protein kinase which catalyses the phosphorylation of casein, protamine and histone by ATP was found in muscle, liver, brain, adipose-tissue and also bacteria. The effectiveness of different cyclic nucleotides in stimulating protein kinase activity varies. The general pattern, however, at low nucleotide concentration is cAMP > cIMP > cGMP > cUMP > cCMP > cTMP.

Several derivatives of cAMP have been prepared which contained alkyl residues in the N-6, and other substituents in the C-2 and C-8 positions. These compounds plus cAMP itself, cIMP and cGMP were tested for their stimulatory effect on the release of various pituitary hormones[11]. The most active were 8-bromo and 8-thio cAMP. cGMP and cIMP produce significant stimulation of the synthesis and release of growth hormones in female rats.

Jefferson et al[12] have put forward the hypothesis that the effects insulin exerts on the mammalian liver to inhibit the production of glucose and urea and to promote the uptake of $K^+$ ions may be due to a decrease in liver cAMP. cAMP has also been found to be an important factor in the inhibition of platelet aggregation[13].

Nature often uses a two-messenger mechanism by which hormones act on effector cells. Basically the endocrine glands receive stimuli

which activate the release of a first messenger, the hormone, which travels to other cells and interacts with specific effector cells[14]. The usual site of interaction is the cell membrane. At the site of interaction a second messenger may be formed which usually functions within the cell to modify enzyme activity and permeability barriers. In some cases the second messenger may stimulate a third messenger (a steroid) which then leaves the specialized tissue to react elsewhere. This succession of events is followed when the hormone epinephrine is released from the endocrine gland and is subsequently exposed to modulators which are capable of inactivating it. Those molecules which survive, interact with adenyl cyclase systems of the effector cell membrane, producing an increased rate of synthesis of cAMP from ATP, the presence of $Mg^{2+}$ ions enhancing the accumulation of the heat-stable cyclic nucleotide.

Fig.1.2. THE SECOND MESSENGER SYSTEM INVOLVING ADENYL CYCLASE

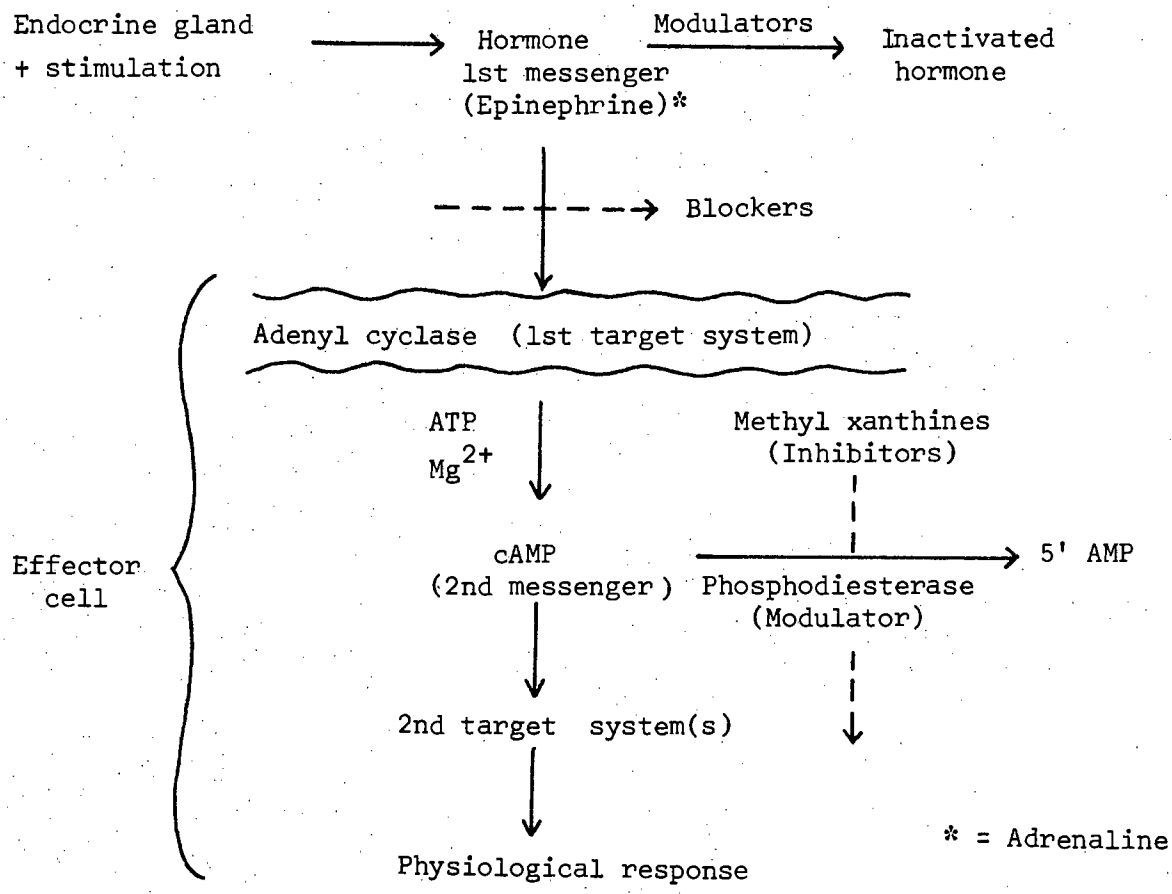

Adenyl cyclase is a particulate fraction of liver homogenate which produces cAMP and the substrate for the reaction is ATP.

The second messenger, in this case cAMP, is also susceptible to inactivation by a modulator, a phosphodiesterase which is specific for mononucleotide 3',5' bonds. Methylxanthines are potent inhibitors of the modulator phosphodiesterase. It is thought that this inhibition is the cause of the pharmacological effects of methyl xanthines. On contact of the cAMP with enzymes of the phosphorylase system, activation occurs and this is partly responsible for the production of glycogenolysis in liver.

Various tissues including liver, heart and fat tissues illustrate the role of the second messenger cAMP. As previously stated the specific physiological response in the liver is glycogenolysis and the target system is the balance between active and inactive phosphorylase. The inotropic response to epinephrine in the heart is under investigation[14].

Epinephrine induces the physiological response of lipolysis in epididymal fat pads where the target system is lipase activation.

There are various other roles which cAMP plays in biological systems including stimulation of hydroxylation of adrenal steroids; inhibition of the release of histamine; involvement in intestinal secretion and other effects of cholera enterotoxin and regulation of the release of thyroid hormones.

## 1.3 Metals in biological systems

During the past two decades there has been considerable progress in understanding the role of metals in biological processes, primarily in the field of metalloproteins. However, in the less specific metal ion reactions where the metal ion is in equilibrium with the substrate the functions of the metal are not as well known.

There are numerous possible roles for metal ions in biological systems ranging from weak ionic effects to highly specific associations. Thus for the alkali metals whose major role is that of a charge carrier, interaction with the protein is slight[15], whereas the metal ions of the redox metalloenzymes are very firmly bound indeed, usually by macrocyclic molecules of the porphyrin type or by strongly polarizable donors. Generally the transition metals act as catalysts often through redoxing and this occurs in the active site of the enzyme (Fe(II) in haemoglobin and Co(III) in the vitamin $B_{12}$ coenzyme[16]). The metal is removed from these metalloenzymes only with extreme difficulty[17] causing loss of activity implying the severance of a specific linkage.

A second group of proteins combine reversibly with several different metal ions these being called the metal-protein complexes[17]. The metal is bound loosely to the protein and readily dissociates causing only some loss of activity. Different metals may substitute for one another in bringing about 'activation' of enzymatic activity. $Mg^{2+}$, $Zn^{2+}$, $Mn^{2+}$ and $Fe^{2+}$, on interaction with enolase, activate the enzyme whilst many other ions form inactive complexes. Metal ions

coordinated in this less specific manner account for approximately 5% of the total heavy metal ion content of the body whilst metal ions bound in metalloproteins account for most of the remaining percentage. Less than 1% is coordinated to amino acids and other low molecular weight ligands. All the work in this thesis falls into this last category.

### 1.3.1 Metals and thiamine

The yeast holoenzyme (conjugated protein, non-amino acid in nature), carboxylase contains $Mg^{2+}$. The action of the coenzyme, cocarboxylase (thiamine pyrophosphate) is reported to function by binding the apoenzyme (the protein component of an enzyme) by means of the $Mg^{2+}$ ion to the pyrophosphate group[4]. However, Schellenberger[5] has postulated that the bonding between N-1' of cocarboxylase and the apoenzyme takes place through the $Mg^{2+}$ ion and that the pyrophosphate is bound to the apoenzyme quite independently of the metal ion in the primary equilibrium. This assumption is supported by the fact that unphosphorylated thiamine has no effect on the primary equilibrium. If the metal ion which is built into the enzyme complex is changed, combination rates alter increasing in the order Mg < Co < Mn < Ca.

Thiamine is decomposed under ordinary heating conditions. The decomposition is accelerated by the presence of $Cu^{2+}$ ions even at as low a concentration as 0,02 ppm[18]. The effect of $Cu^{2+}$ ions is greater than other metal ions studied. The reactions involve, amongst others, the breaking of the thiazole ring to form thiamine disulphide (TDS) and the linking with the amino group to form thiochrome. It

was found that the amounts of TDS and thiochrome varied according to whether the thiamine solution was heated with or without $Cu^{2+}$ ions.

Marzotto and Galzigna[19], have reported data relating to the non-enzymatic hydrolysis of acetylcholine in the presence of both thiamine and Cu(II). Acetylcholine, $CH_3CO_2CH_2CH_2N^+(CH_3)_3$ is the chemical involved in transmission of impulses across synapses between neurons outside the central nervous system[20]. Once released the chemical diffuses across the synapse, exerts its effect at receptor sites of the next cell and is then immediately destroyed by an enzyme called acetylcholinesterase. This destruction is of critical importance. If the acetylcholine were not destroyed, control would be lost since the stimulatory action would then continue indefinitely. Acetylcholinesterase destroys acetylcholine by catalysing its hydrolysis to acetic acid and choline. The latter species may subsequently combine to regenerate the mediator. The physical data related to the non-enzymatic hydrolytic reaction of acetylcholine in the presence of both thiamine and Cu(II) revealed a 1 : 1 thiamine-Cu(II) complex in aqueous solution. Now previous studies show that acetylcholine binds to a 'receptor' zone of the thiamine molecule giving a molecular complex[21] and that thiamine has a catalytic effect on acetylcholine hydrolysis[22]. Therefore, Marzotto et al[23] have demonstrated that Cu(II) inhibits the formation of a thiamine-acetylcholine complex because its affinity for thiamine is higher and the Cu-thiamine complex is more stable. They postulate that the inhibition may be due to several causes, namely, (a) steric hindrance due to Cu(II) occupying the receptor zone of the thiamine molecule, (b) an electronic effect on the pyrimidine ring possibly due to Cu(II)

being bound through coordination to $NH_2$ and N-3', and (c) a slowing down of the C-2 carbanion formation, all of these altering the structure of the receptor zone of the thiamine molecule. Recently an X-ray crystal structure of the Cu-thiamine complex was reported[24] showing that the complex salt $[CuCl_4]$(thiam H) forms with no direct interaction of the thiamine with the metal. This does not necessarily mean that in solution there is no direct interaction of the Cu(II) with the thiamine molecule.

### 1.3.2 Metals and nucleotides

Nucleic acids play a fundamental role in the transmission of genetic information, in the control of the functioning of living cells and in the synthesis of proteins. All of the reactions in which nucleic acids participate in biological systems are mediated by metal ions[25]. Nucleic acids are macromolecules consisting of a backbone of ribose and phosphate moieties to which are attached the various bases. Important nucleotides in biological systems include AMP, GMP, CMP, UMP, TMP and IMP (the monophosphates of adenosine, guanosine, cytidine, uridine, thymidine and inosine) the first five of which make up the nucleic acids the sequence of which constitute the genetic code.

DNA is composed of two chains of polynucleotides which exist in a double helical structure. Each chain consists of sugar rings joined by 3',5' phosphodiester bridges. The chains are held together by hydrogen-bonding between a purine and a pyrimidine base. Adenine base pairs to thymine and cytosine to guanine.

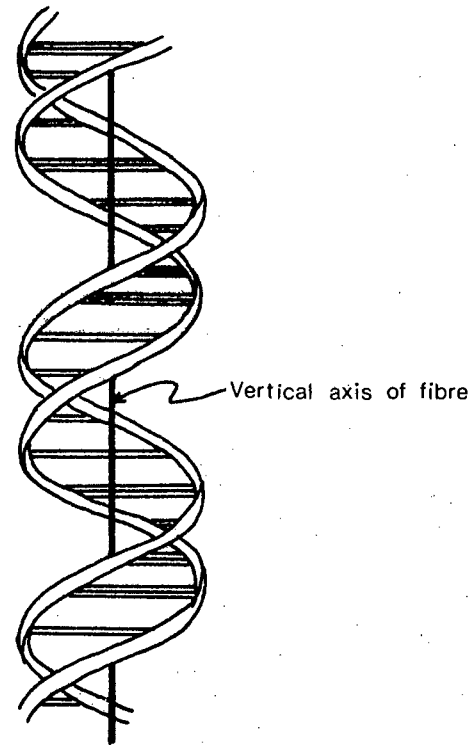


Fig. 1.3 DNA double helix. The horizontal bars represent H-bonding, between pairs of bases and the two strands represent the sugar-phosphate chains.

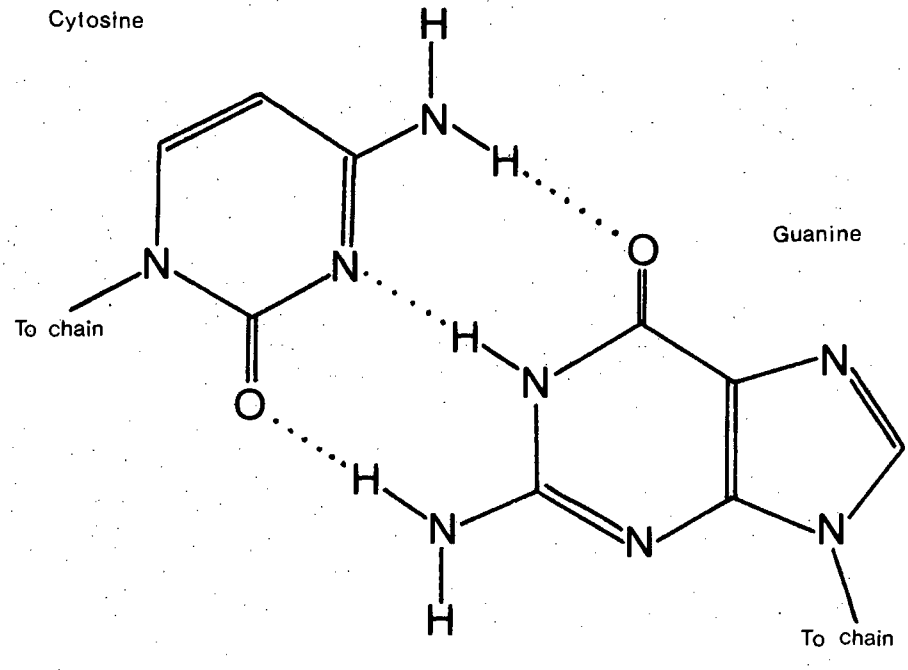


Fig. 1.4 H-bonding of cytosine to guanine.

A metal ion can bind to two sites, the phosphate group and the base. On base binding the helix unwinds due to replacement of protons involved in the base pairing by the metal ion. Binding of the metal to the phosphate would obviously have a different effect. $Mg^{2+}$ ions stabilize DNA due to phosphate binding whilst $Cu^{2+}$ ions destabilize it through binding to the bases[26]. DNA is stabilized by metal binding to the phosphate since the metal counters the negative charges on the phosphate ions in solution therefore negating the repulsion of charges which causes it to unwind.

Now $Cu^{2+}$ ions destabilize DNA and this causes the melting temperature to drop. However, this drop in temperature only occurs at low concentrations of electrolyte. The destabilization effect is countered by a high concentration of salt[25]. Therefore upon heating DNA in the presence of $Cu^{2+}$ and a low concentration of salt, unwinding occurred and on addition of extra salt and cooling of the solution the double helix was regenerated. This was possible since the metal helps form the cross-links between the strands. $Zn^{2+}$ causes reversibility of the unwinding and winding purely by heating and cooling the solution, there being no need for addition of electrolyte. This is due to $Zn^{2+}$ binding less strongly to the bases than $Cu^{2+}$ and results in the double helix reforming more easily from the $Zn^{2+}$ complex of the single stranded DNA than in the case of the $Cu^{2+}$ complex.

Transition metal ions are known to be tightly bound to naturally occurring RNA materials. The extreme difficulty in removing these metals from RNA preparations[73], and the observation that they

stabilize the ordered structure of the RNA molecules, indicate that they may play a significant role in the maintenance of the specific conformation of these nucleic acids. Transfer RNA (tRNA) is one of three different kinds of RNA which have been identified in cells. It is so called since its role is that of transferring information involving interactions with both proteins and other RNA molecules. In order to perform these functions complex secondary and tertiary structures have been adopted by tRNA which are believed to be influenced by the presence of a series of rare nucleosides, in addition to the four common ones. The rare nucleosides include inosine, alkylated and acylated nucleosides, pseudouridine (N-1 of uridine replaced by C), 5,6-dihydrouridine, and thio bases. Several analogous ligands to those quoted above are studied in this work.

Finally, it has been shown[10] that cAMP's stimulatory effect on protein kinase activity is enhanced by $Co^{2+}$ and $Mn^{2+}$. $Ca^{2+}$ produced no protein kinase activity.

## 1.4 The theory of NMR line-broadening and line-shifting.

The basic theory of nuclear-magnetic resonance (n.m.r.) is dealt with in the standard texts[27,28]. Those aspects of n.m.r. which are effected by the presence of paramagnetic metal ions will be discussed here. The present work is concerned chiefly, in information, both structural and otherwise, that can be gained from observation and measurement of (a) the line shape (width at half-height) and (b) the resonance position of n.m.r. lines.

At low radio frequency power the line shape is Lorenztian and independent of $T_1$. The width at half height is related to the spin-spin relaxation rate by the equation

$$\Delta\nu = \frac{1}{\pi T_2} \qquad \text{.....(1.1)}$$

Thus any factors affecting $T_2$ will be reflected in their effect on the line width.

### 1.4.1 Spin-spin relaxation.

Magnetic nuclei interact amongst themselves in addition to interacting with the lattice. Small local magnetic fields, $H_{loc}$, produced by each nuclear magnet act upon their neighbours, as well as the magnetic field $H_o$.

A magnetic dipole produces a field of $\mu/r^3$ gauss at a distance r. Therefore for a proton at a distance of 1Å, the field is approximately 14 gauss. Only neighbours in close proximity have much effect on $H_{loc}$, since as r increases its value decreases very rapidly. Nuclei experience different magnetic fields which causes

broadening of the signal or absorption line. Thus if $H_{loc}$ is the spread of the local magnetic fields then the range in the Larmor precession frequencies is

$$\Delta\nu = \frac{\mu H_{loc}}{I\hbar} \qquad \text{.....(1.2)}$$

In liquids and gases where re-orientation is rapid the average local field is small and a narrow line width is observed but in most solids this is not so and results in a very broadened spectrum.

If the nuclei are precessing in phase at a particular instant, then in the time $(\Delta\nu)^{-1}$ they will be out of phase. This constitutes part of $T_2$, the spin-spin relaxation time, also known as the transverse relaxation time. One nucleus may dephase another causing simultaneous re-orientation or flip-flop of both nuclei. Since the energy comes from the exciting nucleus, the interchange conserves the total energy of the pair. The relative phases of the nuclei change in a time $(\Delta\nu)^{-1}$. This time required for spin exchange causes a further broadening of the signal. Only identical nuclei are capable of spin exchanging whereas unlike nuclei can contribute to $H_{loc}$. Inhomogeneity of the applied field will result in line broadening since gradients present will produce their own $H_{loc}$.

### 1.4.2 Relaxation of nuclei in the vicinity of a paramagnetic centre[29].

The nuclear relaxation times in the solution of a diamagnetic ligand are reduced markedly on addition of small concentrations of paramagnetic solutes. This is because magnetic moments of unpaired electrons are $\sim 10^3$ times greater than the nuclear magnetic moments. The local fields generated by the electron can be coupled to the nuclei by simple

dipole-dipole interaction, or by scalar or hyperfine coupling transmitted through a chemical bond, leading to more efficient nuclear spin relaxation. The relative importance of dipolar and scalar coupling varies with the paramagnetic ion used and the nature of the ligand. Usually for Gd(III) and Mn(II) the dipolar mechanism dominates. Similarly for Cu(II) with non-aromatic ligands the dipolar term dominates[30] but with aromatic ligands this appears not to be the case[31]. For other first row transition metal ions both mechanisms contribute significantly.

The Solomon-Bloembergen equations[32,33] describe the relaxation times $T_1$ and $T_2$ of nuclei bound near a paramagnetic site.

$$\frac{1}{T_{1M}} = \frac{2}{15}\frac{\gamma_I^2 g^2 S(S+1)\beta^2}{r^6}\left(\frac{3\tau_c}{1+\omega_I^2\tau_c^2} + \frac{7\tau_c}{1+\omega_s^2\tau_c^2}\right)$$

$$+ \frac{2}{3}S(S+1)\left(\frac{A}{\hbar}\right)^2\left(\frac{\tau_e}{1+\omega_s^2\tau_e^2}\right) \qquad \text{.....(1.3)}$$

$$\frac{1}{T_{2M}} = \frac{1}{15}\frac{\gamma_I^2 g^2 S(S+1)\beta^2}{r^6}\left(4\tau_c + \frac{3\tau_c}{1+\omega_I^2\tau_c^2} + \frac{13\tau_c}{1+\omega_s^2\tau_c^2}\right)$$

$$+ \frac{1}{3}S(S+1)\left(\frac{A}{\hbar}\right)^2\left(\frac{\tau_e}{1+\omega_s^2\tau_e^2} + \tau_e\right) \qquad \text{.....(1.4)}$$

The first terms in the above expressions represent the dipole-dipole interaction which is modulated by the correlation time $\tau_c$. $\tau_e$ modulates the scalar interactions which are represented by the second term in the equations.

The correlation times are defined as

$$\frac{1}{\tau_c} = \frac{1}{\tau_s} + \frac{1}{\tau_M} + \frac{1}{\tau_r} \qquad \text{.....(1.5)}$$

$$\frac{1}{\tau_e} = \frac{1}{\tau_s} + \frac{1}{\tau_M} \qquad \text{.....(1.6)}$$

where $\tau_r$ is the rotational correlation time, $\tau_M$ is the life-time of the nucleus in the bound state and $\tau_s$ is the electron-spin relaxation time.

The paramagnetic metals may be divided into two classes depending upon their values of $\tau_s$ :

a) Those which broaden a spectrum, which will be dealt with below and

b) those which shift the spectrum which are discussed in 1.4.7.

Mn(II), Cu(II) and Gd(III) have relatively long electronic relaxation times ($\tau_s \approx 10^{-8}$ sec.), $\tau_c$ in equation 1.5 therefore being dominated by $\tau_r$ ($\tau_r \approx 10^{-10}$ sec., $\tau_M \approx 10^{-8}$ sec.) which gives rise to broadening of the spectrum due to large $1/T_{2M}$ values. On the other hand Ni(II) and Co(II) have very short electronic relaxation times ($\tau_s \approx 10^{-12}$ - $10^{-13}$ sec.) and so $\tau_c$ will be dominated by these. This results in $1/T_{2m}$ being two orders of magnitude less for Ni(II) and Co(II) than for Mn(II) and Cu(II).

The two metals used for broadening experiments were Gd(III) and Mn(II) and under the experimental conditions used (i.e. 100 MHz spectrometer),

$$\omega_s = 4 \times 10^{11} \text{ rad. sec.}^{-1}$$

and $$\omega_I \approx 6 \times 10^{8} \text{ rad. sec.}^{-1}$$

hence $\omega_s^2\tau_c^2 \gg 1$ and $\omega_I^2\tau_c^2 \ll 1$.

Resonance frequencies of the protons studied in the broadening experiments showed no discernible shifts. This can be attributed to negligible scalar contribution to the relaxation rates of nuclei not directly bonded to the paramagnetic ion. Other workers[34] confirm this. Therefore equations 1.3 and 1.4 reduce to:

$$\frac{1}{T_{1M}} = \frac{2}{5} \frac{\gamma_I^2 g^2 \beta^2 S(S+1)}{r^6} \cdot 3\tau_c \qquad \text{.....(1.7)}$$

$$\frac{1}{T_{2M}} = \frac{1}{15} \frac{\gamma_I^2 g^2 \beta^2 S(S+1)}{r^6} \cdot 7\tau_c \qquad \text{.....(1.8)}$$

$\gamma_I^2 g^2 \beta^2 S(S+1)$ is a constant for a given nucleus and paramagnetic ion.

1.4.3 Chemical exchange in paramagnetic systems.

Swift and Connick[35] have characterized the effect of chemical exchange on relaxation rates. Where the subscripts A and M denote the free and bound states of the nuclei respectively and f is the ratio of bound nuclei to free nuclei then the relevant equations are:

$$\frac{1}{T_{1OBS}} = \frac{1}{T_{1A}} + \frac{f}{T_{1M}+\tau_M} \qquad \text{.....(1.9)}$$

and

$$\frac{1}{T_{2OBS}} = \frac{1}{T_{2A}} + \frac{f}{\tau_M} \left[ \frac{\frac{1}{T_{2M}} \left( \frac{1}{T_{2M}} + \frac{1}{\tau_M} \right) + \Delta\omega_M^2}{\left( \frac{1}{T_{2M}} + \frac{1}{\tau_M} \right)^2 + \Delta\omega_M^2} \right] \qquad \text{.....(1.10)}$$

If it is assumed that only one ligand is bound to each metal ion, and if the ligand concentration is in large excess of the metal, then

$$f = [M]/[L] .$$

There are several limiting cases of the above equations:

(i) If $\Delta\omega_M^2 >> 1/T_{2M}^2, 1/\tau_M^2$ then

$$1/T_{2p} = f/\tau_M \qquad \text{.....(1.11)}$$

where $$1/T_{2p} = 1/T_{2OBS} - 1/T_{2A} \qquad \text{.....(1.12)}$$

Relaxation occurs through a change in the precessional frequency and $T_{2p}$ is controlled by $\tau_M$.

(ii) If $1/\tau_M^2 >> \Delta\omega_M^2 >> (\tau_M T_{2M})^{-1}$ then

$$1/T_{2p} = f\tau_M\Delta\omega_M^2 \qquad \text{.....(1.13)}$$

Chemical exchange is rapid and so $T_{2p}$ is controlled by the change in the precessional frequency.

(iii) If $1/T_{2M} >> \Delta\omega_M^2; \quad 1/\tau_M^2$ then

$$1/T_{2p} = f/\tau_M \qquad \text{.....(1.14)}$$

Relaxation by $T_{2M}$ is fast, i.e. exchange is slow, and so $T_{2p}$ is controlled by the rate of chemical exchange.

(iv) If $(T_{2M}\tau_M)^{-1} >> 1/T_{2M}^2; \Delta\omega_M^2$ then

$$1/T_{2p} = f/T_{2M} \qquad \text{.....(1.15)}$$

Here exchange is fast and so relaxation is controlled by $T_{2M}$.

Therefore since $\Delta\omega_M$ is small for Gd(III) and Mn(II), since these are broadening reagents rather than shift reagents, equations 1.14 and 1.15 are applicable. For slow chemical exchange $T_{2p}$ is

controlled by $\tau_M$ whereas for fast chemical exchange $T_{2p}$ is controlled by $T_{2M}$. Experimentation was carried out under the conditions of this latter case.

### 1.4.4 Temperature dependence of relaxation rates.

As seen above, equations 1.14 and 1.15 are dependent upon the rate of chemical exchange. Thus under conditions of slow chemical exchange the temperature dependence of $T_{2p}$ is governed by that of $\tau_M$ and under fast chemical exchange conditions by that of $T_{2M}$. This is shown in the following Fig. 1.5.

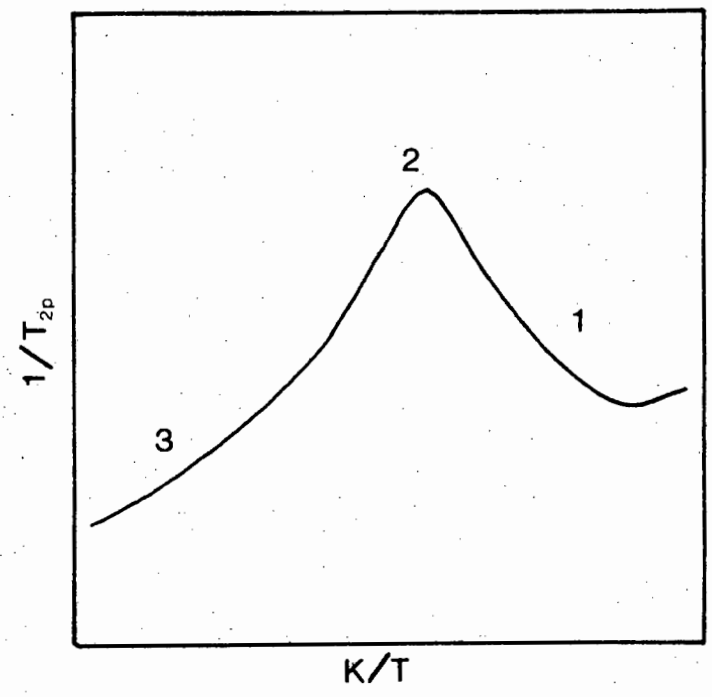


Fig. 1.5 Theoretical curve showing the temperature dependence of $T_{2p}$

Region 1 is the slow-exchange region where $\tau_M$ controls $T_{2p}$. The temperature dependence of $\tau_M$ is:

$$\tau_M = (kT/h)^{-1} \exp. (\Delta H^{\ddagger}/RT - \Delta S^{\ddagger}/R) \quad \ldots\ldots\ldots(1.16)$$

Substituted into 1.14 this gives

$$\ln T_{2p} = \Delta H^{\ddagger}/RT + \text{constant} \qquad \ldots\ldots\ldots(1.17)$$

Therefore on the temperature increasing, $T_{2p}$ decreases and broadening of the spectrum line-widths occurs.

Region 2 is the intermediate region for which there is no simple relationship. The temperature dependence of $T_{2p}$ is therefore extremely complex and difficult to analyse.

Region 3 is that region in which the main interest lies for this work. Fast chemical exchange takes place, $T_{2p}$ being controlled by $T_{2M}$, which is a function of $\tau_r$. $\tau_r$ is given by:

$$\tau_r = \tau_r^{0} \text{ exp. } (E_A/RT) \qquad \ldots\ldots\ldots(1.18)$$

where $E_A$ is the activation energy of rotation. Substitution of this equation into equation 1.8 gives:

$$1/T_{2M} = K \text{ exp. } (E_A/RT) \qquad \ldots\ldots\ldots(1.19)$$

where K is a constant for a particular metal-ion, proton pair.

$$\therefore \ln T_{2p} = -E_A/RT + \text{constant} \qquad \ldots\ldots\ldots(1.20)$$

An increase in temperature thus results in a narrowing of the spectrum line-widths

### 1.4.5 External factors which affect relaxation times.

There are several other factors, mainly instrumental, which may affect the line shape of an n.m.r. resonance. These should, however, be constant during an experiment and so not affect the results. These factors are

(i) Magnetic field inhomogeneity. On the Varian XL100 spectrometer which was used in this study, the magnetic field homogeneity is better than 0,2 Hz.

(ii) Change in bulk susceptibility. Due to the addition of paramagnetic metals to the sample the bulk susceptibility may change. Simple calculations, however, show this to be negligible at the metal-ion concentrations used and tests with internal standards confirm this.

(iii) Viscosity of the medium. As the viscosity of the medium increases so the molecular tumbling rate decreases. This means that the local magnetic fields and inhomogeneities will not be averaged out as well as at the start and so the spectral lines will become broader.

### 1.4.6 Determination of distances, from the broadening data.

In paramagnetic metal complexes, nuclei closest to the metal ion are preferentially broadened. For the metals Gd(III) and Mn(II) the degree of broadening is given by equations 1.1, 1.8 and 1.15. Together these give:

$$\Delta\nu = \frac{1}{\pi T_{2p}} = \frac{f}{15\pi} \frac{\gamma_I^2 g^2 \beta^2 S(S+1)}{r^6} \cdot 7\tau_c \qquad \ldots\ldots\ldots(1.21)$$

$\Delta\nu$ is measured directly from the n.m.r. spectrum. Therefore if every term except for r were known it would be theoretically possible to calculate this metal ion to proton distance. However, the value of $\tau_c$ is unknown and an accurate determination thereof, is often difficult. In order to overcome this drawback relative internuclear distances are determined rather than the absolute distances. Broadening produced by successively increasing concentrations of metal ion is measured and a plot of $\Delta\nu$ versus f drawn. This should produce a straight line whose

slope is proportional to $1/r^6$. Therefore

$$\left(\frac{r_i}{r_{ii}}\right)^6 = \frac{\text{slope ii}}{\text{slope i}} \qquad \text{.....(1.22)}$$

where i and ii denote two ligand protons. The fact that the slopes are proportional to the sixth power of 1/r allows for a relatively large uncertainty in the values of the slopes without sacrificing the accuracy of the distance results.

1.4.7 Pseudo-contact shifts[29,36].

The failure of the dipolar interaction between the unpaired electron spin of some paramagnetic ions and a given nucleus, to average to zero, results in a net shift, the dipolar or pseudo-contact shift.

LaMar et al[37] have shown the magnitude of this shift to be:

$$\partial = D\left\langle\frac{3\text{Cos}^2\theta-1}{r^3}\right\rangle_{av} + D'\left\langle\frac{\text{Sin}^2\theta\text{Cos}2\phi}{r^3}\right\rangle_{av} \qquad \text{....(1.23)}$$

Where $\theta$ is the angle between the principal symmetry axis of the complexed ion and the vector r. D is constant usually of unknown value. The average is taken over the nuclear motions of the molecule, which are rapid on the n.m.r. time scale. If the symmetry of the complex is axial then the last term in equation 1.23 is equal to zero.

For lanthanides, assuming axial symmetry, it is more convenient to measure ratios of the shifts of two nuclei in the same molecule (since D is unknown). Therefore

$$R = \frac{\partial_1}{\partial_2} = \left\langle\frac{3\text{Cos}^2\theta_1-1}{r_1^3}\right\rangle_{av} \Big/ \left\langle\frac{3\text{Cos}^2\theta_2-1}{r_2^3}\right\rangle_{av} \qquad \text{.....(1.24)}$$

It may be noted that if the ratios, $R_i$, of different lanthanides are the same, then it is a reasonable indication of axial symmetry. It is possible to calculate the ratios of observed shifts for any number of probable conformations of the ligand in question for different metal co-ordination sites (if more than one exists). A solution may be obtained when the experimentally observed ratios agree with predicted ones. This does not necessarily give a unique answer, so that extra parameters may be needed to limit the possibilities.

Some lanthanide ions as seen in 1.4.2 give appreciable line broadening with negligible shifts whilst others with very short $\tau_s$ values give the reverse, e.g., $Pr^{3+}$ and $Eu^{3+}$. There are others which give very large shifts but also a certain degree of broadening, e.g. $Dy^{3+}$, $Ho^{3+}$ and $Yb^{3+}$.

The use of various lanthanide ions not only verifies that conditions of axial symmetry are obtained but also that the shifts obtained are due to pseudo-contact interaction alone with no contact shift contributions.

The extent and the direction of shifts of various resonance lines of a particular ligand varies with different lanthanide ions. Thus the choice of lanthanides is limited when proton signals are present in the vicinity of residual HOD - they must be shifted away.

A useful aspect of the lanthanide shift reagents is to shift out a spectrum so that all the lines are easily distinguishable before

commencing a broadening experiment. This eases measurements of the widths at half-height immensely.

A combination of the results gained from these two techniques described, namely broadening and shifting of an n.m.r. spectrum can give extremely useful information on the structure and conformation of the system under study.

## 1.5 Literature survey on relevant line-broadening and line-shifting studies.

Pioneer work on quantitative measurements of metal binding to nucleotides was carried out by Sternlicht et al[34] using $^{31}P$ NMR, employing equations derived by Solomon[32], and Bloembergen[33], and, Swift and Connick[35] (see sections 1.2.2 and 1.2.3 respectively). $T_1$, $T_2$ and shift measurements enabled them to propose that binding of Mn(II), Ni(II), Co(II) and Cu(II) to ATP (adenosine triphosphate) and Co(II) to ITP (inosine triphosphate) occurs simultaneously on the purine ring at N-7 and the phosphate chain, thus giving an intramolecular back-bound monomer. Not all authors agree that the metal in the vicinity of N-7 is actually bound to it. Glassman et al[38] have proposed that an outer-sphere complex is formed in which a water molecule in the metal's inner coordination sphere is hydrogen bonded to N-7.

A similar type of binding is suggested by Gallo et al[39] in their studies on thiamine pyrophosphate with Ni(II). They find broadening of the C-6' proton signal is strongly temperature dependent suggesting that there is an equilibrium involving "folded" and "unfolded" forms, with the unfolded form predominating. In the unfolded form it is proposed that a co-ordinated water molecule hydrogen-bonds to N-1' of the pyrimidine ring. Studies by other workers on the same system with Co(II) and Ni(II)[40] using shift and broadening data from $^{1}H$ and $^{31}P$ n.m.r. spectra propose the above hypothesis as one possibility, the other being a weak interaction of the metal ions to N-1'. Grande et al[41] have shown that Mn(II) binds to the phosphate groups and though they do not mention any base

binding the conformation of the pyrophosphate chain is such that broadening of H-6' is substantial.

Relevant to these studies are the interactions of metal ions with nucleosides where there are no phosphate groups present to compete as binding sites for the metal. Qualitative studies have been carried out on these systems mostly using Cu(II). Inosine and adenosine contain potential chelating groups at N-7 and O-6, and N-7 and N-6 (the amino nitrogen) respectively. Eichhorn et al[42] found that H-8 and H-2 resonances of adenosine in DMSO broadened equally on addition of Cu(II) but the amino group was not broadened. They attributed this to non-chelate binding of the Cu(II) at N-7 plus an equivalent percentage of binding at N-3 and/or N-1. However, one would expect some broadening of the amino group since broadening is a function of the distance, r, of the proton from the metal and binding at N-7 would bring Cu(II) within close proximity of the amino group. It was thought that quantitative work would now be possible on these systems with Cu(II) using the $1/r^6$ broadening dependence but a recent work[31] has lodged some doubt as to whether broadening induced by Cu(II) is completely due to the dipolar mechanism. There may be a significant contribution from the scalar term which would make quantitative determinations impossible.

Inosine was found to bind Cu(II) at N-7 and/or N-1 depending upon the pH of the solution[43,44]. At pH 5,6 both sites are almost equally populated. At elevated temperatures as well as at pHs > 7, N-1 is the preferred binding site. 1-methyl inosine binds Cu(II) only to N-7 whilst 7-methyl inosine binds at N-1 both showing N-3 to be an unfavourable binding site. Other qualitative studies[45] have shown Co(II)

and Mn(II) forming only weak complexes with inosine indicating chelate binding to N-7 and O-6. In none of these studies discussed was metal binding to the ribose ring of any importance except at very high pH.

Various studies have been carried out on the 5'-monophosphates. $^{31}P$ and $^{13}C$ n.m.r. shows that $Mn^{2+}$ ions bind to the phosphate groups at 5'-AMP, 5'-IMP, 5'-CMP, 5'UMP and 5'-TMP[34,46]. In addition to phosphate binding, base binding is found for all the 5'-pyrimidine nucleotides. The metal ion binds near the carbonyl oxygen at C-2 in 5'-CMP and cytidine and near the carbonyl oxygens at C-2 and C-4 in 5'-UMP, 5'-TMP and uridine. Similar line broadening is observed for the base carbons of 5'-CMP as for cytidine and likewise line broadening observed for 5'-UMP is similar to that for uridine. It has therefore been proposed that interaction of the base appears to be independent of the phosphate group. However, broadening of the nucleotide resonances is faster than that of the nucleosides probably due to the additional effect of binding of the metal ion to the phosphate group in the nucleotides. For 5'-IMP the C-5, C-6 and C-8 resonances are preferentially and nearly equally affected by the presence of $Mn^{2+}$ ions indicating that the metal binds near the C-6 carbonyl oxygen as well as near the N-7 position of the base. It must be noted, however, that the $^{13}C$ studies were carried out in concentrated (0.5 - 0.8 M) solutions where base stacking will be pronounced. It is not possible to separate the intramolecular from the intermolecular broadening and therefore these conclusions shown here are somewhat suspect.

Cu(II) can bind to multiple sites on the adenine base with preference for a given site influenced by the position of the phosphate on the ribose[42]. H-8 is broadened preferentially to H-2 in 5'-AMP and

in the cyclic nucleotides, 3',5' cyclic AMP (cAMP) and 2',3' cyclic AMP H-8 and H-2 are broadened equally.

Various workers[36,47] have used shift techniques in order to find the sites of metal binding and additional conformational information about the ligand. They employed the pseudo-contact shift equation[1,24] derived by LaMar et al[37]. Lavallee et al[47] used the lanthanides Pr(III) and Ho(III) in their investigations of cAMP. They found that the ribose and phosphate groups retain the structure found in the crystalline state[48], namely with the phosphate in the energetically favourable chair form and the ribose tending towards a $_4T$ (4'-exo) conformation. The base at pD 5,3 is in the syn conformation with the best agreement at $\phi_{CN} = 86^{\circ}$. This is in disagreement with the results of Barry et al[36] who find that the shift data at pD 5,5 does not give a conclusive result as to which orientation predominates. A mixture of the syn and anti orientations has not been proposed although this would fit the data better. However, at pD 2,0 the shift results show a good fit to the anti conformation with $\phi_{CN} = -34^{\circ}$. $T_1$ and $T_2$ measurements from relaxations with Gd(III) gave similar results at both pD's. The distances found for H-8 and H-2 do not fit either syn or anti calculated distances. The ribose proton distances fit reasonably well for a $^3T$ (3'-endo) conformation. This also disagrees with the former work but it must be noted that the difference in ribose conformations is one of degree rather than of kind.

The shift results do not give a clear indication of the syn/anti ratios and it would seem that relaxation data is more reliable as a means of determining these values.

It is obvious from the survey above that very little quantitative work has been accomplished in this field, either on the sites of metal binding on the ligand, or on the conformations of the ligands themselves. The present work, which attempts to cover these fields, should therefore assist in clearing up many uncertainties.

## 1.6 Objectives of Research

The biological importance of thiamine has been outlined in the previous sections. The present study was undertaken in order to investigate the metal-ion binding sites on model thiamine analogues with the hope that more understanding of some of the thiamine-metal ion interactions would result.

Complexes of thiazoles with a 2-hydroxyethyl side chain were prepared to investigate whether chelate structures through sulphur and oxygen could occur in preference to nitrogen coordination. In addition thiazolium salts were prepared and reacted with metal ions to test the possibility of complex salt formation in preference to direct coordination of the biological ligand.

The importance of studying nucleotide systems is also apparent from the previous sections. Interactions of metal-ions with cyclic nucleotides were undertaken not only to determine the most preferred metal binding sites on the ligands, but perhaps more importantly, to determine quantitatively the conformations of the complexes in solution. This involved the reactions of the cyclic nucleotides with

(i) Gd(III) in order to find syn/anti ratios of the complexes;

(ii) Dy(III) and Ho(III) to find conformational information;

and (iii) Mn(II) to find the preferred binding sites on the ligands.

# C H A P T E R  2.

## STUDIES ON THE SOLID COMPLEXES OF VITAMIN $B_1$ AND SOME RELATED THIAZOLES

## 2.1 Results and Discussion.

The formation of the complex salt $[CoCl_4]$(thiam H) has been suggested[49] when $CoCl_2$ reacts with thiamine chloride hydrochloride. Marzotto et al[50] suggested that with Cu(II) there is direct coordination of a pyrimidine N to the metal. However, a crystal structure has since been reported[24] showing that the complex salt $[CuCl_4]$(thiam H) forms with no direct interaction of the thiamine with the metal. I.R. and electronic spectral data of these complex salts have been reported for useful comparison with the new complexes.

The I.R. spectra (Table 3) suggest that the ligand (thiaz) is monodentate, coordinated through N. Monodentate coordination through S does not seem likely, but cannot be ruled out. The I.R. data for $\nu$(M-ligand) agrees well with data for $\nu$(M-N) in similar thiazole and pyridine complexes[51,52] though values for $\nu$(M-S) in pyridine-thiol complexes[53] are also similar. It also seems unlikely to be bidentate through the S of the thiazole ring and the O of the ethanolic group since the C-O stretching frequency of the hydroxyl group remains virtually unchanged at ~1055 $cm^{-1}$ on complexation. Recently crystal structures of $Co(thiaz)_2Br_2$ (Fig.2.9) and $[CuBr_3thiaz]$(thiaz H) (Fig. 2.1) were determined[54,55] and in both cases coordination of the thiazole ligand to the metal was through N. There seems to be little evidence to support coordination through an alternative site on the thiazole in any of the other complexes prepared here.

The magnetic moments of all the Cu(II) complexes fall in

the range 1,7 - 1,9 B.M. eliminating the possibility of strong Cu - Cu interactions but otherwise giving no indication of the stereochemistry involved.

Table 1. Analytical data and room temperature magnetic moments of the complexes

| Compound | Colour | C% Calc. | C% Found | H% Calc. | H% Found | N% Calc. | N% Found | M% Calc. | M% Found | $\mu_{eff}$ B.M. |
|---|---|---|---|---|---|---|---|---|---|---|
| $[CuCl_4](thiaz\ H)_2$ | Yellow | 29,2 | 29,2 | 4,1 | 4,0 | 5,7 | 5,6 | 12,9 | 13,3 | 1,80 |
| $[CuBr_3\ thiaz](thiaz\ H)$ | Dark red | 24,4 | 24,5 | 3,2 | 3,2 | 4,7 | 4,7 | 10,8 | 10,6 | 1,89 |
| $[CoCl_4](thiaz\ H)_2$ | Blue | 29,5 | 29,7 | 4,1 | 4,1 | 5,7 | 5,8 | | | 4,48 |
| $[CoBr_4](thiaz\ H)_2$ | Blue | 21,6 | 21,8 | 3,0 | 3,1 | 4,2 | 4,4 | | | 3,02 |
| $[CoBr_4](thiaz\ Me)_2$ | Pale blue | 24,2 | 24,3 | 3,5 | 3,4 | 4,0 | 4,2 | | | 4,96 |
| $Cu(thiaz)_2Cl_2$ | Green | 34,2 | 33,9 | 4,3 | 4,3 | 6,6 | 6,6 | 15,1 | 15,5 | 1,72 |
| $Cu(thiaz)_2Br_2$ | Green | 28,3 | 28,8 | 3,5 | 3,7 | 5,5 | 5,1 | 12,5 | 12,7 | 1,76 |
| $Cu(thiaz)Cl_2$ | Brown | 26,0 | 26,3 | 3,3 | 3,4 | 5,0 | 5,0 | | | 1,71 |
| $Cu(thiaz)Br_2$ | Brown | 19,7 | 19,9 | 2,5 | 2,7 | 3,8 | 3,9 | | | 1,85 |
| $Co(thiaz)_2Cl_2$ | Blue | 34,6 | 34,9 | 4,4 | 4,5 | 6,7 | 6,7 | | | 4,28 |
| $Co(thiaz)_2Br_2$ | Blue | 28,5 | 28,7 | 3,6 | 3,7 | 5,5 | 5,6 | | | 4,75 |
| $Co(thiaz)_2I_2$ | Green/ Blue | 24,0 | 24,2 | 3,0 | 3,0 | 4,7 | 4,6 | | | 4,67 |

Table 2. Reflectance Spectra and Electronic Spectra in Nitromethane, of the complexes.

| Compound | State[a] | Absorption max., kK ($\varepsilon_{molar}$ for solution) |
|---|---|---|
| $[CuCl_4]$(thiam H) | R | 24,7 sh.s; 11,0 br.m; 7,6 br.m; 6,1 br.w. |
| $[CuCl_4]$(thiaz H)$_2$ | R | 24,1 sh.s; 10,8 br.s; 7,6 br.m; 6,1 br.m. |
| | N | 11,5 br.s (200) |
| $[CuBr_3$ thiaz](thiaz H) | R | 17,6 sh.m; 16,4 sh.m; 10,1 br.s; 6,1 br.m. |
| | N | 16,0 s (740); 11,2 br.w. |
| $[CoCl_4]$(thiam H) | R | 22,3 w; 19,0 w; 15,1 s; 6,3 br.m; 5,6 br.m. |
| $[CoCl_4]$(thiaz H)$_2$ | R | 22,2 w; 18,9 m; 15,4 s; 7,5 br.m; 6,0 br.m. |
| | N | 17,1 m (310); 15,3 s (470); 5,7 br.w. |
| $[CoBr_4]$(thiaz H)$_2$ | R | 23,0 w; 21,5 w; 15,1 s; 14,3 s; 7,5 br.w; 5,6 br.m. |
| | N | 16,3 m (170); 15,1 sh.s; 14,7 s (310); 7,0 br.w. |
| $[CoBr_4]$(thiaz Me)$_2$ | R | 22,2 w; 18,9 w; 15,8 s; 14,8 s; 6,0 br.m. |
| | N | 16,4 w (280); 15,3 m (620); 14,6 s (760); 7,0 br.w. |
| Cu(thiaz)$_2$Cl$_2$ | R | 29,o sh.s; 14,0 s; 6,1 br.w. |
| | N | 21,8 sh.w (20); 12,6 s (230); 5,3 br.w. |
| Cu(thiaz)$_2$Br$_2$ | R | 24,7 sh.s; 14,6 s; 6,0 br.w. |
| | N | 15,7 m (190); 12,6 s (230); 5,3 br.w. |
| Cu(thiaz)Cl$_2$ | R | 23,6 s; 11,9 br.s; 6,1 br.w. |
| | N | 12,3 s (290); 5,5 br.w. |
| Cu(thiaz)Br$_2$ | R | 24,6 sh.m; 12,5 s; 6,1 br.w. |
| | N | 13,1 s (480); 6,1 br.w. |
| Co(thiaz)$_2$Cl$_2$ | R | 24,1 w; 21,1 w; 19,7 m; 16,8 s; 9,2 br.m; 7,5 br.m; 6,0 br.w. |
| | N | 17,5 sh.m (340); 16,5 s (530); 6,3 br.w. |

Table 2 Continued.

| Compound | State[a] | Absorption max., kK ($\varepsilon_{molar}$ for solution) |
|---|---|---|
| $Co(thiaz)_2Br_2$ | R | 23,6 w; 16,2 s; 15,1 s; 8,8 br.m; 7,3 br.m; 6,0 br.m; 4,5 br.w. |
| | N | 15,7 s (1030); 6,7 br.w. |
| $Co(thiaz)_2I_2$ | R | 25,0 m; 21,6 w; 19,7 w; 15,7 s; 8,7 br.m; 6,0 br.w; 4,5 br.w. |
| | N | 21,5 w; 14,5 s (730); 5,4 br.w. |

[a] R = Diffuse Reflectance ; N = Nitromethane

s = strong, m = medium, w = weak, sh = shoulder, br = broad.

Table 3. Infra red data for the complexes (200 - 400 $cms^{-1}$)

| Compound | ν (thiazolium salts or thiamine chloride hydrochloride) | ν(M-N) | ν(M-X) |
|---|---|---|---|
| ThiamCl HCl | 220(s), 231(m), 348(w) | | |
| $[CuCl_4]$(thiam H) | 236(m) | | 269(m) 296(s) |
| $[CoCl_4]$(thiam H) | 228(w) | | 302(s) 326(s) |
| Thiaz HCl | 220(m) 236(m) 345(w) | | |
| $[CuCl_4]$(thiaz H)$_2$ | 220(m) 236(s) | | 276(sh) 292(s) |
| $[CoCl_4]$(thiaz H)$_2$ | 225(w) 258(m) | | 290(sh) 304(s) 315(s) |
| Thiaz HBr | 217(s) 267(w) 342(m) 364(w) | | |
| $[CuBr_3$ thiaz](thiaz H) | 345(s) 387(w) | 285(w) | 238(s) |
| $[CoBr_4]$(thiaz H)$_2$ | 217(s) 341(m) | | 236(s) 245(sh) |
| Thiaz MeBr | 240(w) 272(s) 330(s) | | |
| $[CoBr_4]$(thiaz Me)$_2$ | 262(m) 293 (w) | | 230(s) 241(s) |
| Cu(thiaz)$_2$Cl$_2$ | | 264(s) | 338(m) |
| Cu(thiaz)$_2$Br$_2$ | | 266(s) | 221(s) |
| Cu(thiaz)Cl$_2$ | | 245(s) | 340(w) |
| Cu(thiaz)Br$_2$ | | 251(m) | |
| Co(thiaz)$_2$Cl$_2$ | | 253(m) | 303(s) 329(s) |
| Co(thiaz)$_2$Br$_2$ | | 245(s) | 266(s) |
| Co(thiaz)$_2$I$_2$ | | 254(m) | 233(s) |

s = strong, m = medium, w = weak, sh = shoulder.

2.1.1 Complex Salts of Cu(II).

The thiazolium salts were found to react in a similar manner to thiamine chloride hydrochloride giving complex salts where the thiazole is not coordinated to the metal. The yellow complex $[CuCl_4](thiaz\ H)_2$ has a reflectance spectrum very similar to that of $[CuCl_4](thiam\ H)$, with broad bands in the 7-11 kK region arising from the tetrahedral $[CuCl_4]^{2-}$ anion and a shoulder at 24,1 kK (Table 2, Fig. 2.2), probably a charge transfer band[56]. It gives a yellow solution in nitromethane with a spectrum that differs a little from the reflectance spectrum of the solid, suggesting that the molecule does not maintain the same configuration in this solution. Most of the I.R. bands (Table 3) found in the spectrum of thiaz HCl are observed in the spectrum of the complex; however, additional strong bands occur at 276 and 292 $cm^{-1}$ which are found only in the complex spectrum and are assigned to $\nu$(Cu - Cl) vibrations in fair agreement with values previously reported for the $[CuCl_4]^{2-}$ anion[57].

The complex formed from $CuBr_2$ and thiaz HBr has the empirical formula ($CuBr_3$thiaz thiaz H). The reflectance spectrum is alike in general shape and band positions to the tetrahedral tetrahalo Cu(II) complex salts (Table 2, and Fig. 2.2) but has additional shoulder bands in the 17 - 19 kK range. This corresponds to a distorted tetrahedral anion $[CuBr_3thiaz]^-$ with an uncoordinated thiazolium cation $(thiaz\ H)^+$. The crystal structure has been determined[55] (Fig. 2.1) confirming this. The I.R. spectrum (Table 3) gives a very strong band at 238 $cm^{-1}$ and a band at 285 $cm^{-1}$ which are tentatively assigned to $\nu$(Cu - Br) and $\nu$(Cu - N) vibrations respectively. There is evidently considerable

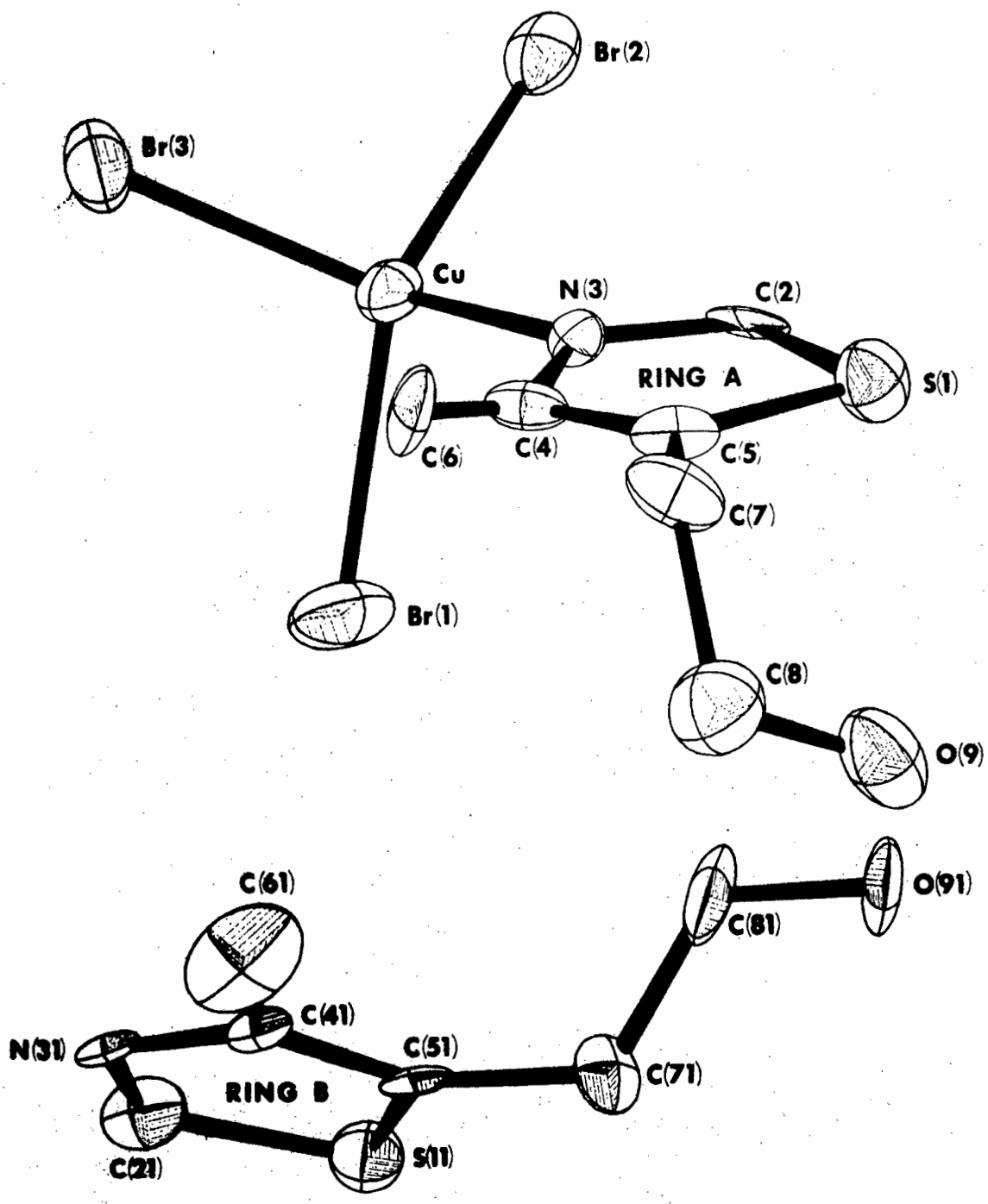


Fig. 2.1 $[CuBr_3thiaz]$ (thiaz H)

loss of the solid complex structure upon dissolution in nitromethane since the dark red solid gives a green solution, the spectrum of which has a strong peak at 16,0 kK.

Fig. 2.2 Reflectance Spectra of (A) $[CuCl_4](thiaz\ H)_2$, (B) $[CuCl_4](thiam\ H)$ and (C) $[CuBr_3\ thiaz](thiaz\ H)$.

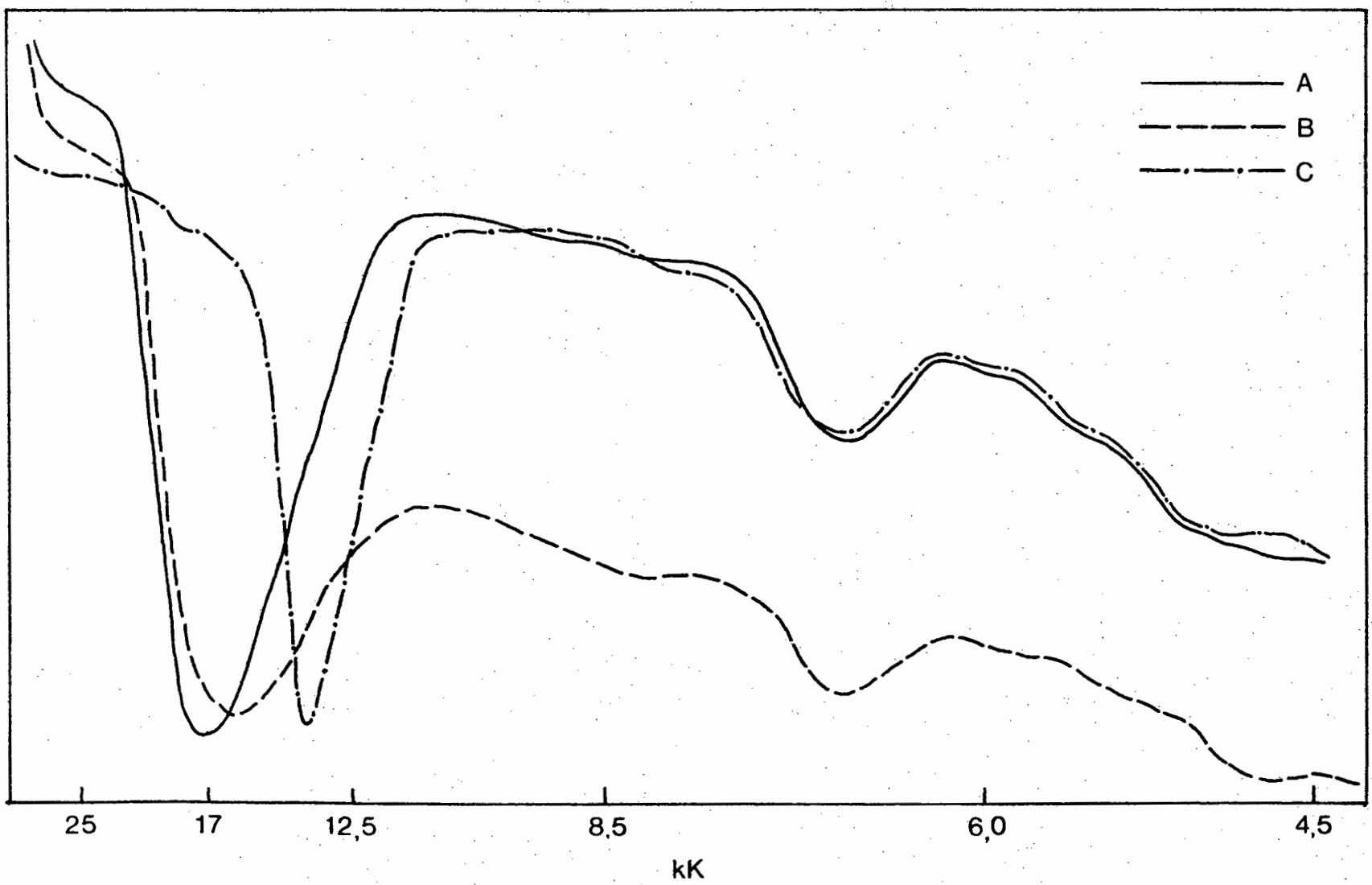

2.1.2 Complex Salts of Co(II).

Talbert et al[49] suggest that $[CoCl_4]$(thiam H) is a complex salt with a tetrahedrally coordinated tetrachloro anion. Similarly, it is suggested that cobalt forms the blue complex salts $[CoX_4]$(thiaz R)$_2$ (X = Cl, R = H; X = Br, R = Me) the halogens being tetrahedrally coordinated. $[CoCl_4]$(thiaz H)$_2$ has a magnetic moment of 4,48 B.M. which is well within the range for tetrahedral Co(II) whilst $\mu_{eff}$ for $[CoBr_4]$(thiaz Me)$_2$ is 4,96 B.M. which is high and falls in the range reported for an octahedral stereochemistry[58]. However, its reflectance spectrum (Table 2, Fig. 2.3) is typical of the tetrahedral $[CoBr_4]^{2-}$ anion[59]. Its spectrum in nitromethane is very similar to the reflectance spectrum suggesting the molecule retains its configuration in this solution; the extinction coefficient of 760 being too high for an octahedral structure but suitable for a tetrahedral structure. So even though its magnetic moment is high (bromo complexes do generally have higher magnetic moments than chloro complexes[59]), its stereochemistry seems to be tetrahedral, probably distorted to some extent. $[CoCl_4]$(thiam H) and $[CoCl_4]$(thiaz H)$_2$ have extremely similar reflectance spectra (Figs. 2.3, 2.4) in good accordance with reported tetrahedral tetrachloro cobalt complexes[59].

$[CoBr_4]$(thiaz H)$_2$ is proposed to have a distorted tetrahedral stereochemistry. Its magnetic moment is 3,02 B.M. which is well below the region recorded for tetrahedral Co(II)[60] and almost that expected for square planar Co(II)[60]. However, its reflectance spectrum (Table 2, Fig. 2.4) is typical of the tetrahedral $[CoBr_4]^{2-}$ anion[59] and unlike that reported for a Co(II) square planar complex[61] which lacked bands in the 14 - 16 kK region.

The far I.R. spectra of these three Co(II) complex salts show most of the bands visible in the thiazolium salts spectra plus additional $\nu$(Co - X) (X = Cl,Br) bands, (Table 3) in excellent agreement with values quoted for tetrahedral tetrahalo Co(II)[57].

Fig. 2.3 Reflectance Spectra of (A) $[CoCl_4]$(thiam) and (B) $[CoBr_4]$(thiaz Me)$_2$.

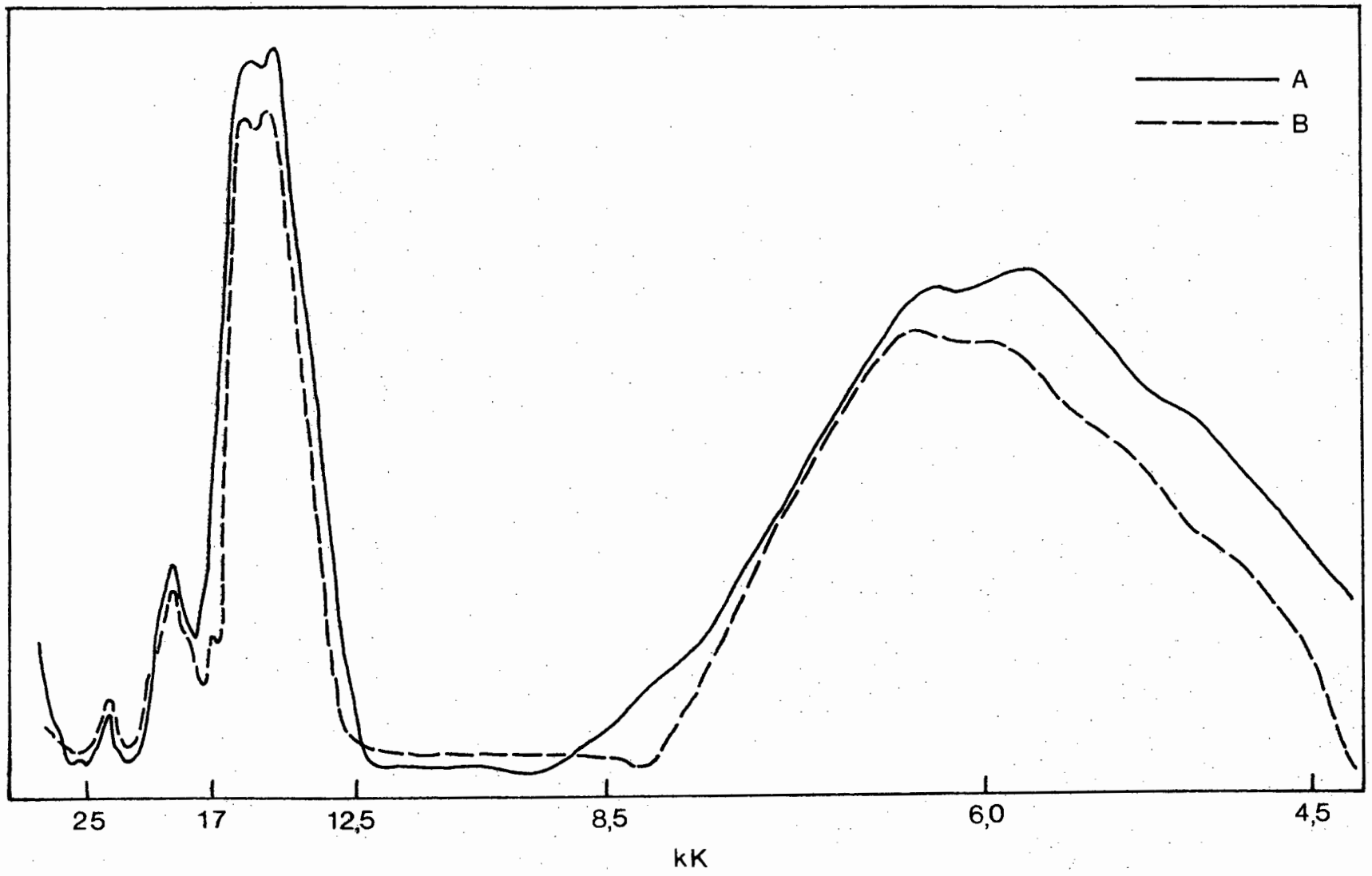

Fig. 2.4 Reflectance Spectra of (A) $[CoCl_4](thiaz\ H)_2$ and (B) $[CoBr_4](thiaz\ H)_2$

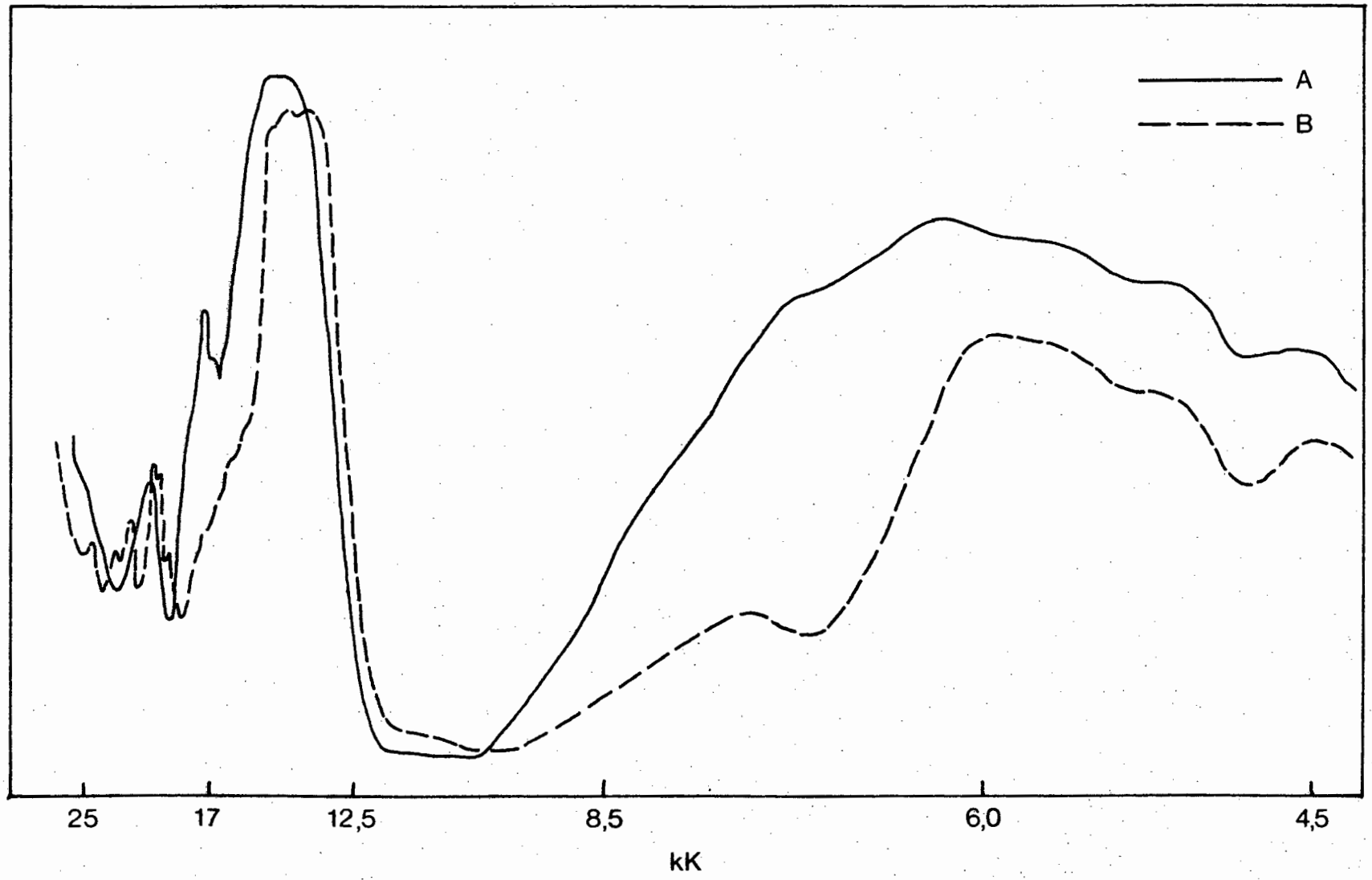

2.1.3 Cu(II) Complexes

The reflectance spectra (Table 2, Figs. 2.6, 2.7) of the green $Cu(thiaz)_2X_2$ (X = Cl, Br) complexes both have strong absorption bands in the 12 - 15 kK range. Two limiting structures are possible, namely, a six coordinate complex where the copper atom is in a tetragonally distorted pseudo-octahedral environment, the halogens of one molecule axially interacting with an adjacent copper atom, and a square planar complex with no axial interaction. As the tetragonal distortion increases from a regular octahedron to the limiting square planar structure so the energy of the absorption band on the electronic spectrum increases from 12 to 22 kK[51,52,62-64]. Both complexes $Cu(thiaz)_2X_2$ (X = Cl, Br) have reflectance spectra characteristic of six coordinate polymeric halogen bridged structures, $Cu(thiaz)_2Br_2$ being slightly more axially distorted with absorption bands at higher energy values. Neither complex can be considered to have a dimeric square pyramidal structure since this is effectively removing one axial bond completely, thus increasing the tetragonal distortion and absorption values of 16 - 19 kK would be expected[52,65].

The electronic and I.R. spectra of these complexes show a strong resemblance to the spectra of $CuX_2$ $(pyridine)_2$ (X = Cl, Br)[52]. The crystal structure of $CuCl_2$ $(pyridine)_2$[66] shows it to be a tetragonally distorted octahedron with four short planar bonds (two Cu-N and two Cu-Cl). These Cu-Cl bonds are effectively terminal Cu-Cl bonds with respect to I.R. stretching frequencies. The remaining bonds are two longer Cu-Cl bonds (Cu's and Cl's from adjacent molecules) at right angles to the plane. The I.R. spectra of $Cu(thiaz)_2Cl_2$ and $Cu(thiaz)_2Br_2$ show strong bands at 264 and 266 $cm^{-1}$ respectively,

which are attributable to ν(Cu-N) vibrations (Fig. 2.5). Bands at 338 and 221 $cm^{-1}$ have been assigned to terminal ν(Cu-Cl) and ν(Cu-Br) modes respectively (Fig. 2.5). Bridging metal to halogen bands which occur at lower wave numbers were not observed probably due to weak axial interactions between the copper and the halogen. The ratio ν(Cu-Br)/ν(Cu-Cl) = 0,65 is consistent with other chloro and bromo species of this type[67].

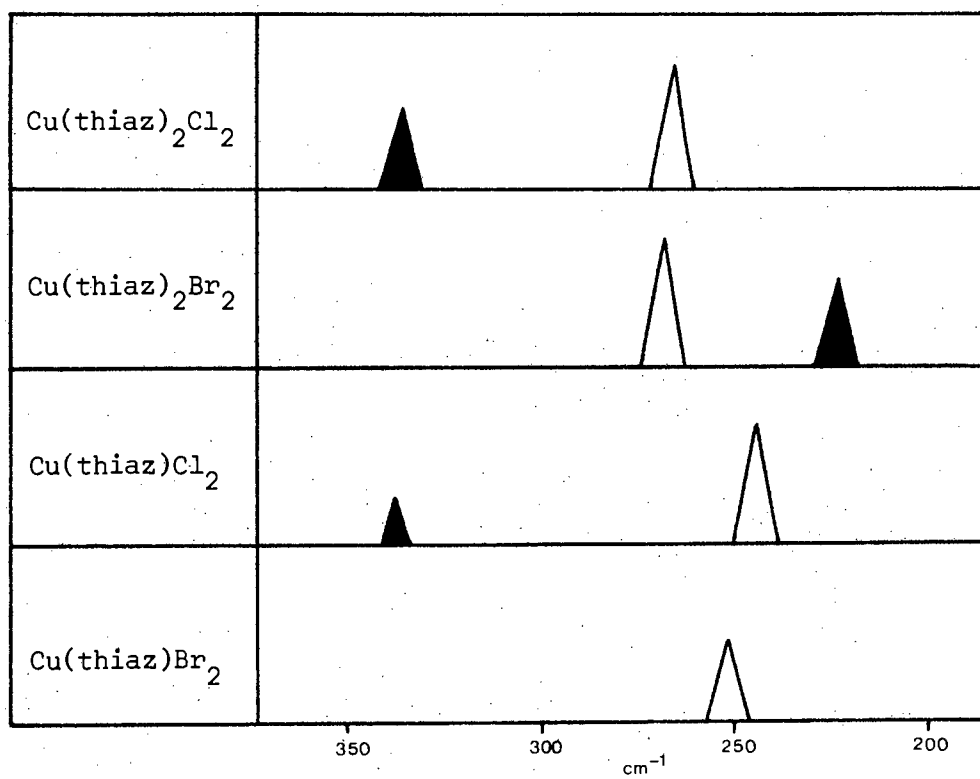


Fig. 2.5 The I.R. spectra of the Cu(II) complexes showing bands due to ν(M-X) vibrations (shaded peaks) and ν(M-N) vibrations (unshaded peaks)

Dimeric square planar structures have been postulated for the brown complexes $Cu(thiaz)X_2$ (X = Cl, Br). Their reflectance spectra are characteristic of this structure[63,68,69] with bands in the 20kK region in accordance with maximum tetragonal distortion (Figs. 2.6, 2.7). The I.R. spectra show strong bands at 245 and 251 $cm^{-1}$ (Fig. 2.5) which

are attributable to $\nu$(Cu-N) vibrations whilst a band at 340 $cm^{-1}$ is assigned to the (Cu-Cl) terminal mode, no bridging mode being found. The electronic spectra of these Cu(II) complexes in nitromethane are similar to the reflectance spectra inferring no great change in stereochemistry in this solution (Table 2).

Fig. 2.6 Reflectance Spectra of (A) $Cu(thiaz)_2Cl_2$ and (B) $Cu(thiaz)Cl_2$

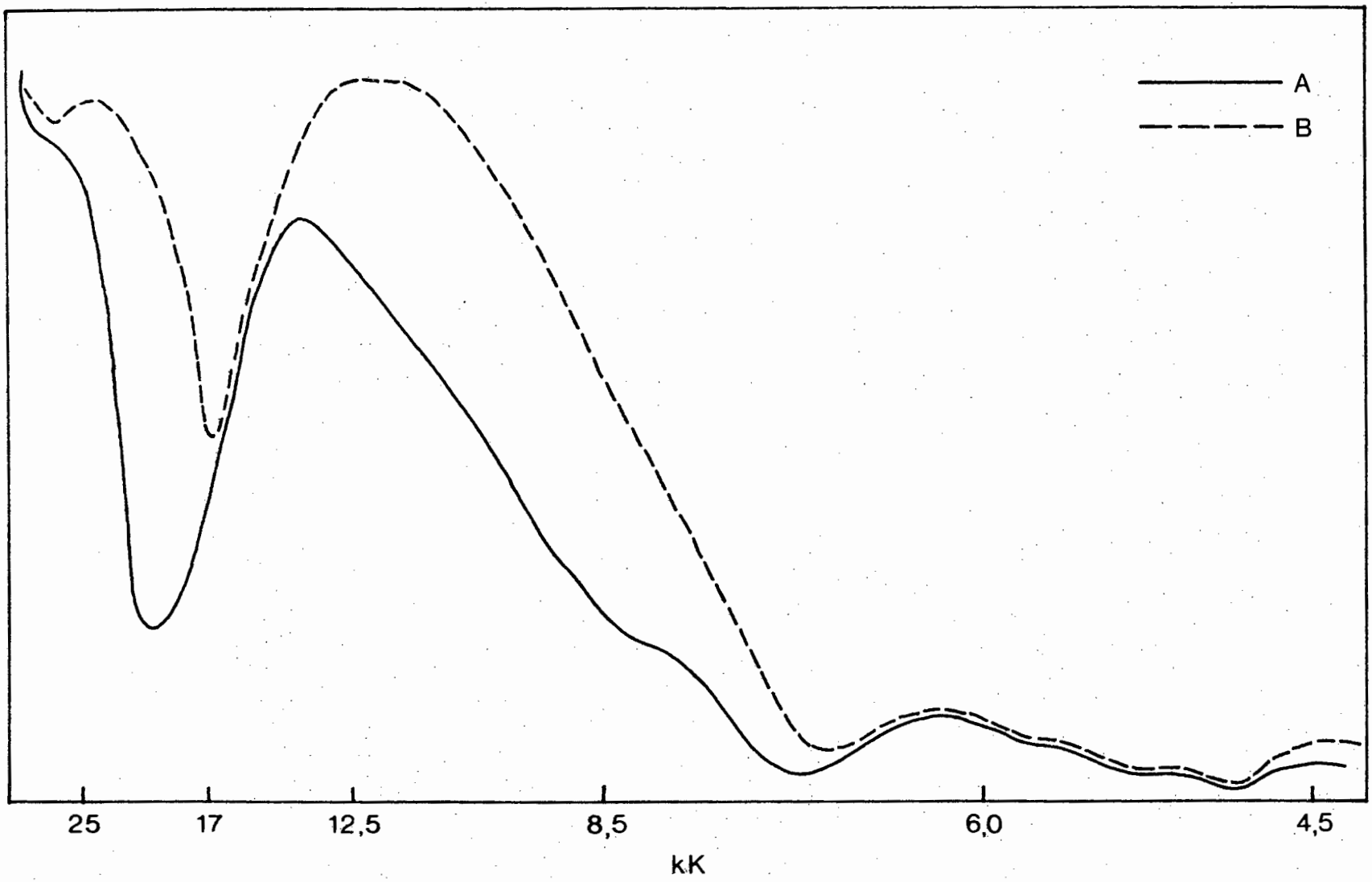

Fig. 2.7 Reflectance Spectra of (A) $Cu(thiaz)_2Br_2$ and (B) $Cu(thiaz)Br_2$.

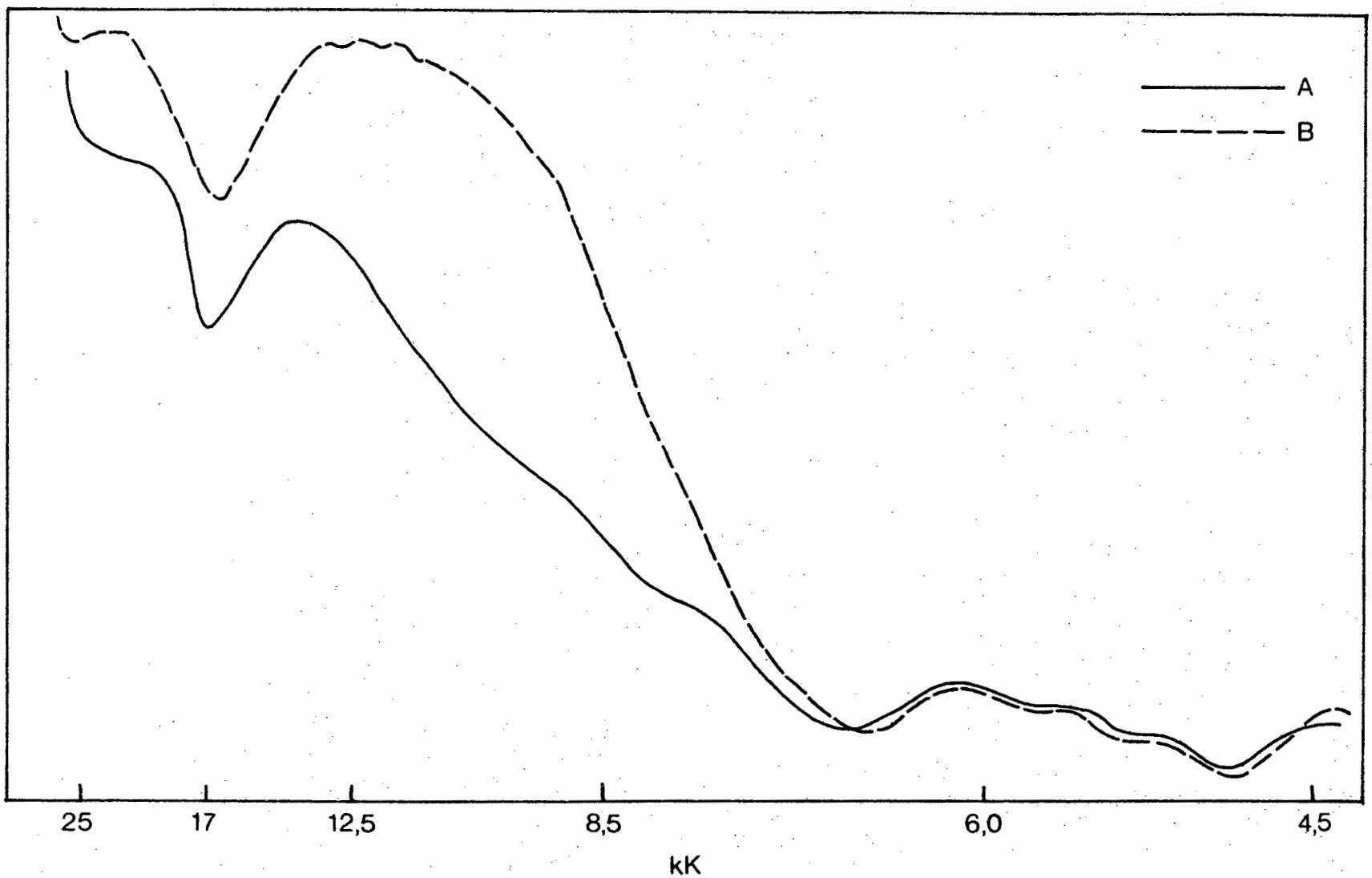

2.1.4 Co(II) Complexes.

The complexes $Co(thiaz)_2X_2$ (X = Cl, Br or I) seem to be straightforward. Their reflectance spectra (Table 2, Fig. 2.10) are typical of Co(II) tetrahedral stereochemistry[51,69,70]. The electronic spectra in nitromethane showed very little change from the reflectance spectrum, implying retention of the tetrahedral stereochemistry in this solution. The complexes $Co(thiaz)_2X_2$ (X = Br, I) have magnetic moments which fall well within the 4,4 - 4,8 B.M. range for tetrahedral Co(II) but $Co(thiaz)_2Cl_2$ has $\mu_{eff}$ = 4,28 B.M. which is low and could be due to distortion of the tetrahedron. The far I.R. spectra were similar to those of tetrahedral Co(II) complexes of 4-methyl thiazole[61], ν(Co-N) vibrations remaining fairly consistent in the region of 250 $cm^{-1}$ (Table 3, Fig. 2.8).

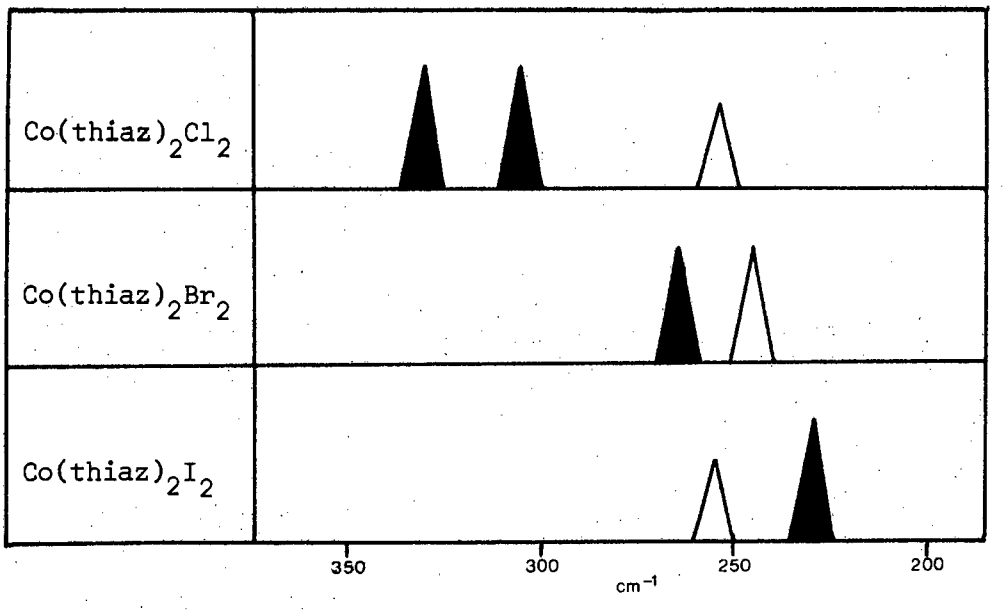


Fig. 2.8 The I.R. spectra of the Co(II) complexes showing bands due to ν(M-X) vibrations (shaded peaks) and ν(M-N) vibrations (unshaded peaks)

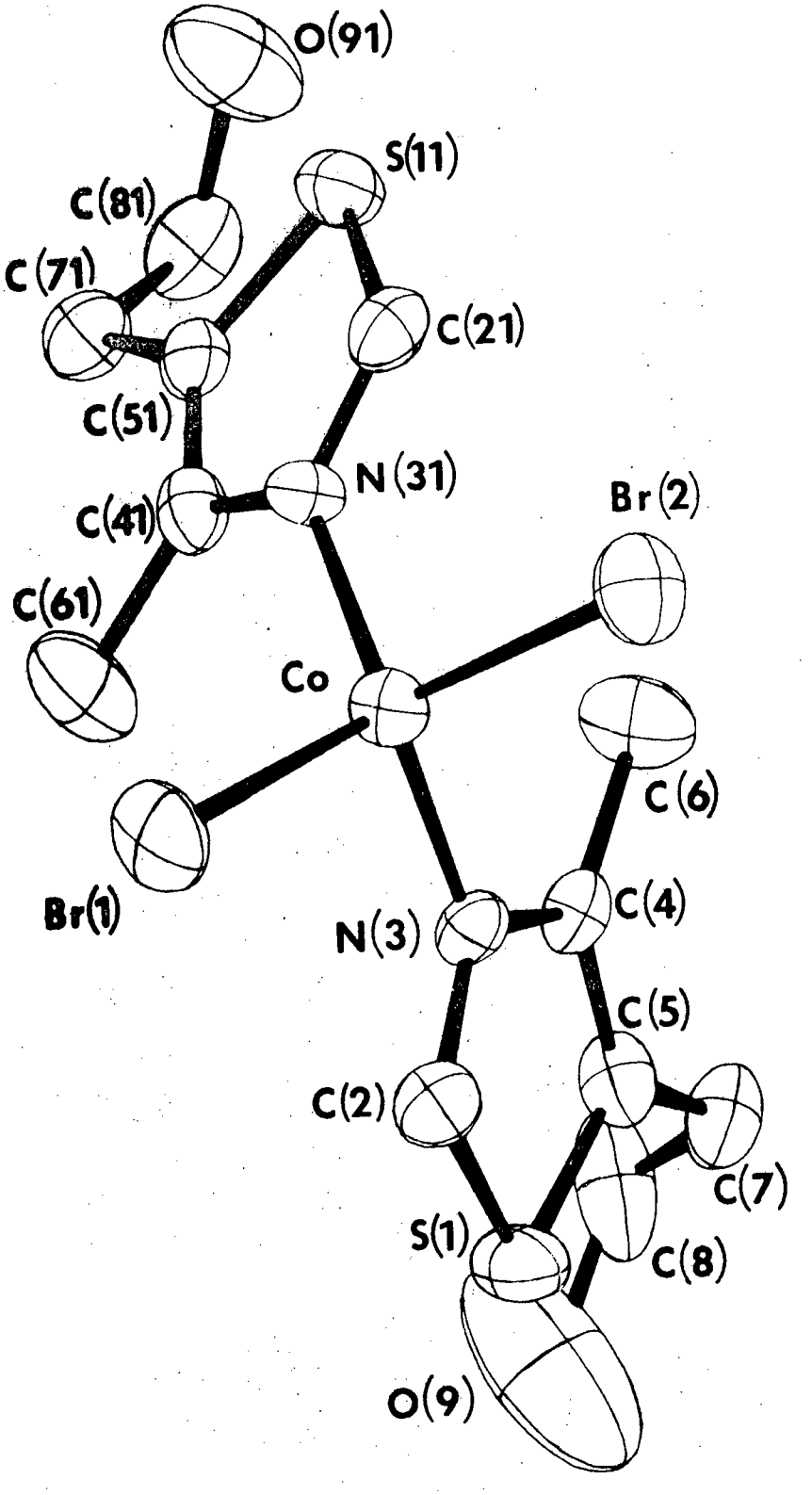


Fig. 2.9 $\underline{Co(thiaz)_2Br_2}$

Fig. 2.10 Reflectance Spectra of (A) $Co(thiaz)_2I_2$, (B) $Co(thiaz)_2Br_2$ and (C) $Co(thiaz)_2Cl_2$.

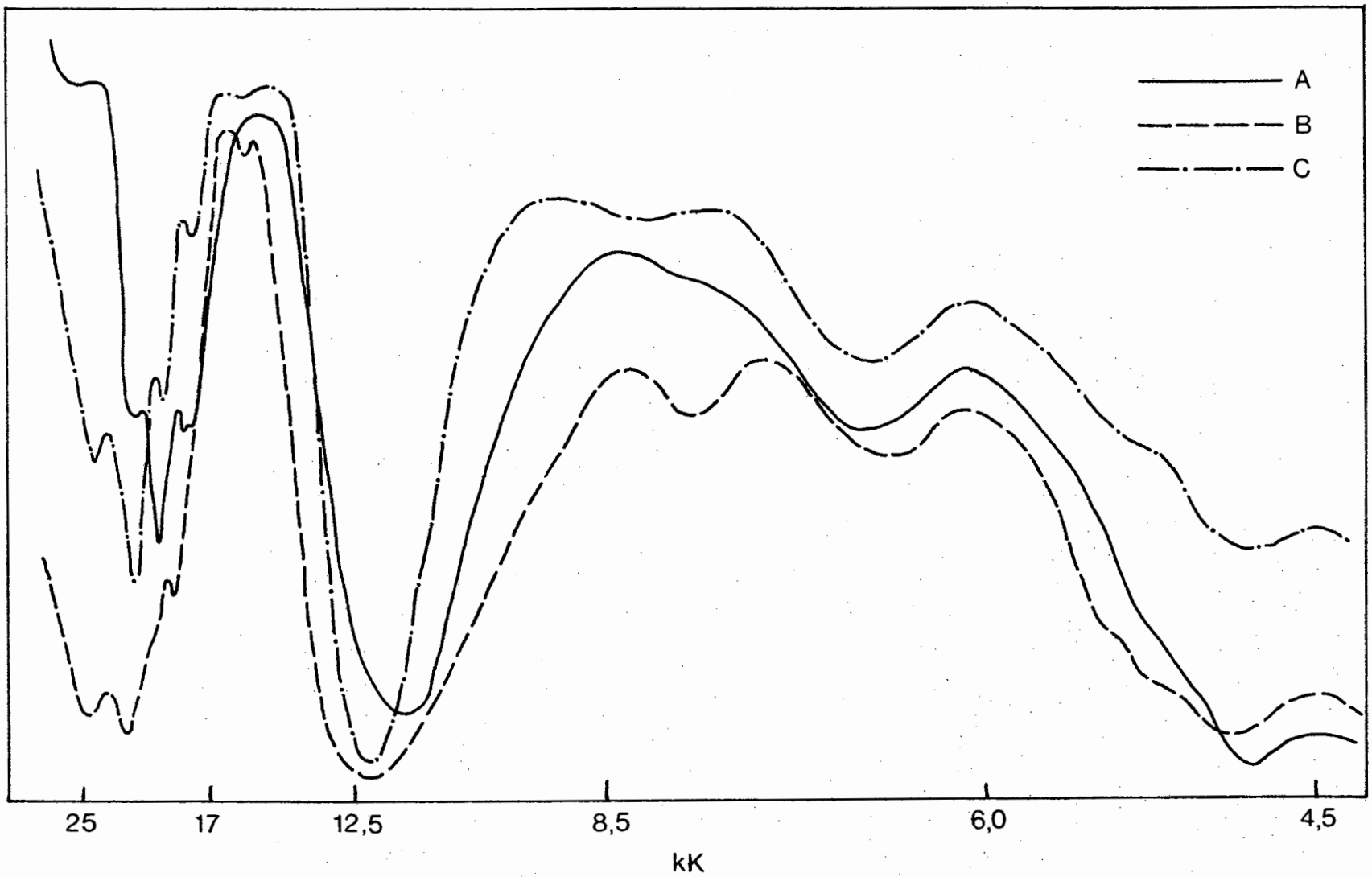

The Co-X bands were assigned giving $\nu$(Co-Br)/$\nu$(Co-Cl) and $\nu$(Co-I)/$\nu$(Co-Cl) ratios of 0,81 and 0,71 respectively in good accordance with those reported by Clark[71].

## 2.2 Experimental.

### 2.2.1 Preparation of ligands.

5-(2-hydroxyethyl)-4-methyl thiazole hydrochloride (= thiaz HCl) was prepared by the bisulphite cleavage of thiamine chloride hydrochloride[8,72]. 1g vitamin was dissolved in excess 2,6 M $NaHSO_3$ and kept at a temperature of 50°C for 1 hour. On cooling the solution, the pyrimidine cleavage product precipitated out and was removed by filtration. The mother liquor was brought up to pH 10 with NaOH and extracted several times with chloroform. The chloroform extracts were extracted with dilute HCl, the acid aqueous extract evaporated in vacuo and the residue was extracted with absolute alcohol.

5-(2-hydroxyethyl)-4-methyl thiazole hydrobromide (= thiaz HBr) was prepared by brominating a solution of thiaz HCl. 0,5 g KOH was added to a solution of 1,6 g of thiaz HCl in MeOH. The volume was reduced and the precipitated KCl was removed by filtration. 1,4 g HBr (excess) was added, the volume further reduced under vacuum and a little EtOH added. A white precipitate of thiaz HBr came out of the solution.

5-(2-hydroxyethyl)-4-methyl thiazole methylbromide (= thiaz MeBr) was prepared by the above procedure using MeBr in place of HBr. After filtration of the KCl the solution was cooled to -5°K to facilitate the addition of an excess of MeBr. The solution was refluxed for several hours before the volume being reduced in vacuo and the thiaz MeBr precipitating out.

5-(2-hydroxyethyl)-4-methyl thiazole (= thiaz) was obtained from Merck and used without further purification.

2.2.2 Preparation of complexes

$Cu(thiaz)_2X_2$ (X = Cl, Br) and $Co(thiaz_2X_2)$ (X = Cl, Br or I). Solutions of the anhydrous metal salt and 5-(2-hydroxyethyl)-4-methyl thiazole in anhydrous methanol were mixed in a 1 : 6 mole ratio and heated. The mixture was evaporated to a small volume and a little 1-propanol added. The crystals formed slowly, were filtered off, washed with 1-propanol and dried in vacuo. In the case of $Cu(thiaz)_2Cl_2$ it was found that brown crystals of $Cu(thiaz)Cl_2$ precipitated in the same solution as the green $Cu(thiaz)_2Cl_2$ crystals. $Cu(thiaz)_2Cl_2$ can be formed exclusively when the proportion of 1-propanol is raised in the mixture of solvents.

$Cu(thiaz)X_2$ (X = Cl, Br). These complexes were prepared as above with the addition of solid KOH in a 1 : 1 mole ratio with 5-(2-hydroxyethyl)-4-methyl thiazole. NaOH may also be used, instead of KOH. Care must be taken to avoid contamination by water which would give hydrated complexes.

$[MX_4]$ (thiaz R)$_2$ (M = Cu, X = Cl, R = H); (M = Co, X = Cl, Br, R = H); (M = Co, X = Br, R = Me) and $[CuBr_3$ thiaz](thiaz H). Solutions of the anhydrous metal salts and thiazolium salts in anhydrous methanol were mixed in a 1 : 6 mole ratio for all complexes except the latter which was mixed in a 1 : 4 mole ratio. The solutions were refluxed for several hours, then evaporated to small volume and

1-propanol added. In the cases of $[CuBr_3thiaz](thiaz\ H)$ and $[CoBr_4](thiaz\ Me)_2$ an oil formed which only crystallized after addition of ether. Solutions of all the remaining complexes precipitated crystals which were filtered, washed with 1-propanol and dried in vacuo. After collecting the yellow flaky crystals of $[CuCl_4](thiaz\ H)_2$ a further precipitation of green $Cu(thiaz)_2Cl_2$ appeared in the same mother liquor.

$[CuCl_4](thiam\ H)$ and $[CoCl_4](thiam\ H)$. These were prepared by procedures of Marzotto et al[50] and Talbert et al[49] respectively by reactions of thiamine chloride hydrochloride with either $CuCl_2$ or $CoCl_2$.

Electronic spectra were measured on a Beckman DK2A spectrophotometer with an attachment for diffuse reflectance spectra. Solution spectra were run in nitromethane. Magnetic moments were measured at room temperature on a Standard Gouy balance which was calibrated with $Hg[Co(SCN)_4]$. I.R. spectra were measured on a Beckman I.R. 12 spectrophotometer using CsI plates and Nujol mulls.

# CHAPTER 3

## NUCLEAR MAGNETIC RESONANCE STUDIES.

## 3.1 Introduction.

The assumptions made in the theory of paramagnetic ion-proton interaction have been tested by previous workers[30] using model compounds of increasing complexity, with Cu(II).

It has been shown that the scalar contribution to $T_2$ is negligible in some cases though it has been reported[31] that this is not always true for Cu(II). There is no evidence of any scalar contribution to $T_2$ measurements in this work using Mn(II) or Gd(III) as the paramagnetic ions.

The first group of ligands investigated were relevant bases and nucleosides. These provide useful information for the study of the pyrimidine cyclic nucleotides and the purine cyclic nucleotides which follow.

## 3.2 Nucleotide nomenclature.

An important parameter in nucleoside and nucleotide conformations is the relative orientation of the essentially planar base ring with respect to the ribose. In the absence of steric hindrance rotation of the base about the glycosidic bond ( (N-9) - (C-1') for a purine base, (N-1) - (C-1') for a pyrimidine base) can occur. If N-3 of a purine, or O-2 of a pyrimidine lie above the plane of the ribose then the conformation is designated "syn"; if N-3 or O-2 point away from the ribose then the conformation is designated "anti". The position of the base is given by the dihedral angle, $\phi_{CN}$, which is defined as the angle between the trace of the plane of the base and the projection of

the (C-1') - (O-1') bond of the ribose ring when viewed along the glycosidic bond[74]. $\phi_{CN}$ is positive if the purine or pyrimidine plane is rotated anticlockwise with respect to the (C-1') - (O-1') bond when viewed with the ribose group in front, provided that the (C-1') - (O-1') bond is coplanar with the base and in the anti conformation when $\phi_{CN} = 0^{\circ}$. Similar rotation clockwise gives a negative $\phi_{CN}$. This is illustrated in Fig. 3.1.

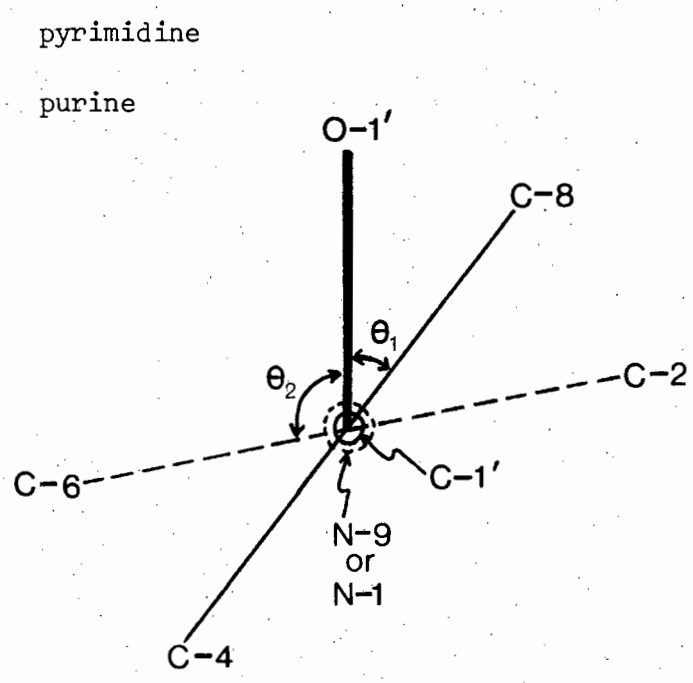


$\phi_{CN} = \theta_1$ (negative)

$\phi_{CN} = \theta_2$ (positive)

Fig. 3.1 The torsion angle, $\phi_{CN}$

When the (C-1') - (O-1') bond is coplanar with the base and the molecule in a syn conformation $\phi_{CN} = \pm 180^{\circ}$, This in general gives negative $\phi_{CN}$ values for anti conformations and positive $\phi_{CN}$ values for syn conformations.

With common nucleotides it is usual to describe the deviations of the atoms of the furanose ring from the least-squares plane

as endo or exo depending on whether they are on the same side or opposite side, respectively, of C-5'. In 3',5' cyclic nucleotides, however, the marked puckering of C-4' brings C-5' into the equatorial plane of the ring. This means that the deviations relative to C-5' are unsuitable and so for this group of compounds the deviations are described relative to the glycosyl nitrogen, N-9 (for purines) or N-1 (for pyrimidines)[75]. That is, endo and exo, mean the deviation is on the same side or opposite side, respectively, of N-9 or N-1. (Fig. 3.2).

The puckering in the cyclic nucleotides ranges from the 3'-endo ($^3T$) form where C-1', C-2', C-4' and O-1' are coplanar to the 4'-exo ($_4T$) form where C-1', C-2', C-3' and O-1' are all coplanar. The symmetrical twist form $^3_4T$ is where C-3' and C-4' are equally deviated from the plane of the other three furanose ring atoms (Fig. 3.2). $^3T_4$ and $_4T^3$ forms are where C-3' and C-4' respectively are predominantly deviated from the plane of C-1', C-2' and O-1'.

Fig. 3.2 The puckering in cyclic nucleotides

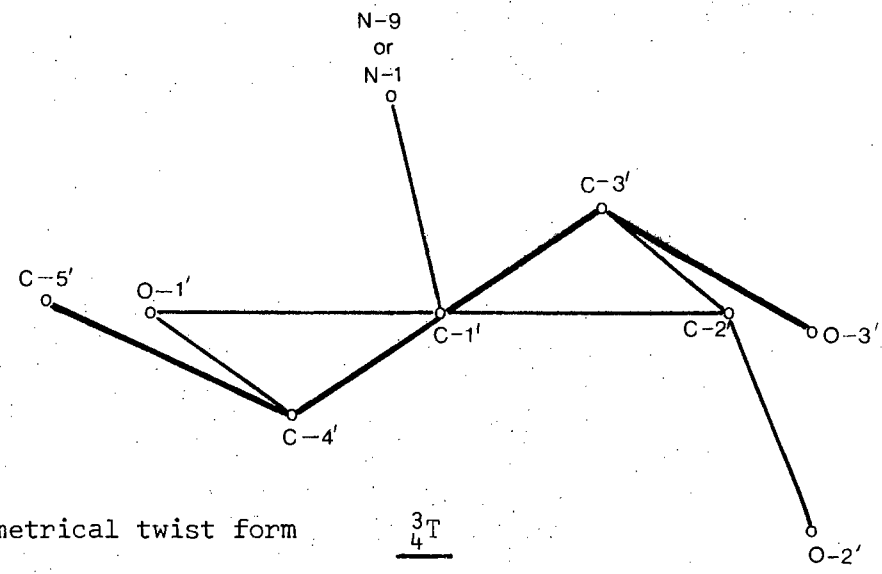


(a) Symmetrical twist form $\underline{{}^{3}_{4}T}$

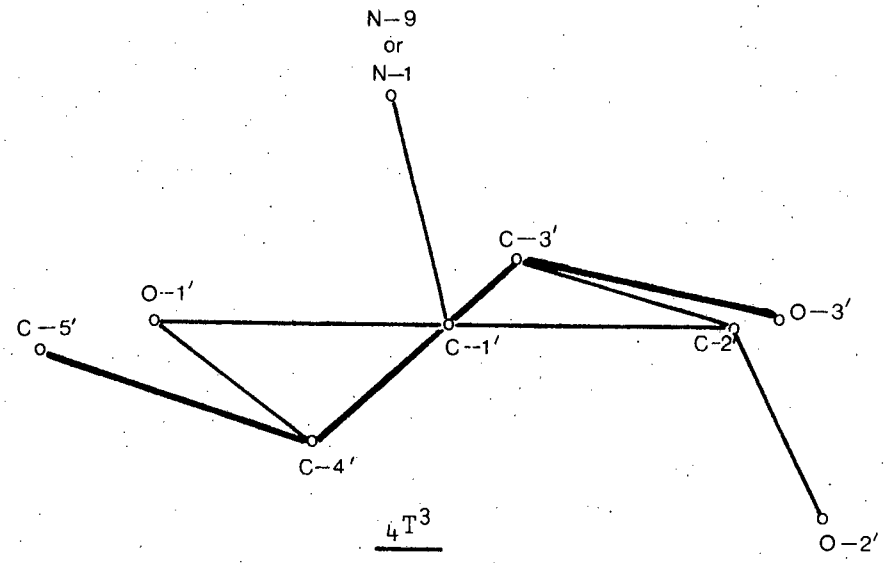


(b) $\underline{{}_{4}T^{3}}$

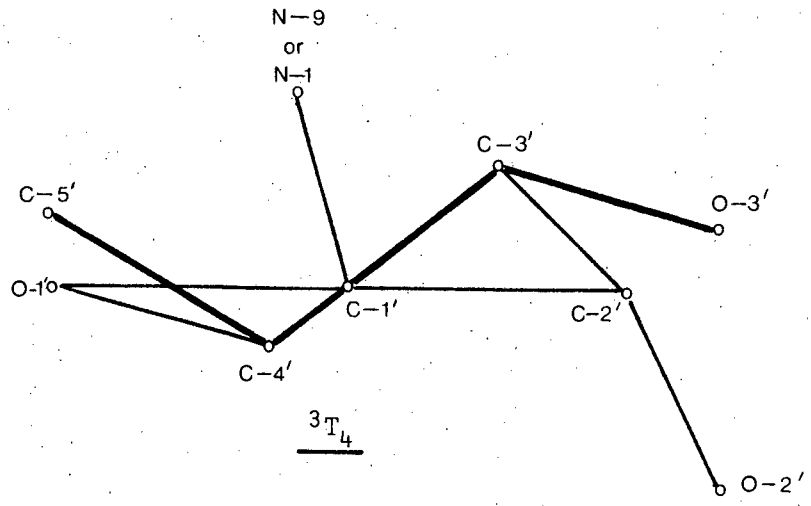


(c) $\underline{{}^{3}T_{4}}$

The phosphate ring of cyclic nucleotides has two conformational possibilities; the chair and the boat forms. All the cyclic nucleotides studied here have been reported to exist in the chair conformation (Fig. 3.3).

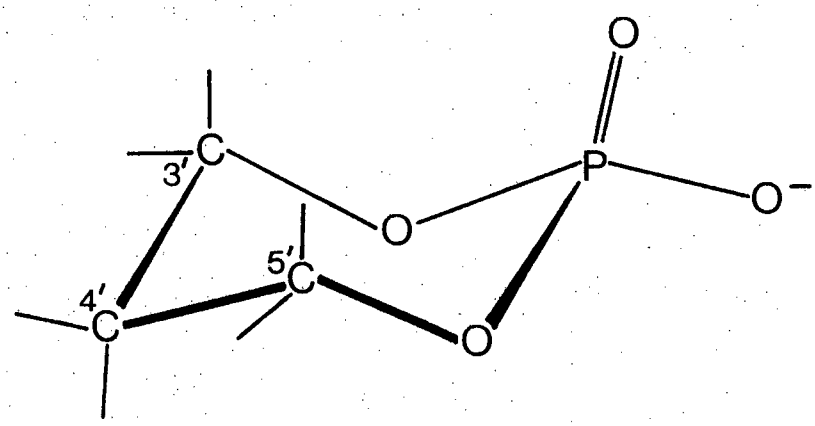


Fig. 3.3 Chair conformation of the phosphate ring

## 3.3 Binding of Mn(II) to some bases and ribosides.

Mn(II) usually binds preferentially to the phosphate group in nucleotides[34,76] but in the absence of phosphates for both bases and nucleosides the metal ion must find alternative binding sites on either the base or the furanose ring. It has been demonstrated that the Mn(II) ions interact with the base in preference to the ribose region of the molecule. Anderson et al[97] report little or no broadening of the H-8, H-2 and H-1' resonances for adenosine and deoxyadenosine in the presence of Mn(II) ions. However, this result differs from results obtained here from the interaction of Mn(II) with adenosine. Qualitative results showed differential broadening of the proton resonances, implying weak but definite binding of the Mn(II) to the nitrogen binding sites.

Broadening experiments were carried out on 1-methyl hypoxanthine, 1-methyl inosine, 9-methyl hypoxanthine and 2',3'-O-isopropylidene inosine. All these ligands have oxygen in the 6-position on the purine ring which is likely to be involved in binding due to Mn(II)'s affinity for binding oxygen. However, it has been reported[77] that in the Mn(II) - $(ATP)_2$ complex the metal simultaneously binds to the phosphate group of one nucleotide and to the N-7 of the second nucleotide for solutions with a very large ratio of ATP molecules to Mn(II) ions. Therefore, N-7 also seems to be a likely contender as a binding site.

Quantitative internuclear distance determinations between the metal ion and a proton are only possible if the condition of fast

chemical exchange is satisfied. Spectra at increasing temperatures show a decrease in line width[30] and a linear relationship between $(fT_{2p})^{-1}$ and $T^{-1}$, confirming rapid chemical exchange.

3.3.1 1-methyl hypoxanthine and 1-methyl inosine with Mn(II).

The spectra of 1-methyl hypoxanthine and 1-methyl inosine are shown in Figs. 3.4(a) and 3.5(a) respectively, together with the proton assignments. H-2 and H-8 are virtually coincident and therefore very difficult to assign. Hydrogen exchange work by Maeda et al[78] has alleviated this problem. They have found that purine derivatives, including natural nucleic acids, undergo hydrogen exchange at their C-8 position. Therefore sample solutions of the ligands in question were heated at 100°C for one hour and then the n.m.r. spectra run. These were compared with the original spectra of these ligands before heating and one peak was found to be considerably reduced in size. This was then assigned to H-8. The size reduction is due to the enhanced hydrogen exchange at C-8 at the raised temperature. All the H-2 and H-8 purine assignments were made using this technique. The spectra after addition of $6{,}3 \times 10^{-4}$M Mn(II) and $7{,}0 \times 10^{-4}$M Mn(II) are shown in Figs. 3.4(b) and 3.5(b) respectively.

Qualitatively it can be seen that the H-8 resonance in both cases is far broader than that of H-2. This means that the Mn(II) on average lies much closer to H-8 than H-2. Since the broadening for both ligands is very similar, it is probable that they bind the Mn(II) at the same site(s); that is either bidentate to O-6 and N-7 or a combination of monodentate binding to O-6 and N-7 separately. This

Fig. 3.4 The effect of Mn(II) on the NMR spectrum of 1-methyl hypoxanthine

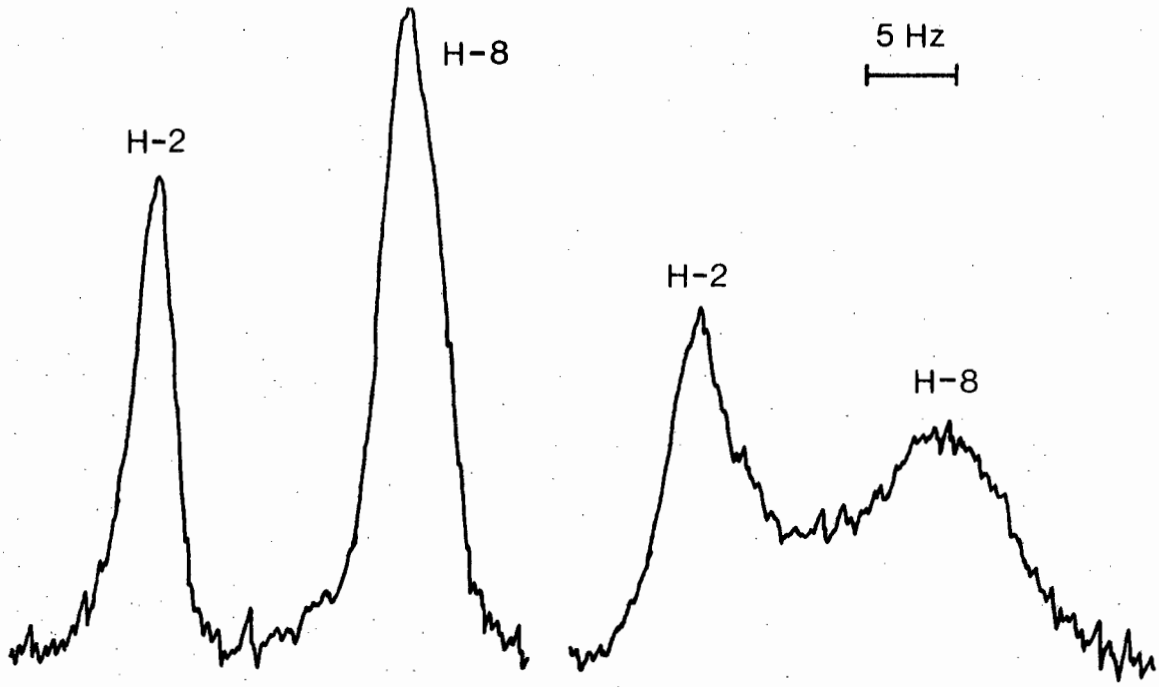


(a) 0,04M ligand
pH 6,6, 23°C

(b) (a) + 6,3 x $10^{-4}$M Mn(II)

Fig. 3.5 The effect of Mn(II) on the NMR spectrum of 1-methyl inosine

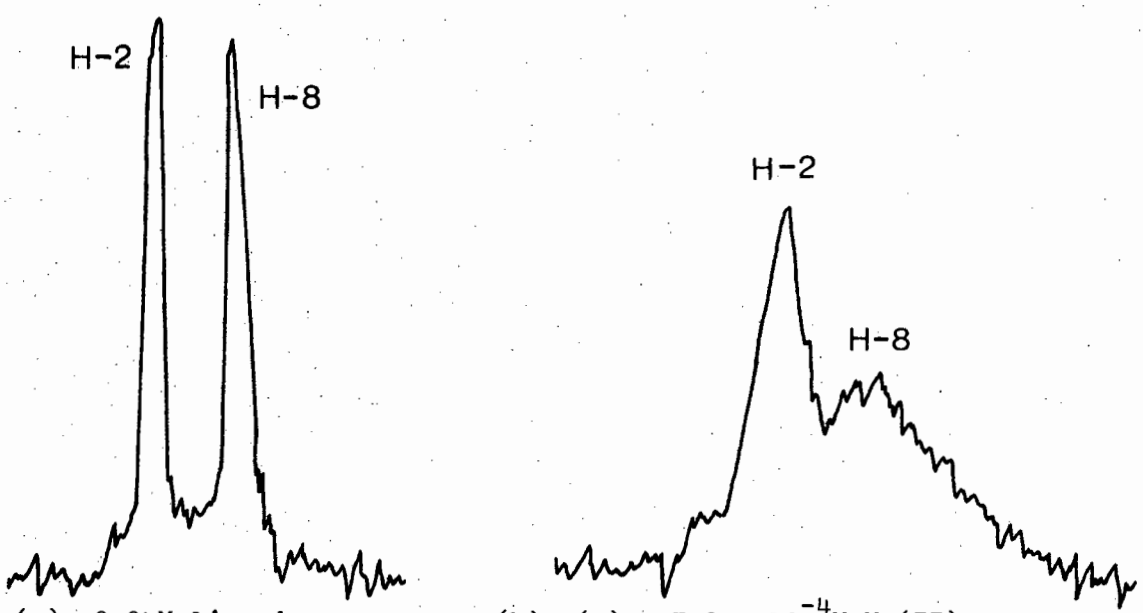


(a) 0,04M ligand
pH 6,3, 23°C

(b) (a) + 7,0 x $10^{-4}$M Mn(II)

(Intensity not to scale)

latter case does not seem as likely as the former but it would be impossible to eliminate this possibility as the time averaged position of the Mn(II) due to these separate monodentate bindings would be extremely close to the bidentate position and so not differentiable.

The results of the broadening observed during the metal titrations are shown in Figs 3.6 and 3.7 in the form of plots of $T_{2p}^{-1}$ vs f. From the relative slopes of these plots the relative metal-proton internuclear distances can be calculated. These are compared to the internuclear distances measured from Drieding models of the complexes in Table 3.1. Binding of Mn(II) to O-6 in the alternative binding site above N-1 is not possible for either of these ligands due to steric hindrance of the methyl group at N-1. N-3 is considered as an unlikely binding site especially for the nucleoside where the ribose ring would hinder any binding at that site. Therefore in Table 3.1 the measured distances from Mn(II) to the protons are those where Mn(II) is bound to N-7 and O-6.

TABLE 3.1

Comparison of measured and experimentally determined proton-metal distances for 1-methyl hypoxanthine - Mn(II) and 1-methyl inosine - Mn(II)

| Complex | Proton | Measured (Å) | Experimental (Å) |
|---|---|---|---|
| 1-methyl hypoxanthine | H-8 | 4,15 | 4,25 |
| - Mn(II) | H-2 | 5,95 | 5,75 |
| 1-methyl inosine | H-8 | 4,15 | 4,25 |
| - Mn(II) | H-2 | 5,95 | 5,85 |

Table 3.1 shows a low error in the values of r. However, even if the error in the relative slopes is as large as 60%, due to the sixth power

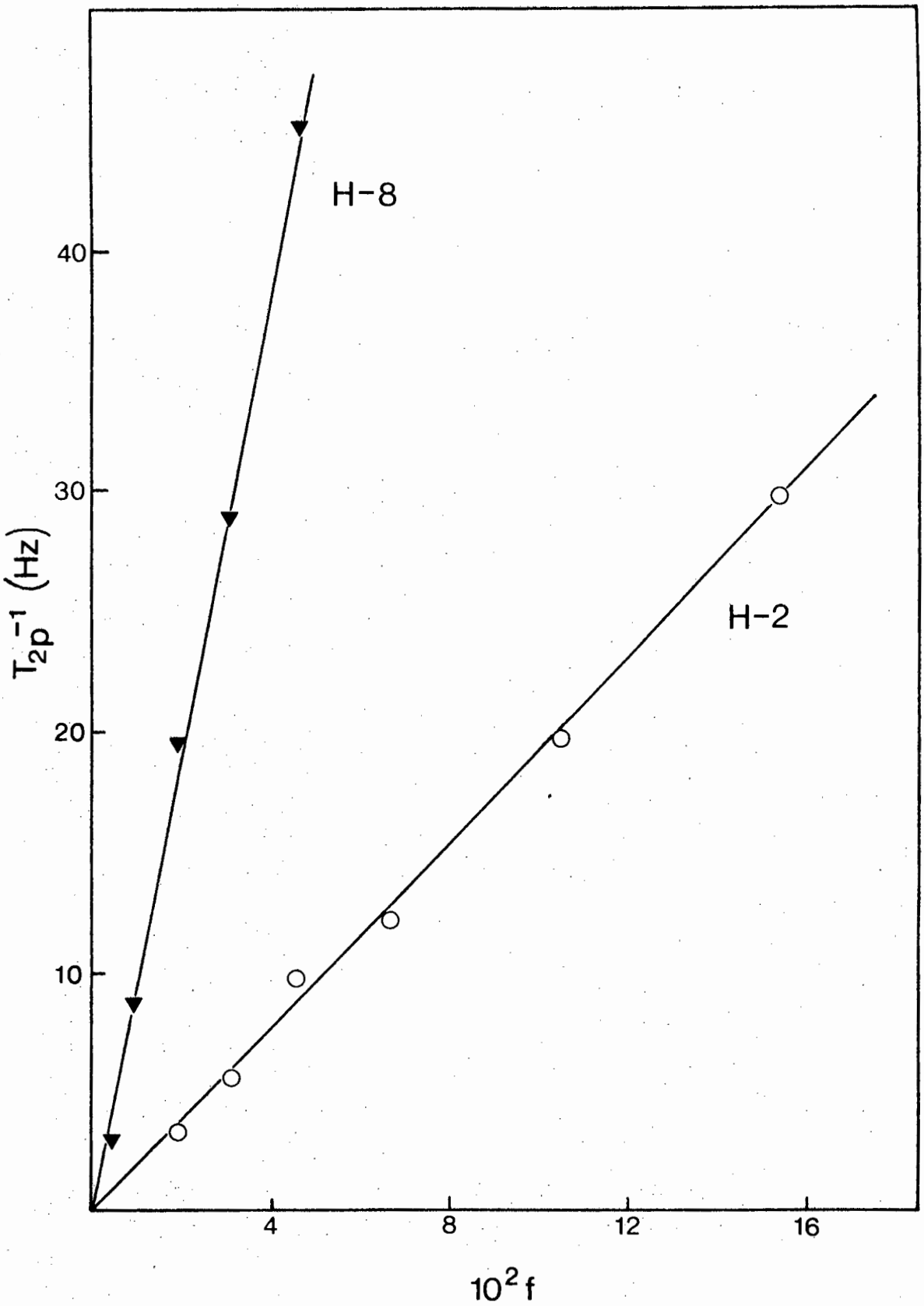


Fig. 3.6 Measured values of $T_{2p}$ for 1-methyl hypoxanthine - Mn(II) as a function of f. pH 6,6, 23°C

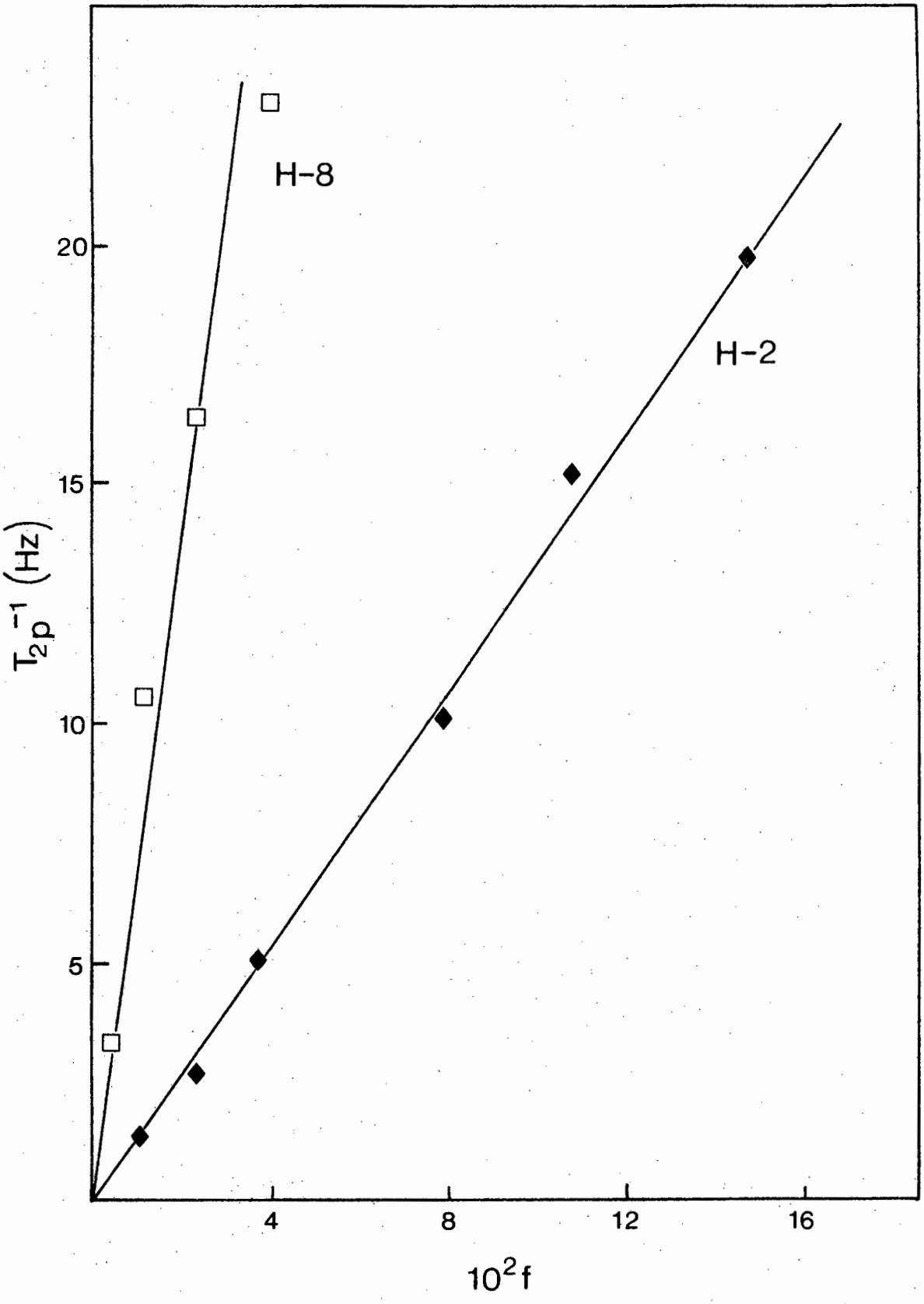


Fig. 3.7 Measured values of $T_{2p}$ for 1-methyl inosine - Mn(II) as a function of f, pH 6,3, 23°C.

of r in equation 1.22, the error in the relative slopes will only be 10%.

The agreement between experiment and theory in Table 3.1 shows that Mn(II) binds in the vicinity of N-7 and O-6, and is probably bidentate. It also lends confidence to the assumptions made in the derivations in section 1.4 and the use of Mn(II) as a paramagnetic ion probe to determine internuclear distances in this type of system.

### 3.3.2 9-methyl hypoxanthine and 2',3'-O-isopropylidene inosine with Mn(II)

The spectra of 9-methyl hypoxanthine and 2',3'-O-isopropylidene inosine are shown in Figs. 3.8(a) and 3.9(a) respectively together with the proton assignments. It can be seen that the H-8 resonance is not always upfield from H-2 as shown in the 2',3'-O-isopropylidene inosine spectrum. This was also assigned using the results of the work of Maeda et al[78]. The spectra, after additions of $2{,}9 \times 10^{-4}$M and $5{,}0 \times 10^{-4}$M Mn(II) to the solutions, respectively are shown in Figs. 3.8(b) and 3.9(b). Again as with the previous two ligands, broadening of H-8 is far greater than H-2 and in the case of 9-methyl hypoxanthine H-2 broadens faster than the methyl resonance.

One would again expect a major binding site to be in the vicinity of O-6 and N-7. However, these two ligands do not have a methyl group attached to N-1 and so binding of O-6 above N-1 is now a distinct possibility. Bidentate binding of Mn(II) to N-1 and O-6 is probably not feasible due to the strain encountered in a four membered

Fig. 3.8 The effect of Mn(II) on the NMR spectrum of 9-methyl hypoxanthine

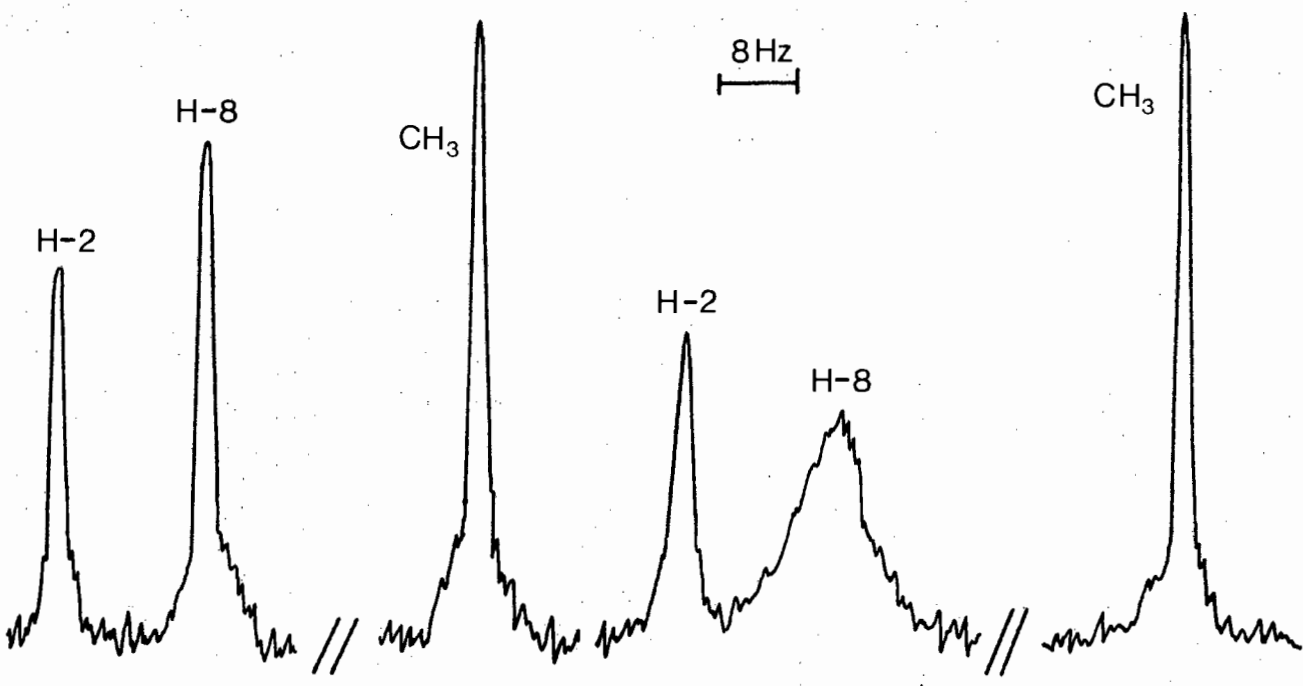


(a) 0,04M ligand
pH 6,3, 40°C

(b) (a) + 2,9 x $10^{-4}$M Mn(II)

Fig. 3.9 The effect of Mn(II) on the NMR spectrum of 2',3'-O-isopropylidene inosine

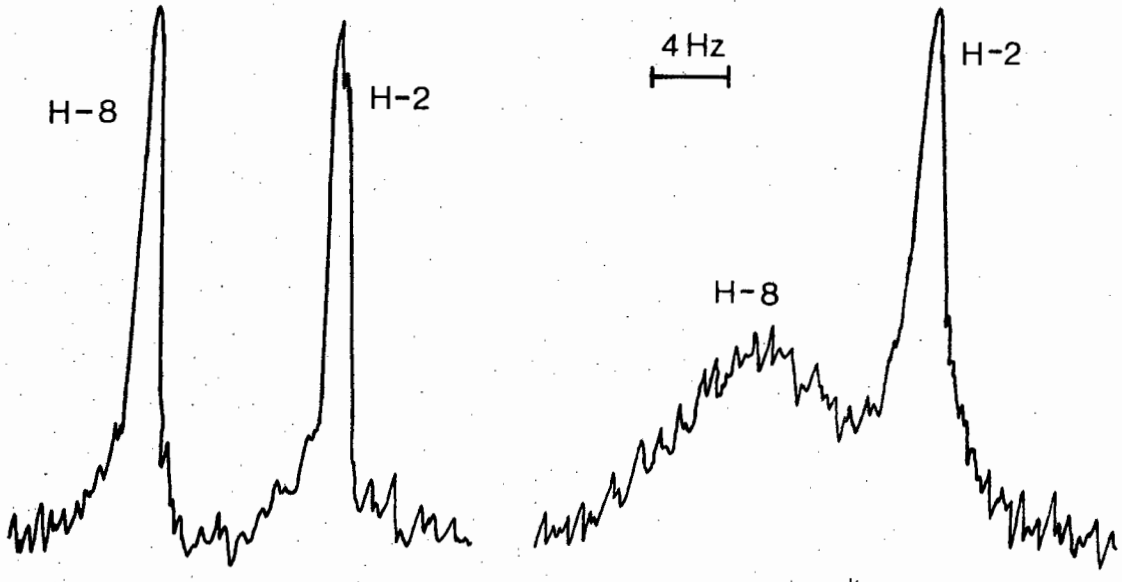


(a) 0,04M ligand
pH 5,5, 50°C

(b) (a) + 5,0 x $10^{-4}$M Mn(II)

(Intensity not to scale)

ring. Binding at N-3 is not likely due to the presence of the methyl or the ribose group at N-9 which would sterically hinder such an attachment.

The results of the broadening observed during the metal titrations of these ligands are plotted (Figs. 3.10 and 3.11) in a similar manner to those of the ligands in 3.3.1, the relative proton-metal internuclear distances then being calculated. Internuclear distances were measured on the Drieding models for Mn(II) bidentately bound to O-6 and N-7 and for Mn(II) monodentately bound to O-6 in the position above N-1. For both ligands the data indicates that Mn(II) only occupies the site in the vicinity of N-7 and O-6. Table 3.2 compares the measured distances from Mn(II) in this preferred binding site to the protons in question, to the experimentally determined distances.

TABLE 3.2

Comparison of the measured and experimentally determined proton-metal distances for 9-methyl hypoxanthine - Mn(II) and 2',3'-O-isopropylidene inosine - Mn(II).

| Complex | Proton | Measured (Å) | Experimental (Å) [a] |
|---|---|---|---|
| 9-methyl hypoxanthine - Mn(II) | H-8 | 4,15 | 4,15 |
| | H-2 | 5,95 | 5,95 |
| | $CH_3$ | 6,50 | 6,55 |
| 2',3'-O-isopropylidene inosine - Mn(II) | H-8 | 4,15 | 3,95 |
| | H-2 | 5,95 | 6,20 |

a Relative to H-2.

Table 3.2 shows very good agreement between experimental and theoretical data and suggests the importance of the O-6, N-7 binding site in preference to any other on the base or ribose ring.

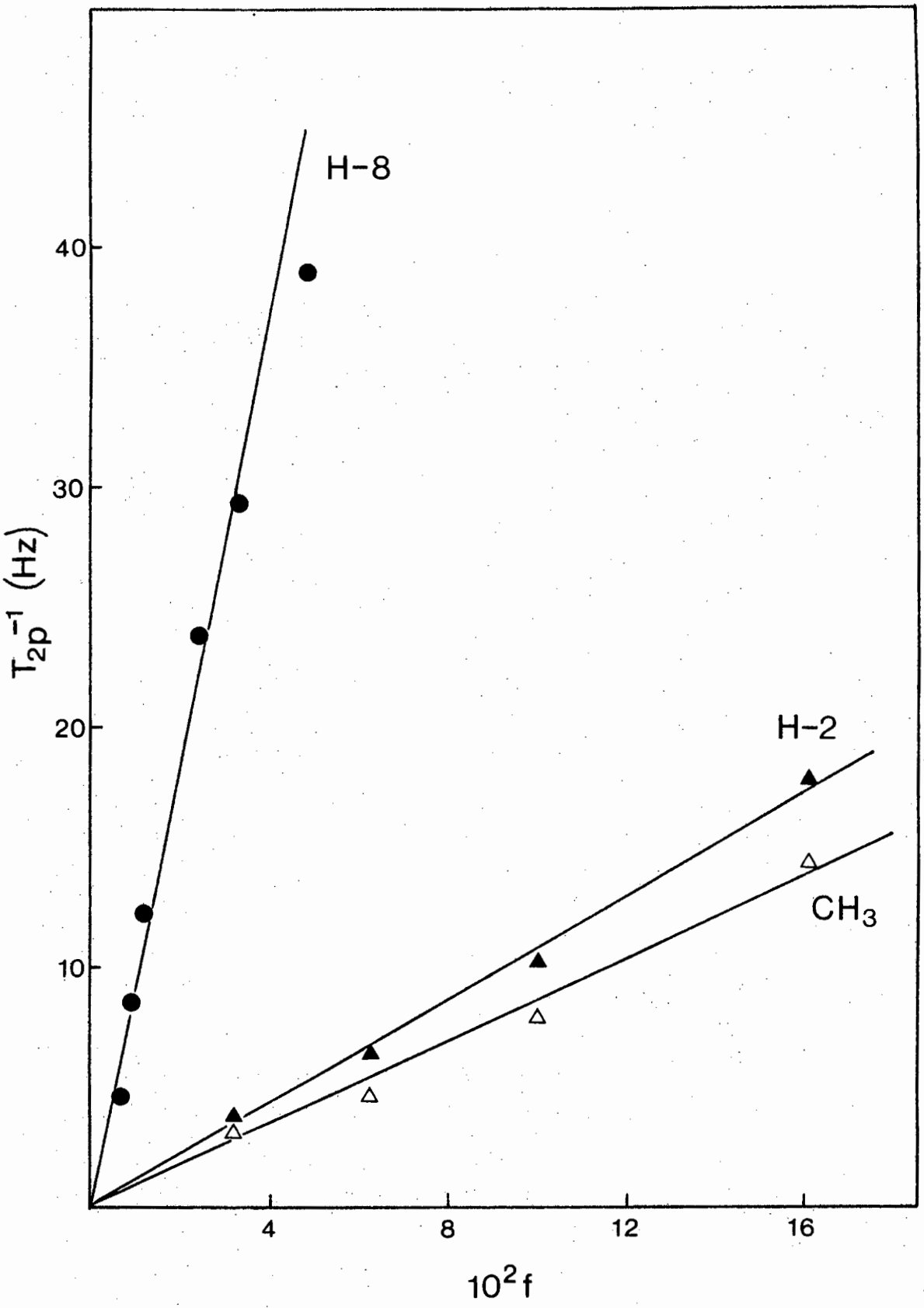


Fig. 3.10 Measured values of $T_{2p}$ for 9-methyl hypoxanthine - Mn(II) as a function of f, pH 6,3, 40°C.

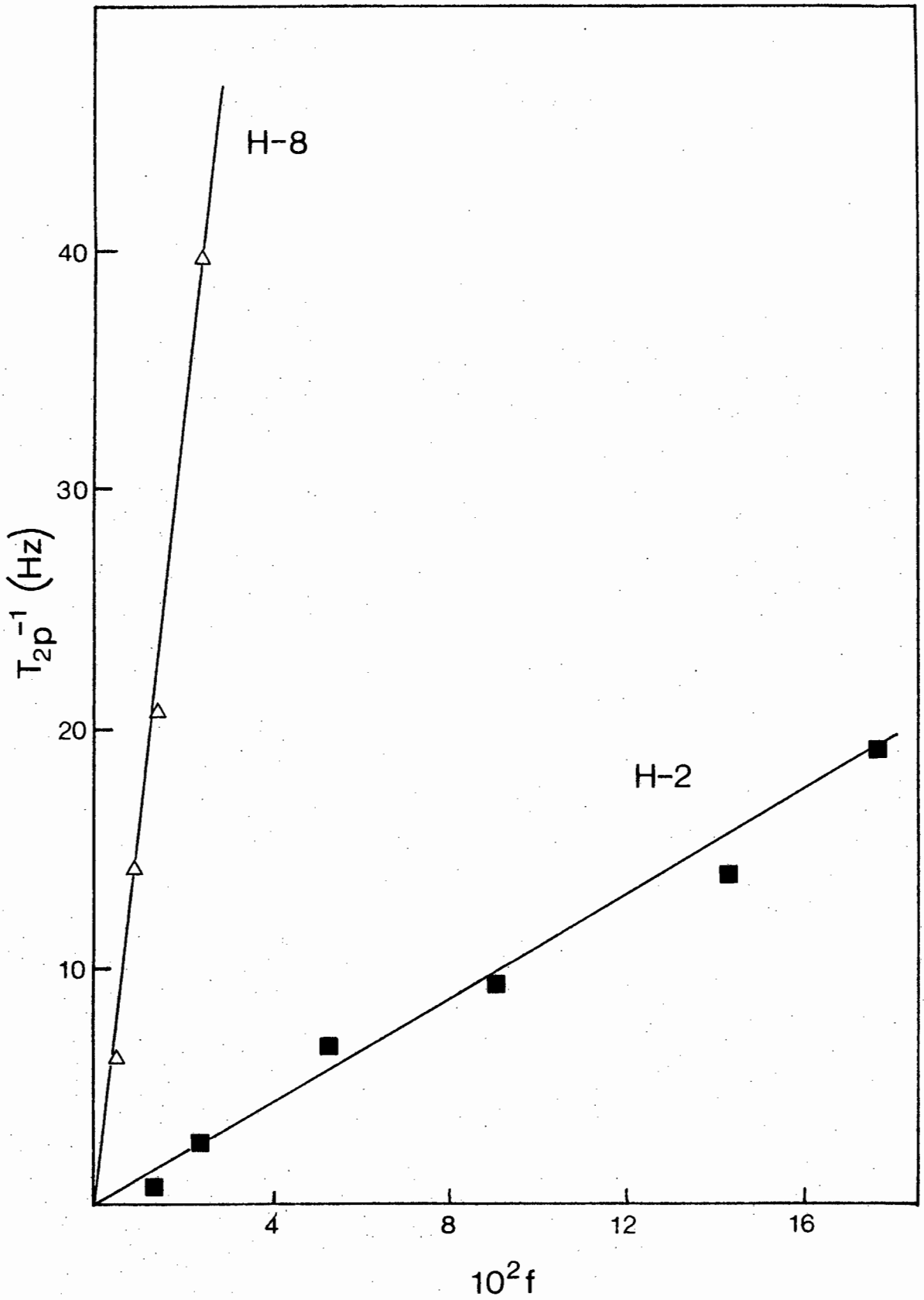


Fig. 3.11 Measured values of $T_{2p}$ for 2',3'-O-isopropylidene inosine - Mn(II) as a function of f, pH 5,5, 50°C.

## 3.4 Conformational studies of some pyrimidine cyclic nucleotides.

Previous studies on all three pyrimidine cyclic nucleotides discussed here (cUMP, cCMP and cTMP) show them to be in the anti conformation. Haschmeyer and Rich[79] have shown by consideration of close contact interaction between base and ribose moieties that the syn conformation is unlikely. Schweizer et al[80] have predicted anti conformations by measuring functional group magnetic anisotropic effects upon furanose proton chemical shifts. Finally, similar potential energy work[81,82] shows that the anti conformation is some 3-4 kcals/mole lower in energy than the syn conformation. cUMP is the only ligand of the three whose X-ray crystal structure has been determined[83]. Two slightly different anti conformers were found, the torsion angles, $\phi_{CN}$, being $-77^{\circ}$ and $-58^{\circ}$. However, the solid state conformation of this molecule is not necessarily that which is found in solution. The ribose conformation is ${}_4T$ in the crystal and here the solution work sharply contrasts this value. ${}^3T$ conformations have been determined for cUMP and cCMP using coupling constants data[84]. A ${}_4T$ conformation has been determined for cTMP[84,85] the difference being attributed to the effect of the absence of the C-2' hydroxy group on the sugar ring.

In this work, both shifting and broadening techniques have been used in order to obtain information pertaining to the ligand conformation in solution.

### 3.4.1 Shift techniques using Dy(III) and Ho(III) with cUMP, cCMP and cTMP.

Data obtained from shifting experiments can be used to determine both syn/anti conformations and ribose conformations. It was hoped that substitution of the shift data into equation 1.29 would easily enable determination of the ribose conformation. However, on inspection of Table 3.3 it can be seen that even though the two extreme ribose conformations are shown, the relative changes of r and θ between the lanthanide ion and the protons in question in the different conformations are slight and hence the alternative δ values are not differentiable.

TABLE 3.3

Theoretical, lanthanide ion induced, relative shift values for the ribose protons of 3', 5' cyclic nucleotides.

| Ribose Confirmation | Proton | $r^a$ (Å) | $\theta^b$ | $\delta^c$ x10$^3$ |
|---|---|---|---|---|
| $_4T$ | H-1' | 7,85 | 15° | 3,7 |
| $^3T$ | H-1' | 8,05 | 19° | 3,2 |
| $_4T$ | H-2' | 6,25 | 34° | 4,3 |
| $^3T$ | H-2' | 6,30 | 35° | 4,o |
| $_4T$ | H-3' | 4,55 | 29,5° | 13,5 |
| $^3T$ | H-3' | 4,55 | 30,5° | 13,0 |
| $_4T$ | H-4' | 6,05 | 0° | 9,0 |
| $^3T$ | H-4' | 6,05 | 0° | 9,0 |
| $_4T$ | H-5'u | 4,75 | 30° | 11,6 |
| $^3T$ | H-5'u | 4,75 | 30° | 11,6 |
| $_4T$ | H-5'd | 5,70 | 22,5° | 8,4 |
| $^3T$ | H-5'd | 5,75 | 22,5° | 8,2 |

a r = Distance from $Ln^{3+}$ to the proton

b θ = Angle between the principal symmetry axis of the complexed ion and the distance vector $\vec{r}$

$$\delta = \frac{3\cos^2\theta - 1}{r^3}$$

Some recent studies of the calculation of the symmetry axis have demonstrated that it is directed along the metal-ligand bond in monodentate systems[86,87]. For complexes in which the lanthanide ion binds to more than one oxygen atom, as in phosphate binding here, the symmetry axis lies along the resultant of the metal-oxygen[88] bonds (Fig. 3.12).

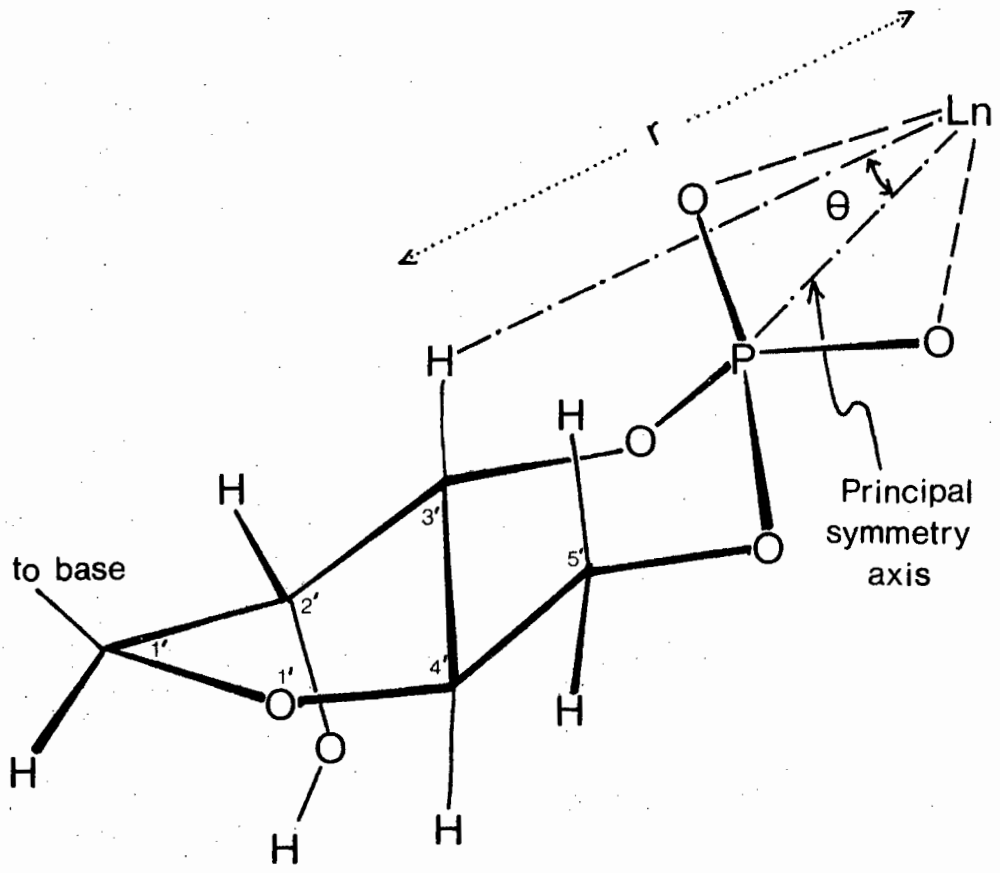


Fig. 3.12 Illustration of the principal symmetry axis, θ and $\vec{r}$ for cyclic nucleotides.

The lanthanide ions best suited to shift experiments are those which produce the greatest shifts and the least broadening. The lanthanides chosen were dysprosium and holmium. Although Pr(III) was quite sufficient to shift out a spectrum in a broadening experiment, Dy(III) and Ho(III) which produce shifts of 9 times and 3,5 times that

of Pr(III) respectively, are needed to obtain the best results. This is due to inconsistancies appearing when the shift is small. In each case the relative shifts were measured for the base protons relative to H-1'.

cUMP. The spectrum of cUMP with the proton assignments is shown Fig. 3.13(a). Figs.3.13(b,c) show the spectrum after addition of Dy(III). Fig. 3.14 shows the pseudo-contact shift, $\delta$, plotted against the total added dysprosium concentration. The shift ratios relative to H-1' are then plotted against lanthanide concentration, Fig. 3.15. There is a linear variation which is due to the ionic strength effect of the added lanthanide solution. To remove this effect the ratios are extrapolated to zero metal concentration. The ratio values, R, at zero metal concentration are shown in Table 3.4 together with results from Ho(III) shift experiments. The similarity of the results indicates axial symmetry of the complex.

TABLE 3.4

Ratios of pseudo-contact shifts to that of H-1' at zero metal concentration for cUMP

| $Ln^{3+}$ | R (H-6) | R (H-5) |
|---|---|---|
| $Dy^{3+}$ | 0,57 | -0,11 |
| $Ho^{3+}$ | 0,46 | -0,13 |

cCMP. The spectrum of cCMP with the proton assignments is shown in Fig. 3.16(a) whilst Figs.3.16(b,c) show the shifts after addition of Dy(III). The pseudo-contact shift versus added dysprosium concentration plot and shift ratio versus dysprosium concentration plot are shown in

Fig. 3.13 Shifting of the cUMP NMR spectrum with Dy(III)

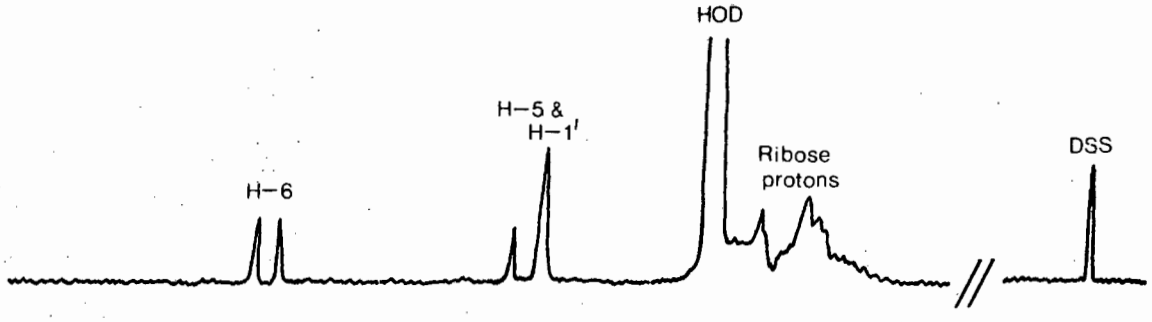


(a) cUMP 0,02M pH 5,5, 23°C

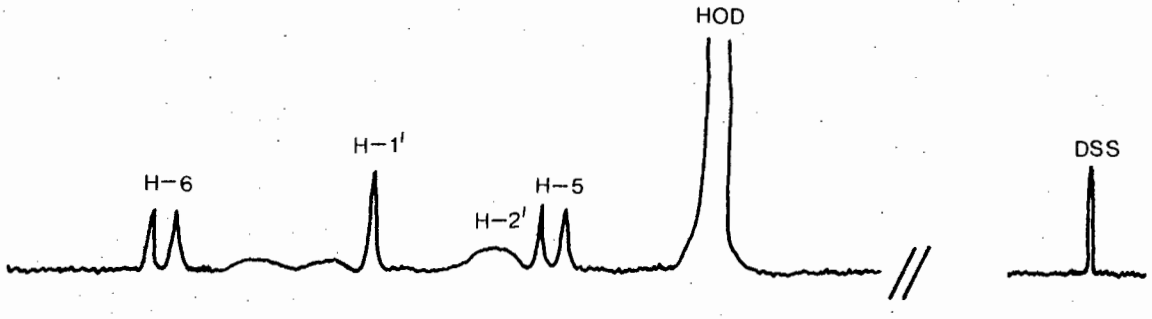


(b) (a) + 4µl Dy(III) satd. solution.

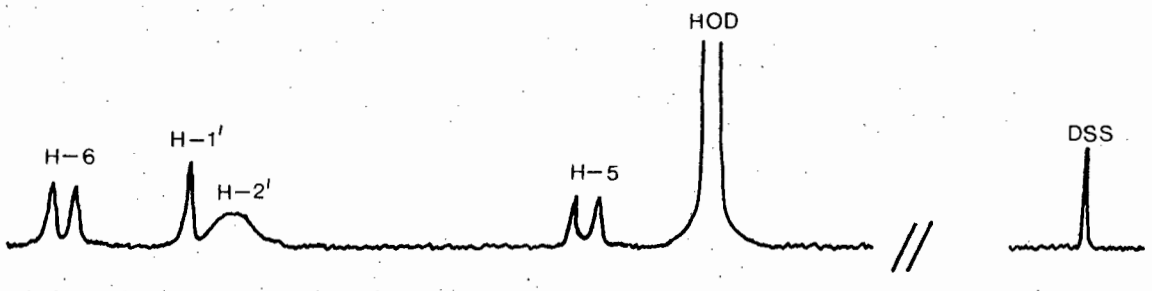


(c) (a) + 8µl Dy(III) satd. solution.

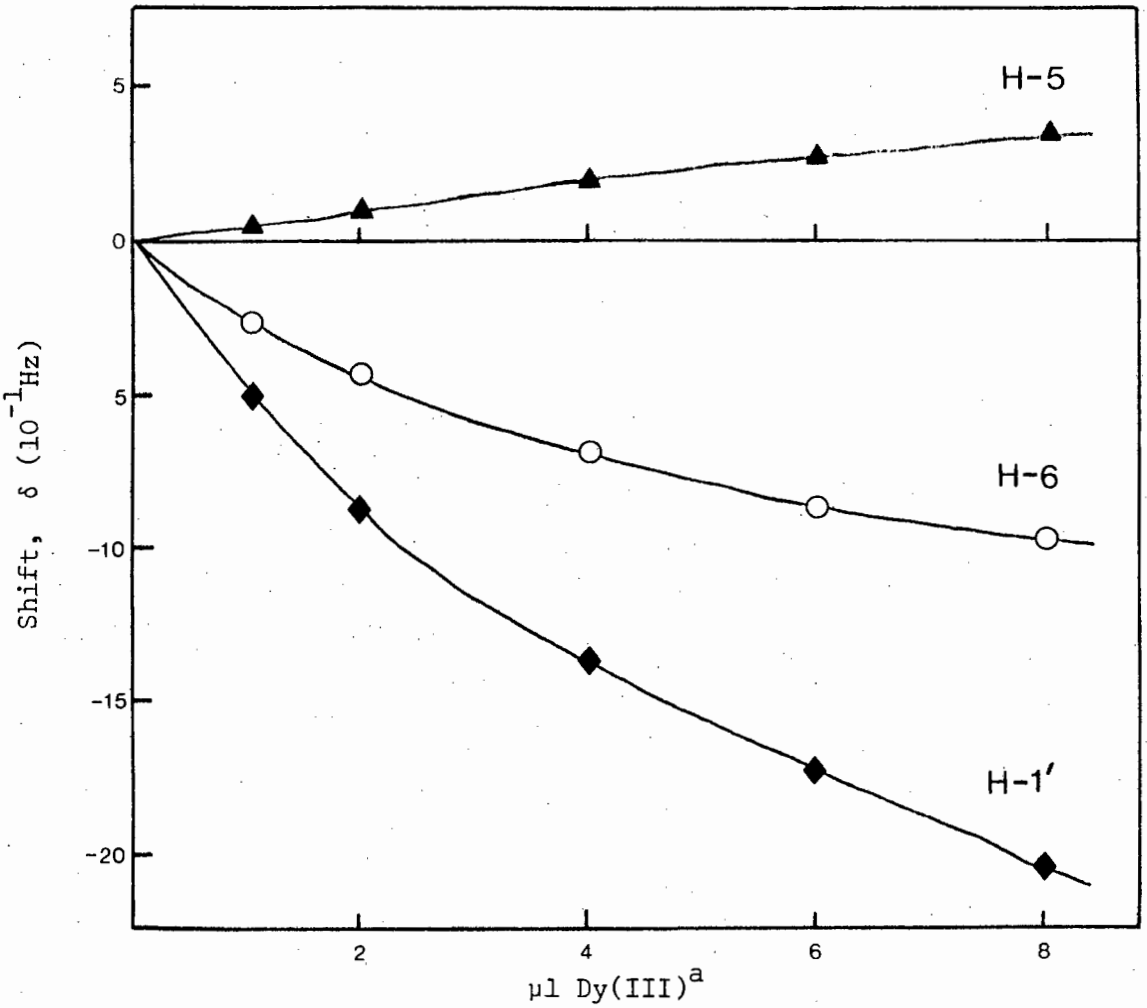


Fig. 3.14 Titration curve for cUMP with Dy(III), ph 5,5, 23°C.

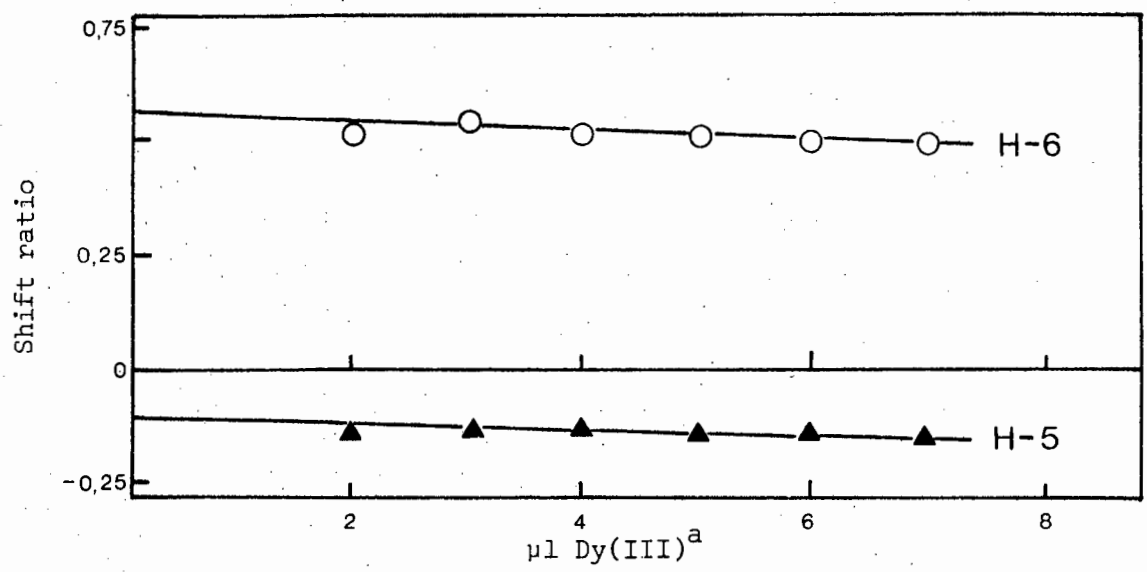


Fig. 3.15 Shift ratios relative to H-1'

[a] Saturated solution of Dy(III)

Fig. 3.16 Shifting of the cCMP NMR spectrum with Dy(III).

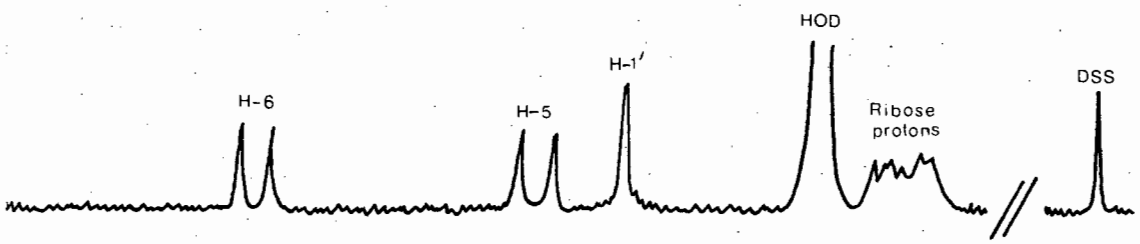


(a) cCMP 0,02M, pH 5,0, 23°C

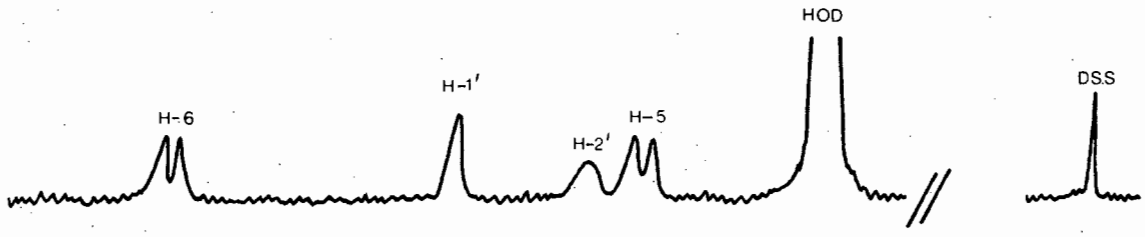


(b) (a) + 3,5 µl Dy(III) satd. solution

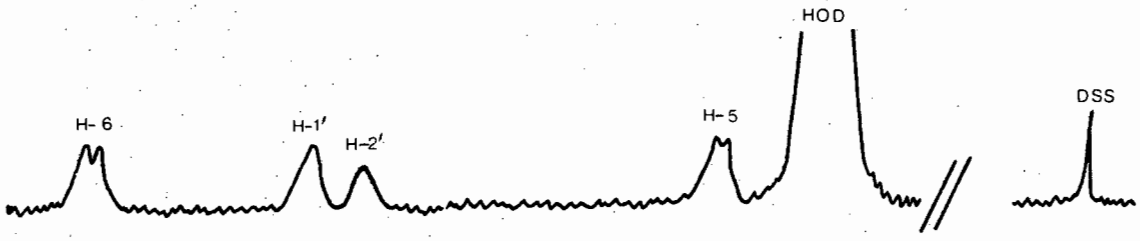


(c) (a) + 8µl Dy(III) satd. solution

Figs. 3.17 and 3.18 respectively. The ratio values, R, at zero lanthanide concentration are shown in Table 3.5 and are fairly similar to those of cUMP.

TABLE 3.5

Ratios of pseudo-contact shifts to that of H-1' at zero metal concentration for cCMP.

| $Ln^{3+}$ | R (H-6) | R (H-5) |
|---|---|---|
| $Dy^{3+}$ | 0,88 | -0,10 |

cTMP. The spectrum of cTMP with the proton assignments is shown in Fig. 3.19(a) and Figs. 3.19(b,c) show the shifts after addition of Dy(III). The pseudo-contact shift and shift ratio versus dysprosium concentration are shown in Figs. 3.20 and 3.21 respectively. Even though a methyl group replaces the proton at C-5 very little change is found in the results. Ho(III) once again gives very similar results, the ratio values being shown in Table 3.6 as well as the Dy(III) results.

TABLE 3.6

Ratios of pseudo-contact shifts to that of H-1' at zero metal concentration for cTMP.

| $Ln^{3+}$ | R (H-6) | R ($CH_3$) |
|---|---|---|
| $Dy^{3+}$ | 0,59 | -0,16 |
| $Ho^{3+}$ | 0,54 | -0,19 |

The results in Tables 3.4 - 3.6, inclusive, can be used to

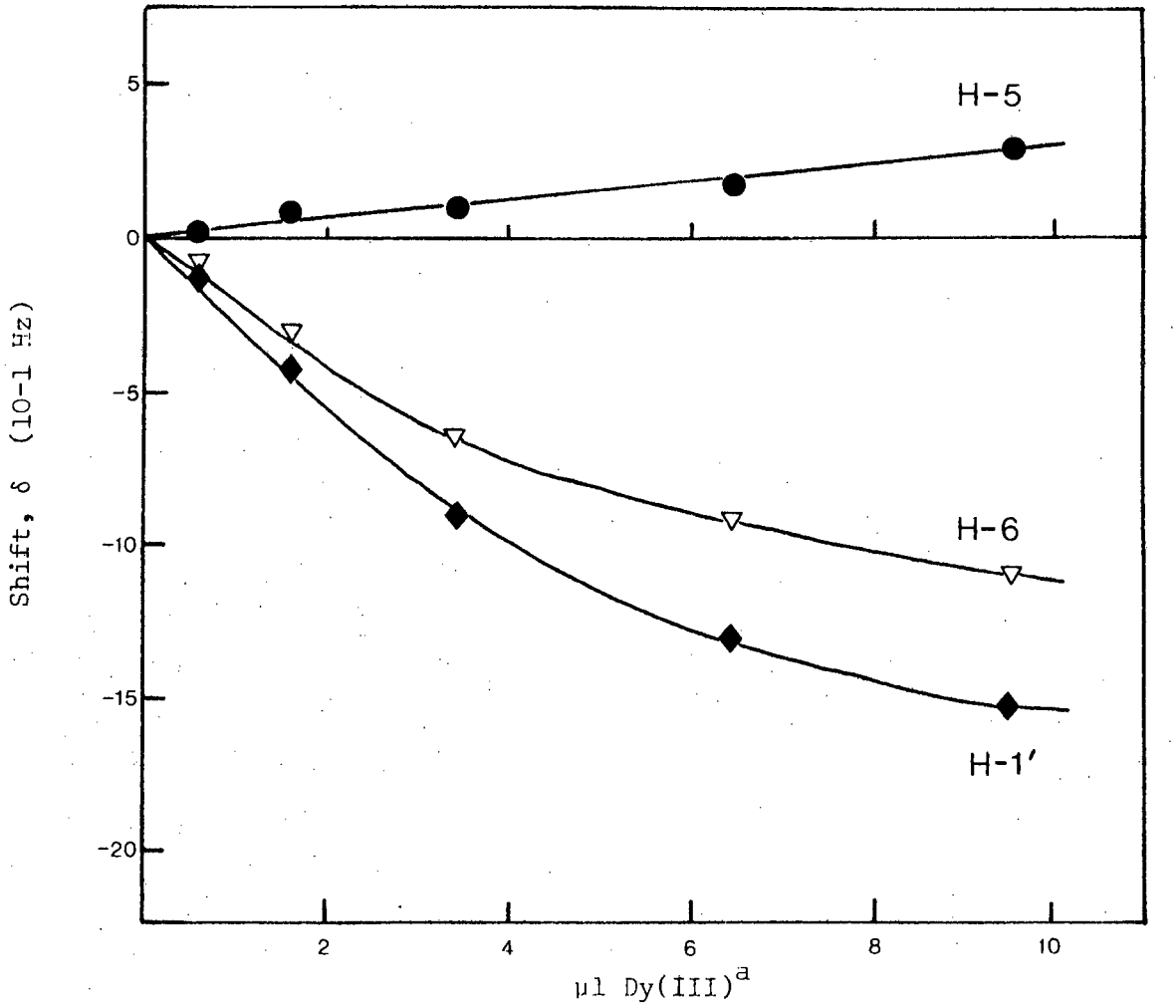


Fig. 3.17 Titration curve for cCMP with Dy(III), pH 5,0, 23°C.

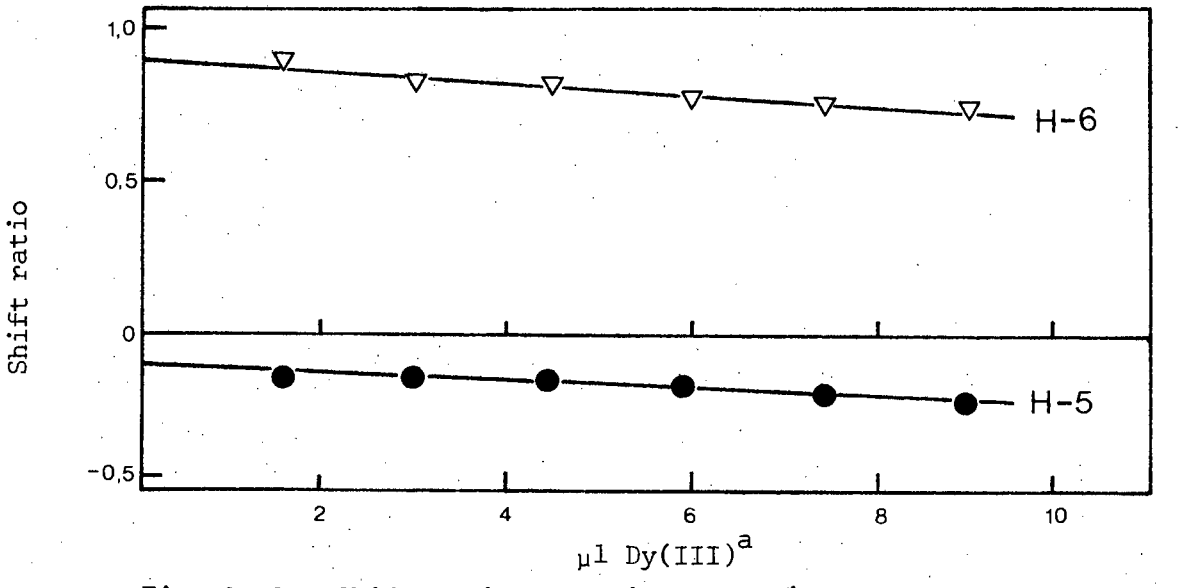


Fig. 3.18 Shift ratios relative to H-1'.

[a] Saturated solution of Dy(III).

Fig. 3.19 Shifting of the cTMP NMR spectrum with Dy(III)

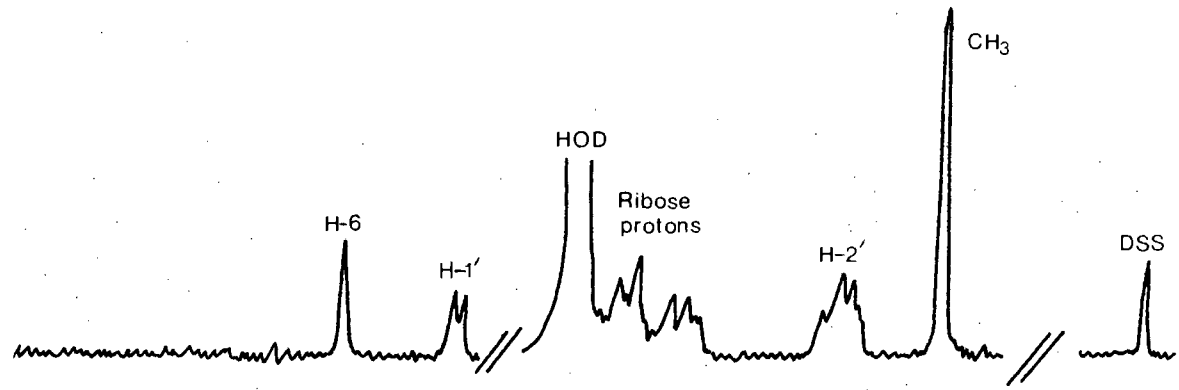


(a) cTMP 0,02M, pH 5,4, 23°C

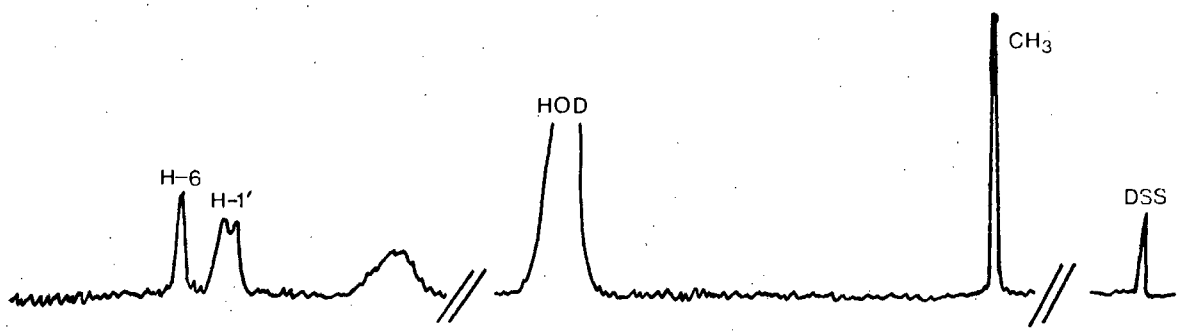


(b) (a) + 8µl Dy(III) satd. solution

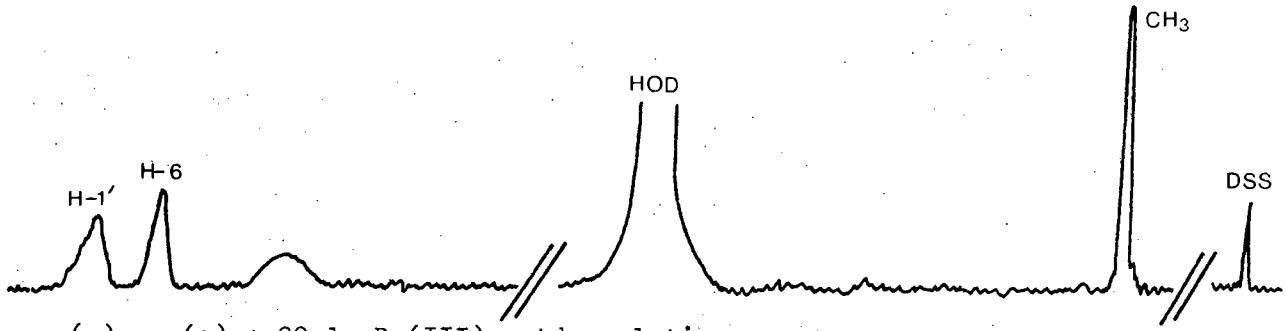


(c) (a) + 20µl Dy(III) satd. solution

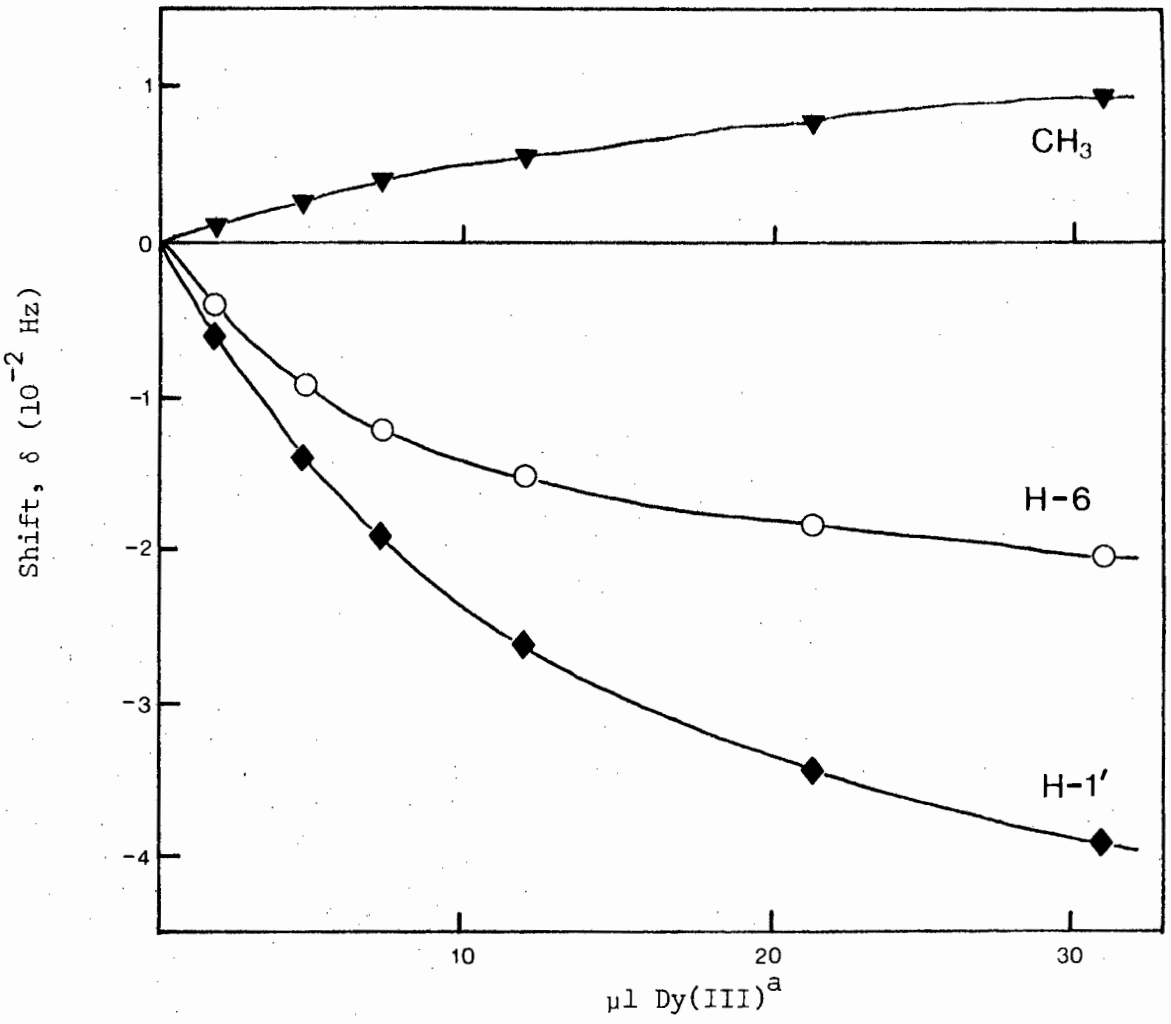


Fig. 3.20 Titration curve for cTMP with Dy(III), pH 5,4, 23°C.

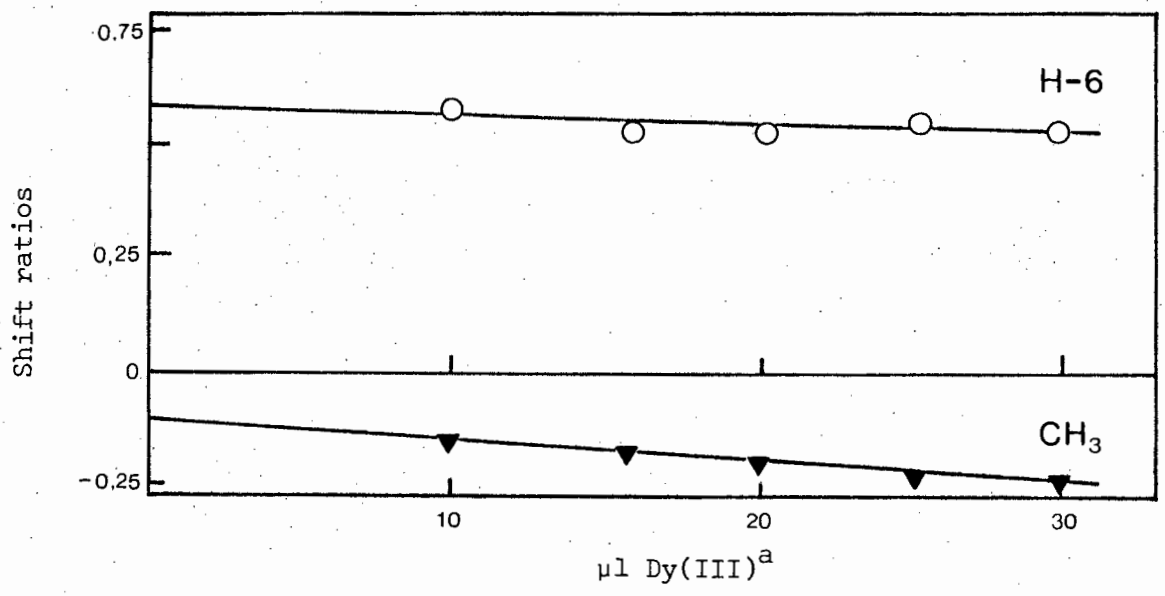


Fig. 3.21 Shift ratios relative to H-1'.

[a] Saturated solution of Dy(III).

predict the syn/anti conformations of the complexes and the ribose conformations.

Theoretical data was compiled and is presented in Tables 3.7 and 3.8. The X-ray crystal structure of cUMP has been determined[83] and shows the molecule to be in an anti conformation, $\phi_{CN} = -68^{\circ}$. Therefore this torsion angle was used in the theoretical calculations for cUMP. Since crystal structures of cCMP and cTMP have not been determined the anti torsion angle used for the theoretical calculations was the value found for the bottom of the potential energy well for these ligands, calculated by Yathindra et al[81] and is $-50^{\circ}$. No pyrimidine cyclic nucleotides, other than those with large substituents at C-6, have been reported in the syn conformation. Nevertheless, theoretical data is necessary in order to see if it differs substantially from anti data and hence whether the method is sensitive to differentiating between the two. The syn torsion angles used, were also found from potential energy wells[81] the value being $135^{\circ}$. Drieding models were used to measure r and $\theta$ and then the $\delta$ values were calculated. Tables 3.7 and 3.8 differ due to slight changes in conformation of the model when measuring the parameters. In Table 3.7 the angles (C-2) - $\widehat{(N\text{-}1)}$ - (C-1') = $117^{\circ}$ and (C-6) -$\widehat{(N\text{-}1)}$ - (C-1') = $121^{\circ}$ are used, these being the angles found in the cUMP crystal structure[83]. However, in Table 3.8 calculations involving the complex in the anti conformation used (C-6) - $\widehat{(N\text{-}1)}$ - (C-1') = $135^{\circ}$ and calculations involving the complex in the syn conformation used (C-1) - $\widehat{(N\text{-}1)}$ - (C-1') = $131^{\circ}$. This is effectively moving the base away from the ribose ring in order to reduce steric effects. This is analogous to the crystal structure of cAMP[48]. If this movement can occur in the crystalline form it is reasonable to expect it in solution

TABLE 3.7

Theoretical values[a] for the ratios of the pseudo-contact shifts of the base protons relative to that of H-1'.

| | Anti | | Syn | |
|---|---|---|---|---|
| cUMP[b] | H-6 | H-5 | H-6 | H-5 |
| Ribose Conf. | | | | |
| $^3T$ | 1,32 | -0,16 | 0,42 | 0,15 |
| $^3T_4$ | 1,07 | -0,13 | 0,44 | 0,21 |
| $_4T$ | 0,87 | 0,15 | 0,51 | 0,26 |
| cCMP[c] | | | | |
| Ribose Conf. | | | | |
| $^3T$ | 1,12 | -0,16 | 0,40 | 0,14 |
| $^3_4T$ | 0,90 | 0,01 | 0,47 | 0,23 |
| $_4T$ | 0,77 | 0,17 | 0,51 | 0,26 |
| cTMP[c] | | $CH_3$ | | $CH_3$ |
| Ribose Conf. | | | | |
| $^3T$ | 1,16 | -0,39 | 0,41 | 0,13 |
| $^3_4T$ | 0,94 | -0,13 | 0,48 | 0,24 |
| $_4T$ | 0,81 | 0,03 | 0,51 | 0,26 |

[a] $(C\text{-}2) - (\widehat{N\text{-}1}) - (C\text{-}1') = 117^\circ$; $(C\text{-}6) - (\widehat{N\text{-}1}) - (C\text{-}1') = 121^\circ$

[b] anti $\phi_{CN} = -68^\circ$; syn $\phi_{CN} = 135^\circ$

[c] anti $\phi_{CN} = -50^\circ$; syn $\phi_{CN} = 135^\circ$

TABLE 3.8

Theoretical values[a] for the ratios of the pseudo-contact shifts of the base protons relative to that of H-1'.

| | Anti | | Syn | |
|---|---|---|---|---|
| cUMP[b] | H-6 | H-5 | H-6 | H-5 |
| Ribose Conf. | | | | |
| $^3T$ | 0,54 | -0,16 | 0,41 | 0,17 |
| $^3T_4$ | 0,48 | -0,08 | 0,51 | 0,18 |
| $_4T$ | 0,50 | 0,10 | 0,50 | 0,28 |
| cCMP[c] | | | | |
| Ribose Conf. | | | | |
| $^3T$ | 0,74 | -0,09 | 0,39 | 0,17 |
| $^3_4T$ | 0,62 | 0,15 | 0,49 | 0,17 |
| $_4T$ | 0,66 | 0,18 | 0,48 | 0,25 |
| cTMP[c] | | $CH_3$ | | $CH_3$ |
| Ribose Conf. | | | | |
| $^3T$ | 0,77 | -0,39 | 0,40 | 0,17 |
| $^3_4T$ | 0,67 | -0,19 | 0,50 | 0,18 |
| $_4T$ | 0,70 | 0,03 | 0,51 | 0,23 |

[a] anti (C-6) - $\widehat{(N\text{-}1)}$ - (C-1') = 135°: syn (C-2) - $\widehat{(N\text{-}1)}$ - (C-1') = 131°

[b] anti $\phi_{CN} = -68°$; syn $\phi_{CN} = 135°$

[c] anti $\phi_{CH} = -50°$; syn $\phi_{CN} = 135°$

where the freedom of movement is not restricted by packing factors.

Comparison of the experimental data for cUMP, Table 3.4, with that in Table 3.7 shows no fit at all, for either the syn or anti conformations or a combination of the two. However, comparison with data in Table 3.8 shows a good fit for an anti conformation of the complex and a $^{3}T$ ribose conformation. This is in agreement with all previous solution studies on cUMP[81,82,84]. In the same manner cCMP experimental data does not correspond well with the data in Table 3.7 though a mixture of syn and anti conformations could give the correct agreement. However cCMP is reported to be in the anti conformation[81,82] in solution and since the data in Table 3.8 for cCMP in this conformation, agrees with the experimental data, it seems the likely solution. The ribose conformation which best fits the experimental data is also $^{3}T$ which again corresponds to previous work[84]. cTMP follows the pattern of the other two ligands, whereby the less sterically hindered conformations of the complex in which the base is pushed away from the ribose ring, give data corresponding to that found experimentally. The data again fits the anti conformation but the ribose preferred conformation is $_{4}T^{3}$. Kainosho et al[84] find cTMP to be in a $_{4}T$ conformation which is almost the same as $_{4}T^{3}$ since even the movement of the ring from one extreme to the other is fairly small due to the restrictions imposed by the cyclic phosphate.

Since the $\phi_{CN}$ values used were only the central values of a fairly wide potential energy well, further calculations were made using values $20^{\circ}$ on either side of those used in order to ascertain the possible error in the results. Table 3.9 shows that the differences are negligible.

TABLE 3.9

Theoretical values for the ratios of the pseudo-contact shifts showing the effects of changing $\phi_{CN}$.

| cUMP[a] | $\phi_{CN}$ | H-6 | H-5 |
|---|---|---|---|
| | $-48^{\circ}$ | 1,18 | -0,13 |
| | $-68^{\circ}$ | 1,32 | -0,16 |
| | $-88^{\circ}$ | 1,15 | -0,13 |

[a] Anti conformation, Ribose conformation $^{3}T$.

### 3.4.2 Broadening techniques using Gd(III) and Mn(II) with cUMP, cCMP and cTMP

Data obtained from broadening the proton resonances with Gd(III) may be used to confirm the syn/anti populations of the ligands whilst the Mn(II) broadening data, in combination with the results obtained from the previous experiments, may be used to determine binding sites and percentage occupation times of these sites by the Mn(II).

cUMP - Gd(III)

The spectrum of cUMP is shown in Figure 3,22(a). Since H-5 and H-1' overlap, Pr(III) was added in order to shift the resonances and so separate them, Fig. 3.22(b). H-5 and H-6 are coupled and so to facilitate width at half height measurements they were decoupled from each other, Fig. 3.22(c). With the spectrum in this form the broadening experiments were carried out. The spectrum after addition of $2.9 \times 10^{-4}$M Gd(III) is shown in Fig. 3.22(d). Qualitatively the H-6 resonance is broader than that of H-5 but since H-6 is closer to Gd(III) in both syn and anti conformations quantitative determinations are necessary.

The results of the broadening observed during the metal titration are shown in Fig. 3.23 in the form of a plot of $T_{2p}^{-1}$ versus f. Gd(III) can bind to the base portion of cUMP as shown by the differential broadening of the proton resonances of uridine on addition of the metal. Thus corrections have been made to the relative slopes measured on the plots in Fig. 3.23. This corrected data is reported in Table 3.10.

Fig. 3.22 Broadening of the cUMP NMR spectrum with Gd(III)

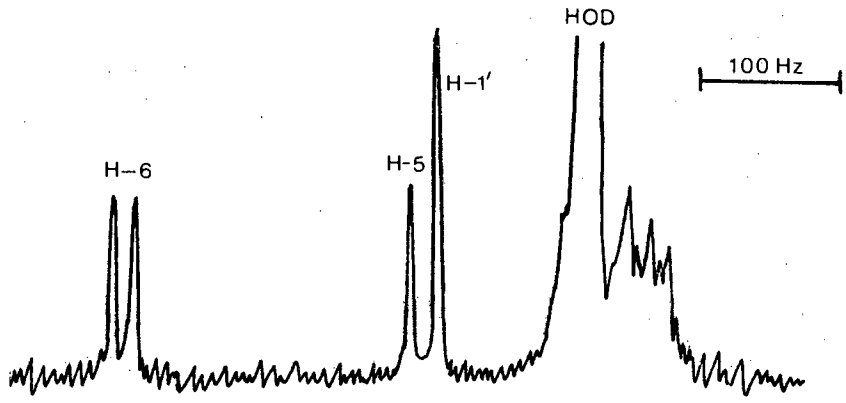


(a) cUMP 0,04M, pH 5,3, 23°C

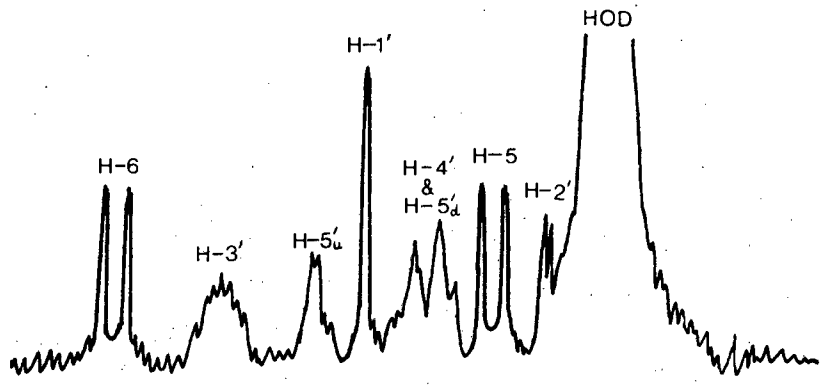


(b) (a) + 20µl ~3M, Pr(III)

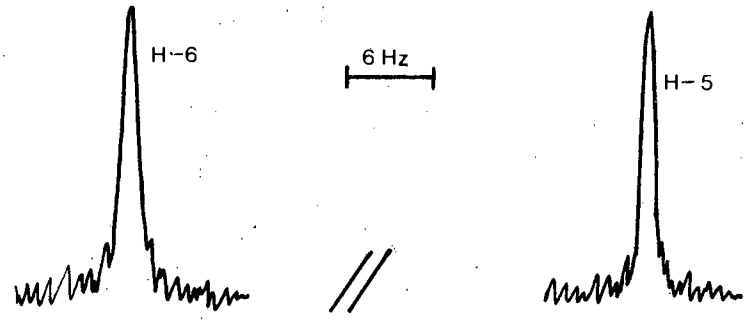


(c) The proton resonances H-6 and H-5 after decoupling

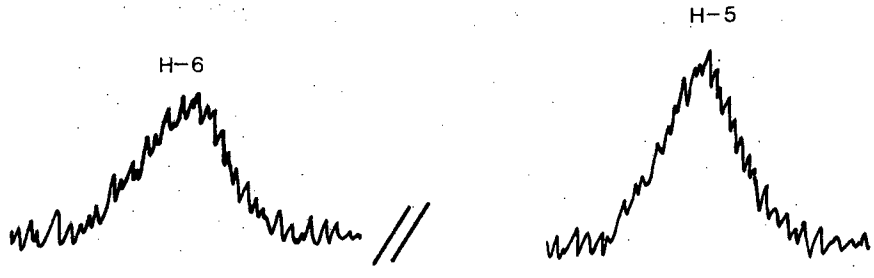


(d) (c) + 2,9 x $10^{-4}$M, Gd(III)

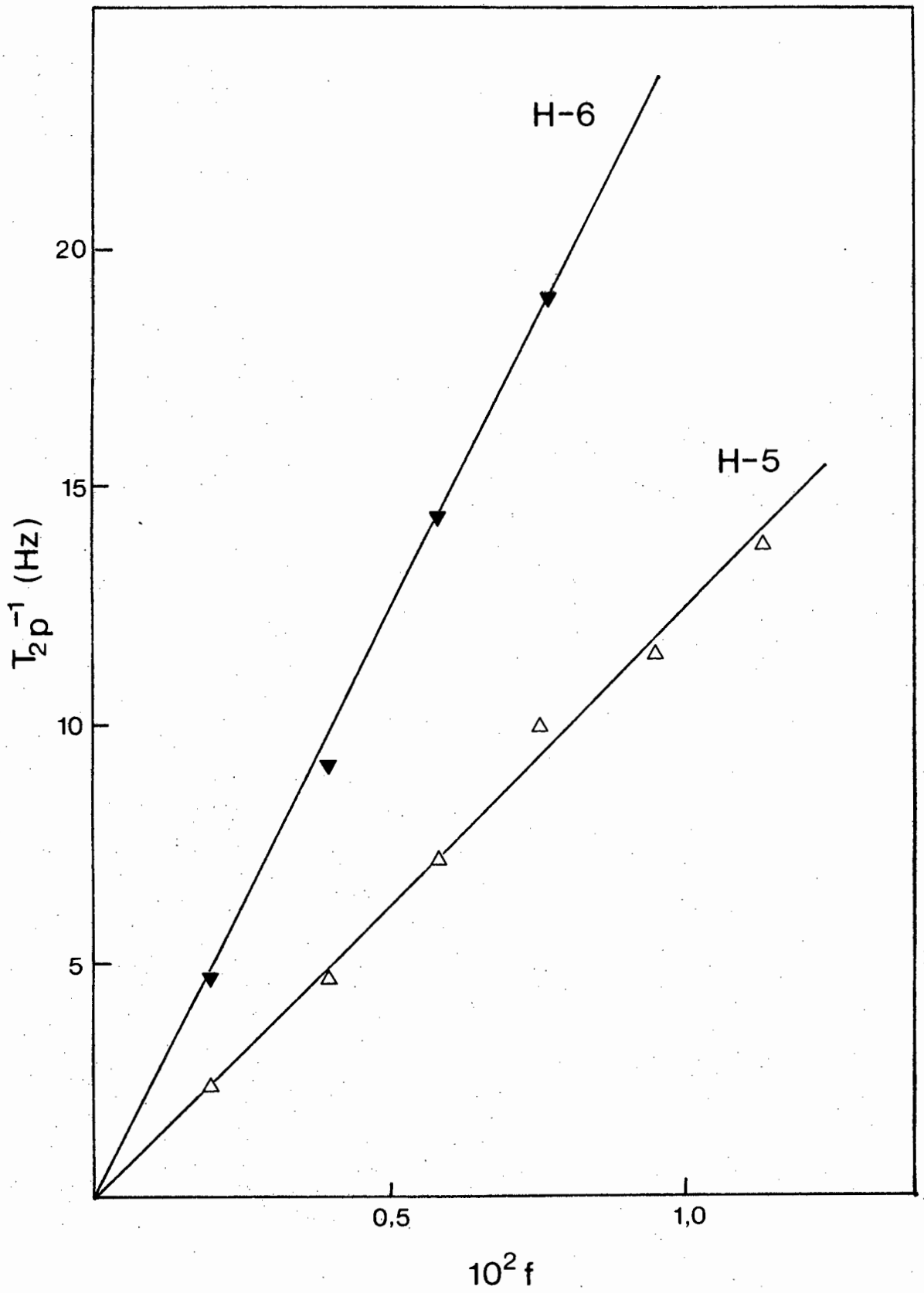


Fig. 3.23 Measured values of $T_{2p}$ for cUMP - Gd(III) as a function of f, pH 5,3, 23°C.

TABLE 3.10

Relative slopes of H-5 and H-6 in terms of $1/f\ T_{2p}$ after corrections for base binding.

| Proton | Slope |
|---|---|
| H-5 | 725 |
| H-6 | 2286 |

From these relative slopes the relative metal-proton internuclear distances can be calculated and compared to the relative internuclear distances measured on a Drieding model of the complex in the anti conformation with the sugar ring in the $^3T$ conformation, and $\phi_{CN} = -68^{\circ}$, (Table 3.11).

TABLE 3.11

Comparison of measured and experimentally determined relative proton-metal distances for cUMP - Gd(III).

| Proton | Measured | Experimental |
|---|---|---|
| H-5 | 1,32 | 1,21 |
| H-6 | 1 | 1 |

There is fair agreement here between experiment and theory. However, due to the relative proton-metal distances of H-5 and H-6 to Gd(III) in the syn conformation, being fairly similar to those in the anti conformation for pyrimidine cyclic nucleotides, this experimental procedure is not very sensitive for syn/anti determinations for this group of complexes.

cCMP - Gd(III)

The spectrum of cCMP is very similar to that of cUMP but H-5 and H-1' do not overlap and therefore no shift reagent was necessary. The broadening follows a similar pattern to that of cUMP, the relative slopes after correction for base binding being shown in Table 3.12.

TABLE 3.12

Relative slopes of H-5 and H-6 in terms of 1/f $T_{2p}$ after corrections for base binding.

| Proton | Slope |
|---|---|
| H-5 | 742 |
| H-6 | 1103 |

The relative metal-proton internuclear distances are again compared with the relative internuclear distances measured on a Drieding model of the complex in an anti conformation, the sugar ring in $^3T$ conformation and $\phi_{CN} = -50^\circ$ (Table 3.13).

TABLE 3.13

| Proton | Measured | Experimental |
|---|---|---|
| H-5 | 1,3 | 1,1 |
| H-6 | 1 | 1 |

cTMP - Gd(III)

The spectrum of cTMP differs from the previous two cases in

that the methyl resonance in place of H-5, occurs upfield of the HOD resonance. However, the broadening is very similar, on addition of Gd(III). The corrected relative slopes of $CH_3$ and H-6 are shown in Table 3.14.

TABLE 3.14

Relative slopes of $CH_3$ and H-6 in terms of 1/f $T_{2p}$ after corrections for base binding.

| Proton | Slope |
|---|---|
| $CH_3$ | 628 |
| H-6 | 1646 |

The relative metal-proton internuclear distances are compared with the relative internuclear distances measured on a Drieding model of the complex in the anti conformation, this time with the sugar ring in a $_4T^3$ conformation, and $\phi_{CN} = -50^{\circ}$ (Table 3.15).

TABLE 3.15

Comparison of the measured and experimentally determined relative proton-metal distances for cTMP - Gd(III).

| Proton | Measured | Experimental |
|---|---|---|
| $CH_3$ | 1,17 | 1,17 |
| H-6 | 1 | 1 |

The experimental results here agree perfectly with the theory and so confirm the shift results and other workers' results[80-2].

cTMP - Mn(II)

Assuming that the cTMP - Mn(II) complex retains the same anti conformation and the same $_4T^3$ sugar conformation as the cTMP-Gd(III) complex further calculations have been made in order to establish the binding sites and the percentage binding times of Mn(II) at each specific site.

The spectrum of cTMP is shown in Fig. 3.24(a) and the spectrum after H-1' and H-2' have been decoupled one from the other in Fig. 3.24(b). This spectrum was then broadened with Mn(II) Fig. 3.24(c) showing the resonances after the addition of 1,6 x $10^{-3}$M Mn(II). The results of the broadening observed during the metal titration are shown in Fig 3.25.

There are several possible binding sites for Mn(II) on cTMP and these are illustrated in Fig. 3.26.

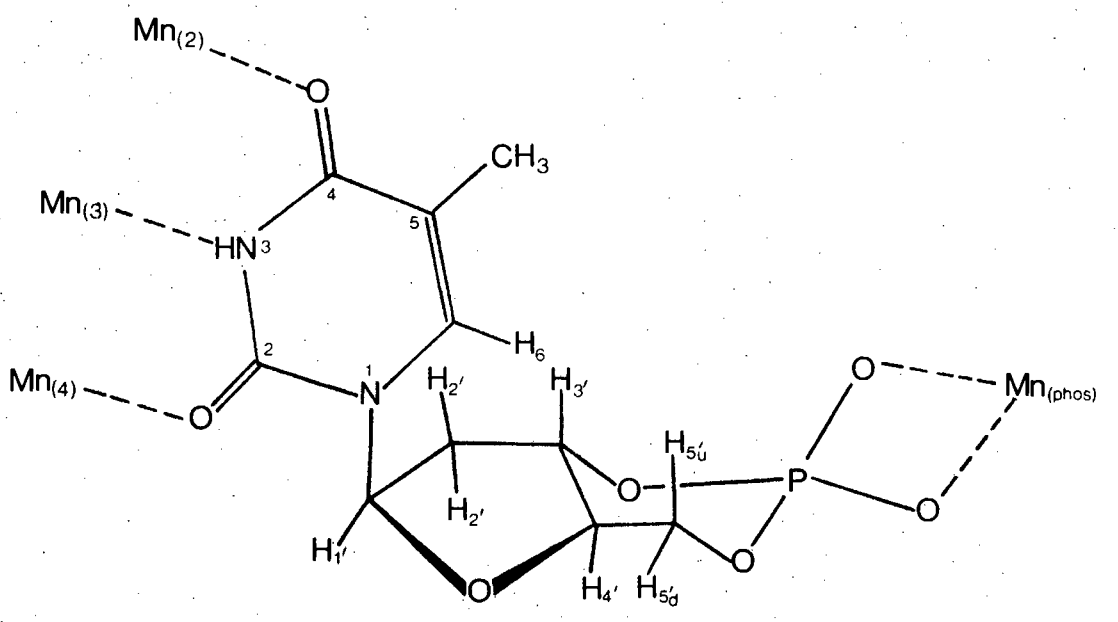


Fig. 3.26. Possible binding sites for Mn(II) on cTMP.

Fig. 3.24 Broadening of the cTMP NMR spectrum with Mn(II)

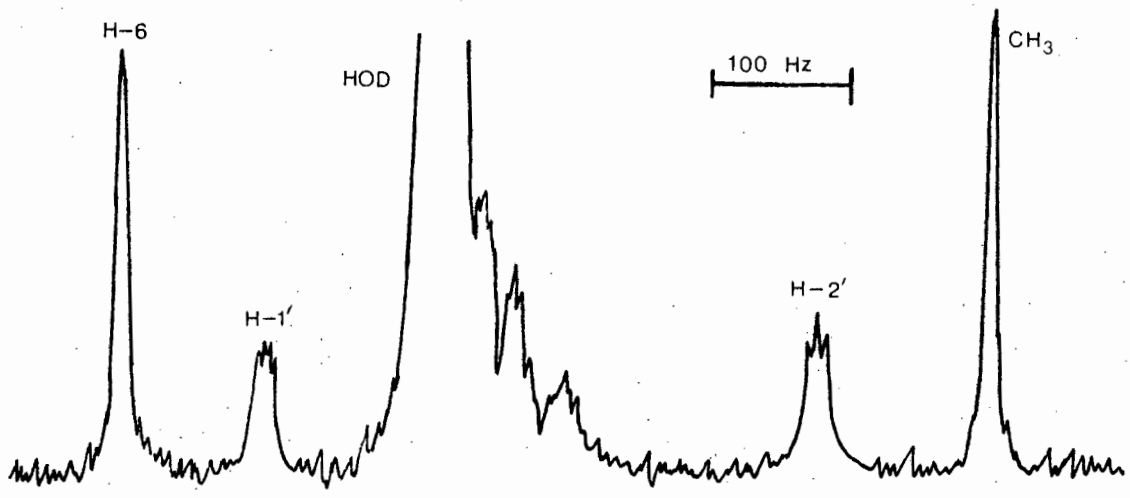


(a) cTMP, 0,04M, pH 6,2, 23°C

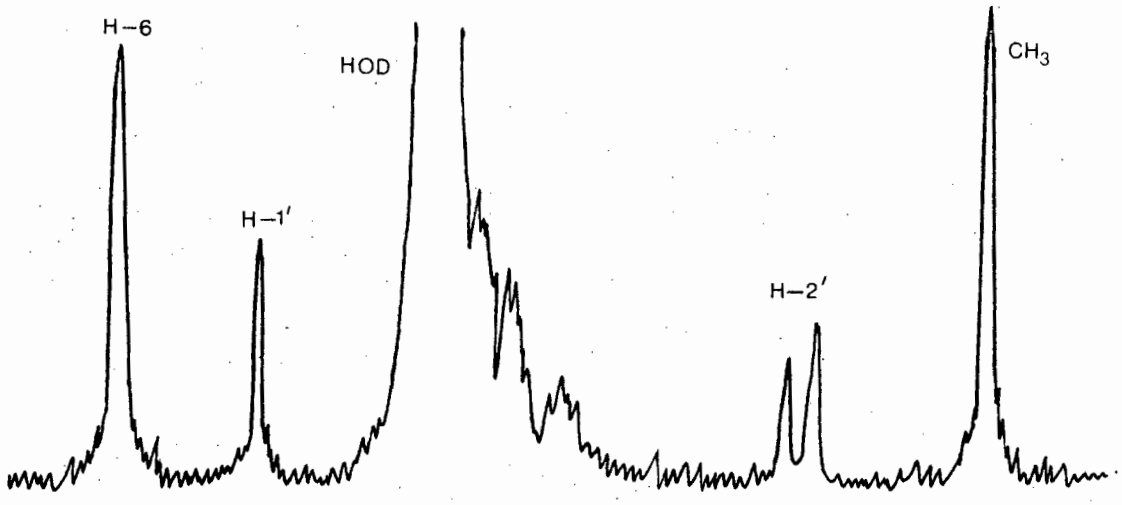


(b) Resultant spectrum after decoupling of H-1' and H-2'

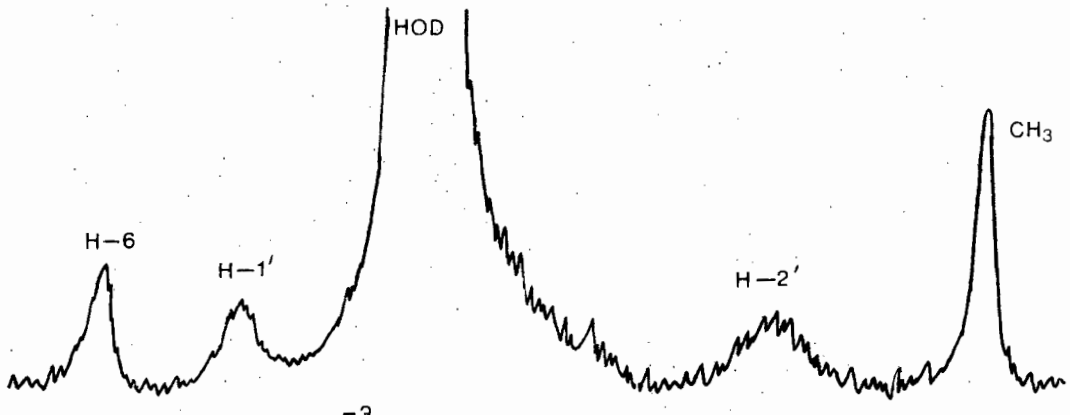


(c) (b) + 1,5 x $10^{-3}$M Mn(II)

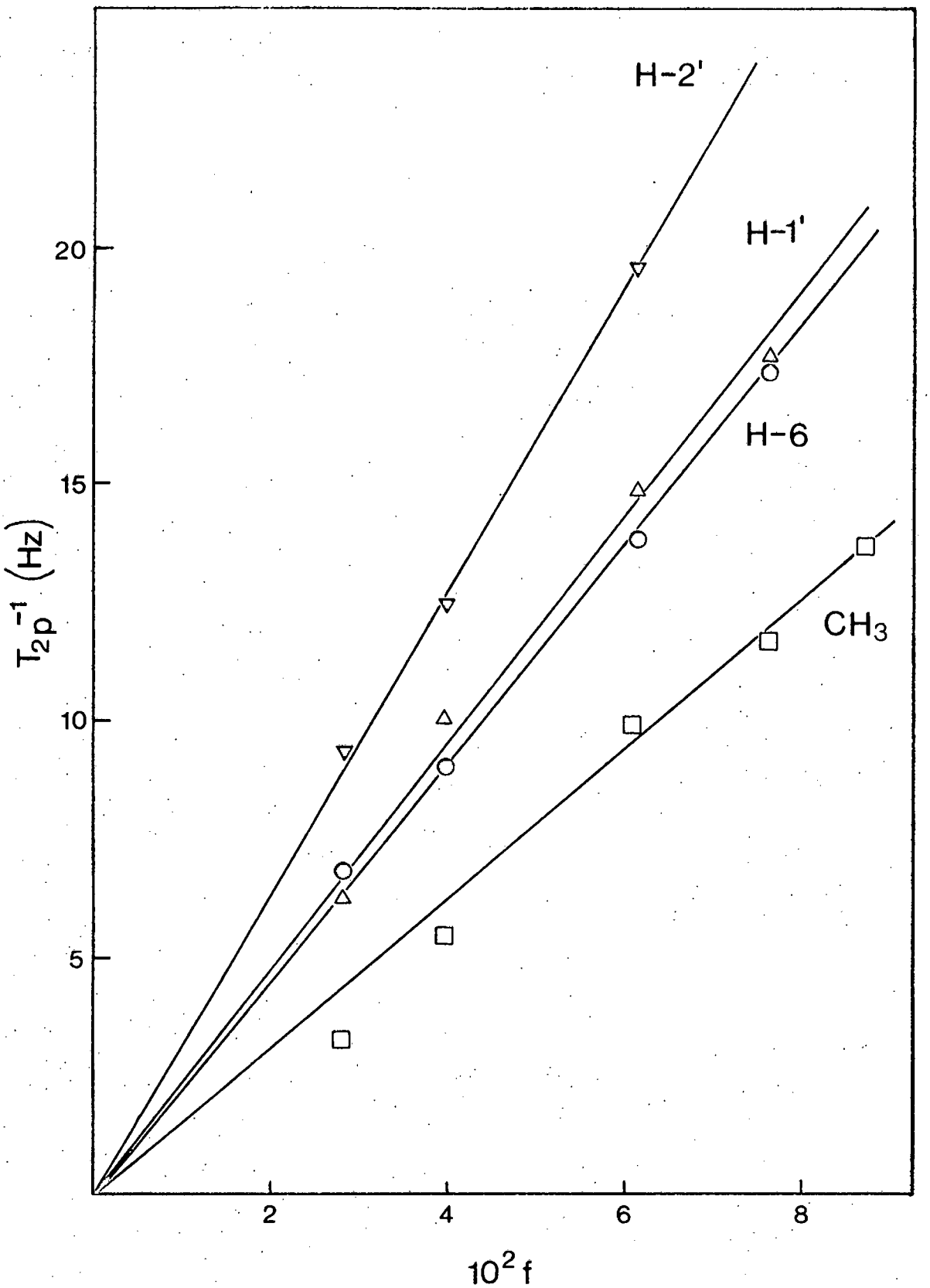


Fig. 3.25 Measured values of $T_{2p}$ for cTMP - Mn(II) as a function of f, pH 6,2, 23°C.

The alternative binding sites on O-4 and O-2 are sterically hindered by the $CH_3$ group and H-1' respectively.

On a Dreiding model of the cTMP - Mn(II) complex the metal-proton distances were measured for each different possible binding site. With this information and the relative slopes of the protons, a computer programme found the best fit to be as follows in Table 3.16.

TABLE 3.16.

Percentage binding times for Mn(II) with cTMP.

| Mn(II) binding site | % Time for metal at site |
|---|---|
| $Mn_{(2)}$ | 10 |
| $Mn_{(3)}$ | 0 |
| $Mn_{(4)}$ | 3 |
| $Mn_{(phos)}$ | 87 |

The K values for each proton for the above solution were very close indicating a very good fit for the data. The possibility of Mn(II) binding bidentately to O-4 and N-3 for some time and bidentately to O-2 and N-3 at other times must be considered. It is probably not as likely as the monodentate binding already described since four membered rings of this nature are likely to be strained. However, since these positions are very close to Mn(II) monodentately bound to O-4 and O-2 the computer programme would not be able to differentiate between the two.

cUMP - Mn(II)

The assumptions made for the cUMP - Mn(II) complex are that

the ligand is in the anti conformation and that the ribose is in the $^3T$ conformation. The Mn(II) titration with cUMP caused broadening, the resultant relative slopes in terms of 1/f $T_{2p}$ for the observed protons are shown in Table 3.17.

TABLE 3.17

Relative slopes for H-5, H-6, H-1' and H-5'u in terms of 1/f $T_{2p}$

| Proton | Slope |
|---|---|
| H-5 | 289 |
| H-6 | 316 |
| H-1' | 131 |
| H-5'u | 557[a] |

[a] H-5'u is a corrected value for the slope, due to a different $\tau_c$ value (see section 3.5.2).

There are several different possible binding sites for Mn(II) on cUMP and these are illustrated in Fig. 3.27.

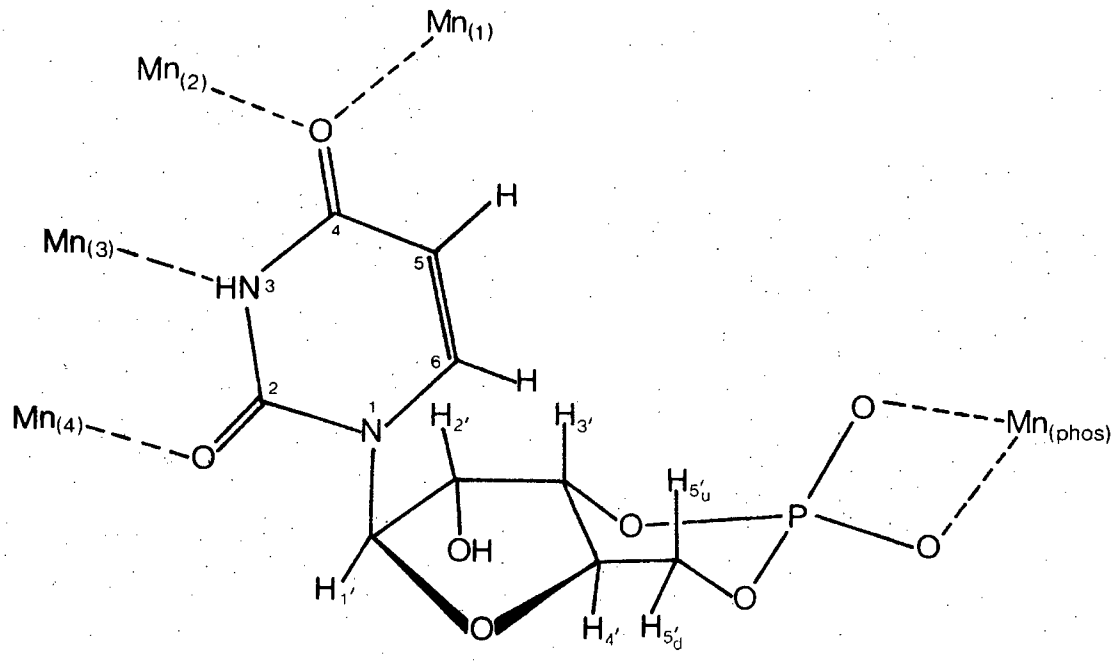


Fig. 3.27 Possible binding sites for Mn(II) on cUMP

Since there was no Mn(II) binding at site $Mn_{(3)}$ (bonded to N-3) in cTMP there is no reason why there should be binding there for cUMP and so this site has been excluded from the possibilities. Site $Mn_{(1)}$ is not very likely since the distance from Mn(II) to H-5 is slightly less than the sum of the van der Waals radii, but nevertheless it is used in the calculations as a possible site. The best fit found by the computer programme using the experimental slopes and the theoretical metal-proton distances is shown in Table 3.18.

TABLE 3.18.

Percentage binding times for Mn(II) with cUMP

| Mn(II) binding site | % Time for metal at site |
|---|---|
| $Mn_{(1)}$ | 0 |
| $Mn_{(2)}$ | 27 |
| $Mn_{(4)}$ | 5 |
| $Mn_{(phos)}$ | 68 |

The K values for each proton in the above solution were the same which lends confidence to the method used and the resultant data.

Again as with cTMP bidentate binding of Mn(II) to O-4 and N-3, and to O-2 and N-3 could not be easily differentiated from the monodentate binding considered.

cCMP - Mn(II)

The assumptions made for the cCMP - Mn(II) complex are the same as for cUMP - Mn(II), namely, an anti conformation and the ribose in the $^3T$ conformation.

The resultant relative slopes in terms of 1/f $T_{2p}$ determined from the broadening during the Mn(II) titration with the ligand, are shown in Table 3.19.

TABLE 3.19

Relative slopes for H-5, H-6 and H-1' in terms of 1/f $T_{2p}$

| Proton | Slope |
|---|---|
| H-5 | 285 |
| H-6 | 675 |
| H-1' | 801 |

cCMP has an amine group at C-4 in contrast to the oxygen in both cTMP and cUMP. Nitrogen does not tend to bind Mn(II) as well as oxygen but sites where Mn(II) is bonded to N-4 must be considered as possibilities. The possible binding sites on cCMP are shown in Fig. 3.28.

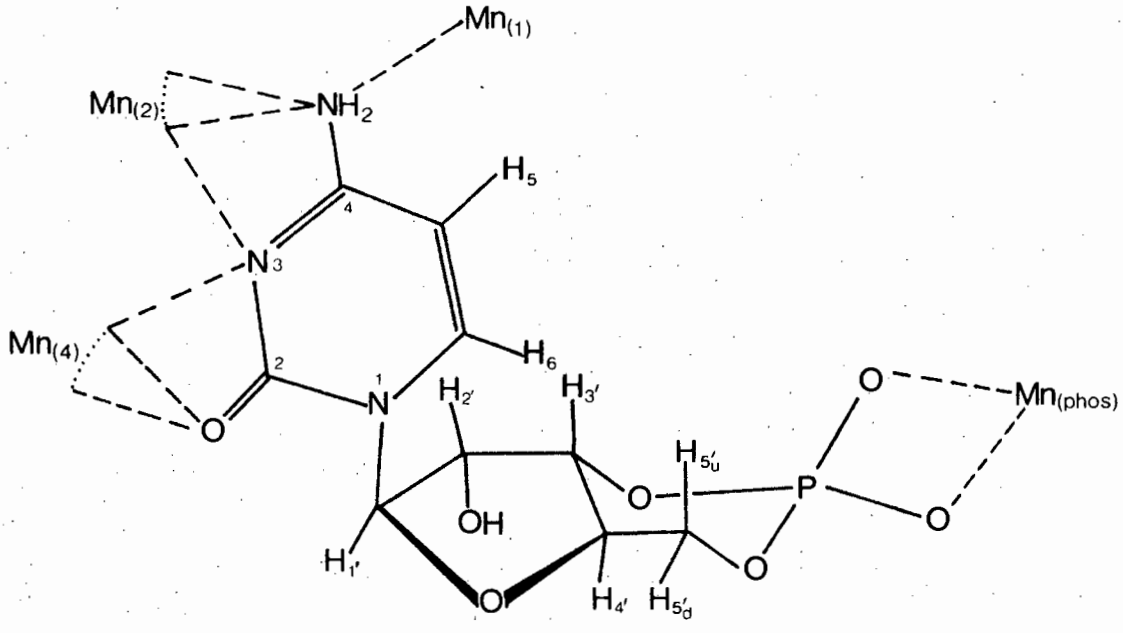


Fig. 3.28 Possible binding sites for Mn(II) on cCMP

$Mn_{(1)}$ site here, is not taken into account in the calculations since due to N-4 having $sp^3$ hybridization as opposed to the $sp^2$ hybridization of O-4, the Mn(II) is brought even closer to H-5, well within the sum of the van der Waals radii. Since nitrogen does not bind Mn(II) to the same extent as oxygen $Mn_{(2)}$ might well bind bidentately to N-4 and N-3 for extra stability, though the four membered ring may prevent this. Due to the uncertainty of mono- or bidentate binding here the sites reported in Table 3.20 are for the range of mono to bidentate binding positions and the percentage times are also quoted within a small range.

TABLE 3.20.

Percentage binding times for Mn(II) with cCMP.

| Mn(II) binding site | % Time for metal at site |
|---|---|
| $Mn_{(2)}$ | 4 - 10 |
| $Mn_{(4)}$ | 13 - 21 |
| $Mn_{(phos)}$ | 75 - 77 |

Of interest in the above table is the relative rise in binding time at the $Mn_{(4)}$ site. This is probably due to O-2 being a better Mn(II) binder than the nitrogens available.

In all the systems studied here with Mn(II), the phosphate group has been the favoured binding site and this is to be expected since the possibility of binding to two oxygens is offered, the four membered ring not being strained due to the tetrahedral angle O - $\hat{P}$ - O.

### 3.4.3 General Discussion

The results put forward in the previous sections 3.4.1 and 3.4.2 show that both shifting and broadening techniques are reliable methods in conformational studies. The anti conformation found for all the complexes, and the ribose conformations of $^{3}T$ for cUMP and cCMP and $_{4}T^{3}$ for cTMP agree very well with results found using totally different methods. This shows that the presence of the metal does not affectively alter the conformation of the ligand under study.

All the theoretical measurements were made where the base and ribose ring were moved away from each other giving a more energetically favourable conformation of the ligand. This variable parameter is not mentioned by any of the previous workers and it seems therefore that it has not been taken into account. This present study shows that it is an important factor and should be taken into careful consideration when attempting conformational work with this type of ligand.

## 3.5 Conformational studies of some purine cyclic nucleotides.

Recent studies on purine cyclic nucleotides have dealt mainly with cAMP (adenosine 3',5' cyclic phosphate) and to a lesser extent with cIMP (inosine 3',5' cyclic phosphate). The purine cyclic nucleotides under study here are cIMP, 8-methylthioadenosine 3',5' cyclic phosphate (an analogue of cAMP) and 6-chloropurine riboside 3',5' cyclic phosphate. Conformational work reported on this type of ligand is both limited and conflicting.

Studies on cAMP have also been undertaken in these laboratories. Gd(III) broadening experiments have indicated that cAMP exists approximately 40% of the time in a syn conformation and the other 60% in an anti conformation[90].

Potential energy studies by Yathindra et al[81] on cIMP and cAMP predict that the former favours a syn conformation to an anti by 70:30, whilst the latter shows a preference for an anti conformation rather than a syn conformation by 70:30. Saran et al[82] report a global energy minimum at $\phi_{CN} = 90^{\circ}$ and a local one at $\phi_{CN} = -90^{\circ}$ for purine cyclic nucleotides, both being borderline between syn and anti conformations. Using lanthanide shift techniques on cAMP Lavallee et al[47] report that there is only one conformational state of the molecule at pD 5,3 and this is where $\phi_{CN} = 86^{\circ}$ (in the syn conformation). Klee and Mudd[89] have suggested on the basis of large differences in ORD amplitudes between adenosine and cAMP, that the latter is predominantly syn. However, Schweizer and Robins[80] interpret their PMR and Fourier Transform $^{31}P$ spectra results as indicating the existence of an anti conformation for cAMP. Their work on some 8-substituted cAMPs is applicable to the present study. They predict

preference for a syn conformation for both 8-thioadenosine 3',5' cyclic phosphate and 8-methylaminoadenosine 3',5' cyclic phosphate. Finally, cIMP is proposed to be primarily anti since a significant deshielding was seen at H-2' and H-3'. All the above work by Schweizer and Robins is, however, open to some degree of doubt as the solutions used were 0.25M, at which concentration significant stacking effects would come into play.

Blackburn et al[85] using coupling constant data have shown the furanose ring of cAMP to be $^{3}_{4}T$. They also conclude that the cyclic phosphate ring is locked in the chair conformation and not in the more flexible boat conformation. Kainosho et al[84] predict slightly different ribose conformations also from coupling constant data finding $^{3}T$ conformations for both cAMP and cIMP. Barry et al[36] suggest a $^{3}T$ ribose conformation using shift data as well as predicting an anti conformation, $\phi_{CN} = -34^{\circ}$ for cAMP at pH 2,0. Their relaxation data on cAMP gave no conclusive results.

Finally, crystal structures have been determined for both cAMP[48] and cIMP[91]. cAMP shows two molecules in the asymmetric unit which have different conformations about the glycosidic bond, one being syn with $\phi_{CN} = 102^{\circ}$ and the other anti with $\phi_{CN} = -50^{\circ}$. The other structural details of the molecules are the same, namely with a $_{4}T$ ribose conformation and the phosphate ring in the chair configuration. cIMP is in the anti conformation with $\phi_{CN} = -22^{\circ}$. The ribose is in a $^{3}T_{4}$ conformation. This information, while being valuable is not necessarily that which is found in solution.

The present study involves percentage syn/anti determinations and then with the aid of these results Mn(II) binding sites and their percentage occupations will be treated.

3.5.1 Broadening techniques using Gd(III) with cIMP, 6-chloropurine riboside 3',5' cyclic phosphate and 8-methylthioadenosine 3',5' cyclic phosphate.

Gd(III) is used here as the broadening agent in order to study the syn/anti conformations of these purine cyclic nucleotides quantitatively. The assumption is made that the molecule spends nearly all its time in either a syn or an anti conformation and negligible time in any intermediary conformation. The assumption is based on potential energy calculations[81]. The adaptation of equation 1.21 to suit this assumption is shown in the experimental section 3.6.

cIMP - Gd(III)

The spectrum of cIMP is shown in Fig. 3.29(a) and after addition of Pr(III) in Fig. 3.29(b). This shifted spectrum, which enables the ribose proton resonances to be differentiated, was used for the broadening experiments, Fig. 3.29(c) showing the spectrum after addition of $6,3 \times 10^{-4}$ M Gd(III). The results of the broadening observed during the metal titration are shown in Fig. 3.30 in the form of a plot of $T_{2p}^{-1}$ vs. f. Since cIMP has an oxygen donor site on the base it is possible that there is some base binding of the Gd(III). This is verified by the differential broadening of inosine proton resonances caused by Gd(III). Therefore a correction has been made to the slopes of the plots shown in Fig. 3.30 the results for the base protons being shown in Table 3.21.

TABLE 3.21

Slopes, in terms of $1/f\ T_{2p}$, for the cIMP base protons after correction for base binding

| Proton | Slope |
|---|---|
| H-2 | 144 |
| H-8 | 1296 |

Fig. 3.29 Broadening of the cIMP NMR spectrum with Gd(III)

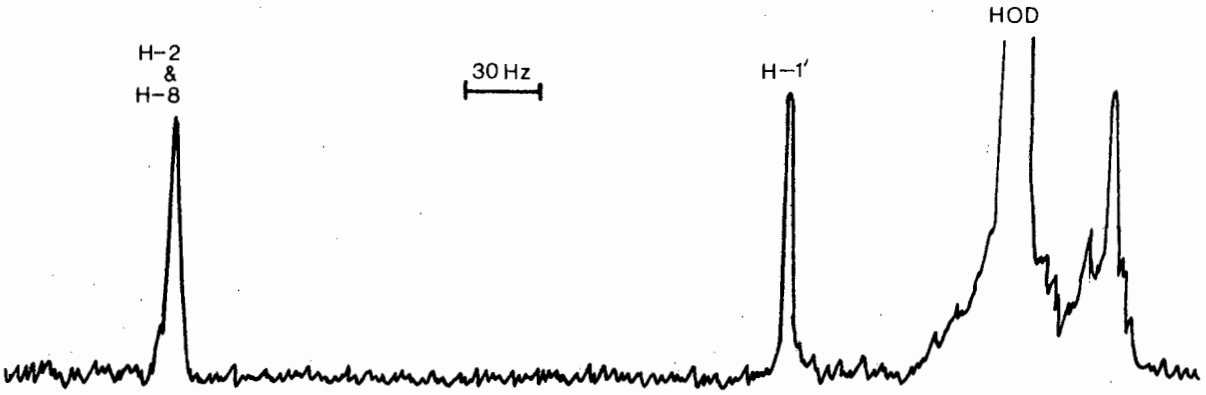


(a) cIMP, 0,04M, pH 5,5, 23°C

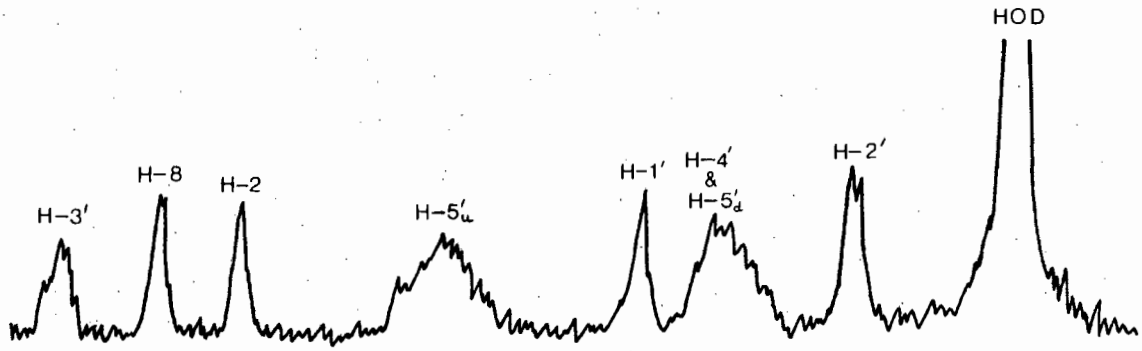


(b) (a) + 50µl ~3,3M Pr(III)

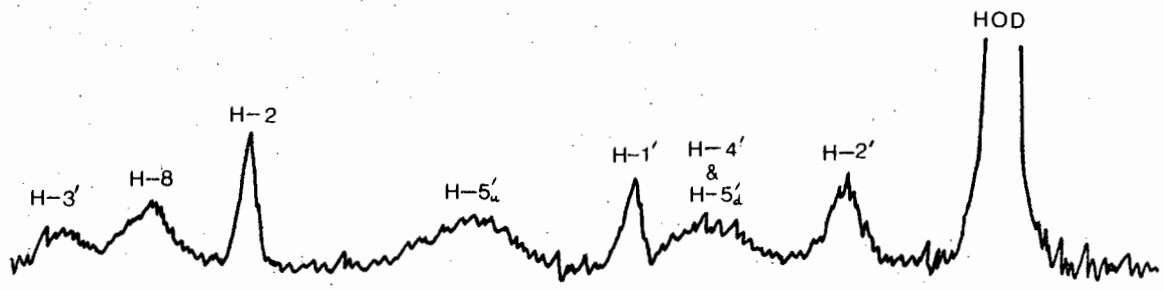


(c) (b) + 6,3 x $10^{-4}$M Gd(III)

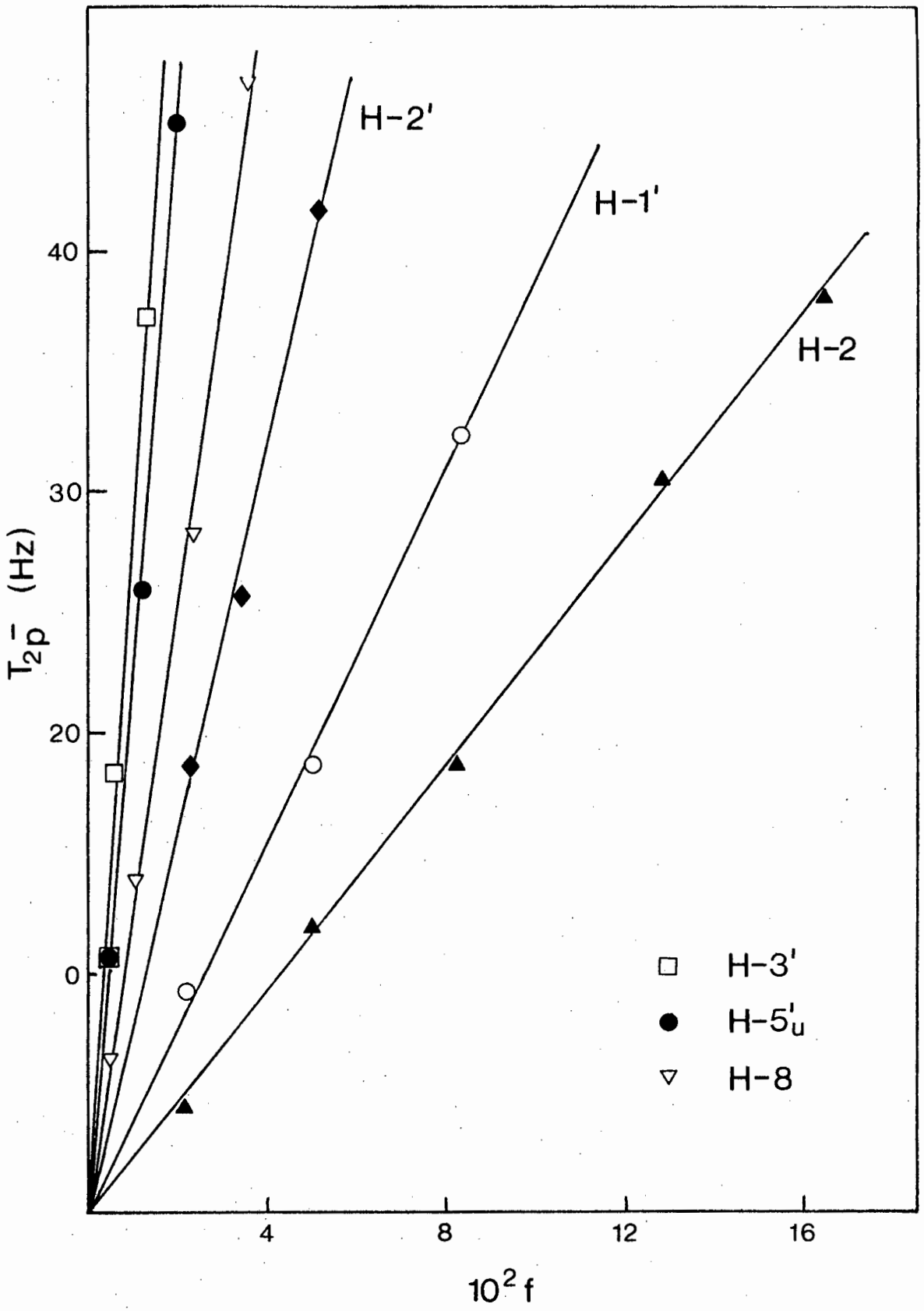


Fig. 3.30 Measured values of $T_{2p}$ for cIMP - Gd(III) as a function of f, pH 5,5, 23°C.

From these slope values the relative metal-proton internuclear time-averaged distances can be calculated. Measurements of the broadening caused by Gd(III) on the H-2 and H-8 resonances of cIMP, in the absence of Pr(III), gave final slope values in terms of $1/fT_{2p}$, in the same ratio as those values found in the presence of a substantial concentration of Pr(III). This means that any effect the Pr(III) might have on the system is negligible in terms of changing the conformation of the complex in solution. Since the cIMP - Gd(III) complex is not in a rigid conformation but in a rapid syn/anti equilibrium, the Gd(III), with respect to the base, can occupy two alternative positions, one whilst the molecule is in a syn conformation, and the other whilst it is in an anti conformation. Thus Gd(III), although it is bound only to the phosphate oxygens, can have two binding sites or positions in space with respect to the H-2 and H-8 base protons. These theoretical distances from Gd(III) to the protons were measured on a Dreiding model of the complex for chosen $\phi_{CN}$ values and ribose conformations. The $\phi_{CN}$ values selected were those values corresponding to the centre of the potential energy wells reported by Yathindra et al[81] and they are $-60^{\circ}$ (anti) and $120^{\circ}$ (syn). Values $20^{\circ}$ on either side of these were also used to test the errors involved in small rotations about the glycosidic bond. In addition $\phi_{CN}$ (anti) values corresponding to the cIMP crystal structure[90] and $\sim 20^{\circ}$ less were used, namely $\phi_{CN} = -22^{\circ}$ and $\phi_{CN} = 0^{\circ}$. The ribose conformation was also varied from ${}_4T$ to ${}^3_4T$ through to ${}^3T$. The computer analyses of the percentage time Gd(III) spends at each of the two sites, (which are effectively the percentage syn and anti times for the complex) are shown in Table 3.22 for all the possible combinations of conformations.

TABLE 3.22

The experimentally determined percentage times cIMP - Gd(III) spends in the syn and anti conformations.

| Ribose Conf. | Syn $\phi_{CN}$ | Anti $\phi_{CN}$ | % syn | % anti |
|---|---|---|---|---|
| $_4T$ | 140° | -80° | 5,0 | 95,0 |
| | 120° | -80° | 3,5 | 96,5 |
| | 100° | -80° | 3,5 | 96,5 |
| | 140° | -60° | 6,2 | 93,8 |
| | 120° | -60° | 4,3 | 95,7 |
| | 100° | -60° | 4,3 | 95,7 |
| | 140° | -40° | 4,1 | 95,9 |
| | 120° | -40° | 2,9 | 97,1 |
| | 100° | -40° | 2,9 | 97,1 |
| | 140° | -22° | 1,7 | 98,2 |
| | 120° | -22° | 1,2 | 98,8 |
| | 100° | -22° | 1,2 | 98,8 |
| | 140° | 0° | No fit | |
| | 120° | 0° | No fit | |
| | 100° | 0° | No fit | |
| $^3T$ | 140° | -80° | 5,7 | 94,3 |
| | 120° | -80° | 3,0 | 97,0 |
| | 100° | -80° | 3,1 | 96,9 |
| | 140° | -60° | 6,0 | 94,0 |
| | 120° | -60° | 3,2 | 96,8 |
| | 100° | -60° | 3,3 | 96,7 |
| | 140° | -40° | 4,8 | 95,2 |
| | 120° | -40° | 2,5 | 97,5 |
| | 100° | -40° | 2,7 | 97,3 |
| | 140° | -22° | 3,9 | 96,1 |
| | 120° | -22° | 2,0 | 98,0 |
| | 100° | -22° | 2,2 | 97,7 |
| | 140° | 0° | No fit | |
| | 120° | 0° | No fit | |
| | 100° | 0° | No fit | |

TABLE 3.22 (Contd.)

| Ribose Conf. | Syn $\phi_{CN}$ | Anti $\phi_{CN}$ | % syn | %anti |
|---|---|---|---|---|
| $^3_4T$ | 140° | -80° | 7,9 | 92,1 |
| | 120° | -80° | 5,3 | 94,7 |
| | 100° | -80° | 5,3 | 94,7 |
| | 140° | -60° | 7,9 | 92,1 |
| | 120° | -60° | 5,3 | 94,7 |
| | 100° | -60° | 5,3 | 94,7 |
| | 140° | -40° | 6,4 | 93,6 |
| | 120° | -40° | 4,2 | 95,8 |
| | 100° | -40° | 4,2 | 95,8 |
| | 140° | -22° | 2,9 | 97,1 |
| | 120° | -22° | 1,9 | 98,1 |
| | 100° | -22° | 1,9 | 98,1 |
| | 140° | 0° | No fit | |
| | 120° | 0° | No fit | |
| | 100° | 0° | No fit | |

Table 3.22 shows a remarkably small range in syn and anti values over a fairly wide range of conformational variables. Hence even if the ribose conformation is not known exactly nor the torsion angles exactly very little accuracy is lost as a result. The most generally reported ribose conformation reported for cIMP is $^3T$ and this would, on average, mean that for 96,5% of the time the molecule would be in an anti conformation and the remaining 3,5% in a syn conformation.

All the previous measurements were made on Dreiding models of the complex, where (C-4) - ($\hat{N}$-9) - (C-1') = 137° for the syn conformation and (C-8) - ($\hat{N}$-9) - (C-1') = 138° for the anti conformation. These angles are those reported in the crystal structure of cAMP[48] and for the same reasons stated in 3.4.1 it is a reasonable assumption to expect their existence in solution.

6-chloropurine riboside 3',5' cyclic phosphate - Gd(III).

Gd(III) broadening was carried out on the ligand proton resonances in the same way as the cIMP - Gd(III) experiment. A small amount of ethylenediaminetetraacetic acid (EDTA) was added to the solution to prevent precipitation. Pr(III) was again used to shift the spectrum so that ribose proton resonances could be observed. The slopes in terms of $1/fT_{2p}$ measured from the $T_{2p}^{-1}$ vs. f plot are shown in Table 3.23.

TABLE 3.23

Slopes in terms of $1/fT_{2p}$, for the 6-chloropurine riboside 3',5' cyclic phosphate protons.

| Proton | Slope |
|---|---|
| H-2 | 845 |
| H-8 | 885 |
| H-1' | 463 |
| H-2' | 928 |
| H-3' | 6286 |
| H-5'u | 4485 |

pH 1,7, 23°C

Since no experimentation in the form of either potential energy work on a crystal structure has been done on this ligand, $\phi_{CN}$ values corresponding to the cAMP crystal structure[48] have been used. Thus with the use of the H-2 and H-8 slope values and the various distance measurements the percentage times in the syn and anti conformations have been calculated (Table 3.24).

TABLE 3.24

The experimentally determined percentage times 6-chloropurine riboside 3',5' cyclice phosphate - Gd(III) spends in the syn and anti conformations.

| Ribose Conf. | Syn $\phi_{CN}$ | Anti $\phi_{CN}$ | % Syn | % Anti |
|---|---|---|---|---|
| $_4T$ | 122° | -70° | 56,4 | 43,6 |
| | 102° | -70° | 55,4 | 44,6 |
| | 82° | -70° | 64,7 | 35,3 |
| | 122° | -50° | 56,3 | 43,7 |
| | 102° | -50° | 55,3 | 44,7 |
| | 82° | -50° | 64,6 | 35,4 |
| | 122° | -30° | 50,4 | 49,6 |
| | 102° | -30° | 49,4 | 50,6 |
| | 82° | -30° | 59,0 | 41,0 |
| $^3T$ | 122° | -70° | 35,7 | 64,3 |
| | 102° | -70° | 35,8 | 64,2 |
| | 82° | -70° | 53,0 | 47,0 |
| | 122° | -50° | 36,9 | 63,1 |
| | 102° | -50° | 36,9 | 63,1 |
| | 82° | -50° | 54,2 | 45,8 |
| | 122° | -30° | 31,2 | 68,8 |
| | 102° | -30° | 31,3 | 68,7 |
| | 82° | -30° | 47,9 | 52,1 |
| $^3_4T$ | 122° | -70° | 42,3 | 57,7 |
| | 102° | -70° | 41,1 | 58,9 |
| | 82° | -70° | 54,1 | 45,9 |
| | 122° | -50° | 41,2 | 58,8 |
| | 102° | -50° | 40,0 | 60,0 |
| | 82° | -50° | 52,9 | 47,1 |
| | 122° | -30° | 35,6 | 64,4 |
| | 102° | -30° | 52,9 | 47,1 |
| | 82° | -30° | 35,6 | 64,4 |

The above results indicate the need in this case to know the

ribose conformation since the percentages change by approximately 15% as the ribose changes from a $_4T$ conformation to a $^3T$ conformation. There is a greater range of percentage values within a set of results for one particular ribose conformation than for the previous results for cIMP - Gd(III). In each case the results which differ the most are when considering the $\phi_{CN}$ syn value of 82°. On the potential energy diagram[81] for cAMP this value is just out of the energy well range and falls at a very high energy value. It is therefore a very unlikely conformation for the molecule and these results should not be taken into account. If a $^3T$ conformation which has been found to be preferable for several other purine cyclic nucleotides[84] is equally so for this ligand then the average percentage syn and anti times are 34,6% and 65,4% respectively. Although the anti conformer still dominates it is much reduced, the results being very similar to those found for cAMP which has also been investigated in our laboratories[83].

Angles where (C-4) - ($\hat{N}$-9) - (C-1') = 137° for the syn conformation and (C-8) - ($\hat{N}$-9) - (C-1') = 138° for the anti conformation were again used. In these experiments the Gd(III) and Pr(III) will be bound not only to the phosphate group but to EDTA with water molecules taking up any remaining vacant sites. This obviously forms a fairly bulky complex but studies on the Dreiding models show that at these angles where the ribose is pushed away from the base no additional steric hindrance is encountered. In addition Dobson et al[92] report no effects other than solubility factors produced by the addition of EDTA to their experiments with cytidine 5'-monophosphate and Ln(III) ions.

8-methylthioadenosine 3',5' cyclic phosphate - Gd(III).

Gd(III) was used to broaden the spectrum of 8-methylthioadenosine 3',5' cyclic phosphate after Pr(III) had been added to shift the spectrum. The slope for each proton in terms of $1/fT_{2p}$ was measured from the plot of $T_{2p}^{-1}$ vs. f. No correction to the slopes is necessary for base binding, since the addition of Gd(III) to adenosine gave no differential broadening of the protons. This is expected since adenosine has no suitable oxygen binding sites. Table 3.25 shows the measured slope values for each observable proton.

TABLE 3.25

Slopes in terms of $1/fT_{2p}$ for the 8-methylthioadenosine 3',5' cyclic phosphate protons.

| Proton | Slope |
|---|---|
| $H_2$ | 2786 |
| $CH_3$ | 573 |
| $H_1'$ | 986 |
| $H_3'$ | 11264 |
| $H_5'u$ | 16292 |

pH 5,4, 23°C

Due to the large methylthio group attached to the adenine ring at C-8 there are severe conformational restrictions to the complex in both syn and anti conformations. Firstly, the only ribose conformation possible due to steric factors is the $_4T$ conformation. For any other conformation there is a large base - ribose interaction.

Secondly, in the anti conformation (C-8) - (N-9) - (C-1') = 138° is used but in the syn conformation no movement of the base away from the ribose is possible since it causes H-1' to interact with the methylthio group. $\phi_{CN}$ values used are the same as in the previous experiment. In connection with the S-Me proton time averaged distance measurements, the S-Me group was allowed restricted rotation only. No atoms were permitted closer than the sum of their van der Waals radii. The percentage syn and anti times were calculated by a computer programme using the above data, the results being reported in Table 3.26.

TABLE 3.26

The experimentally determined percentage times 8-methylthioadenosine 3',5' cyclic phosphate - Gd(III) spends in the syn and anti conformations.

| Ribose Conformation | Syn $\phi_{CN}$ | Anti $\phi_{CN}$ | % Syn | % Anti |
|---|---|---|---|---|
| $_4T$ | 122° | -70° | 77,4 | 22,6 |
| | 102° | -70° | 75,3 | 24,7 |
| | 82° | -70° | 87,6 | 12,4 |
| | 122° | -50° | 77,4 | 22,6 |
| | 102° | -50° | 75,3 | 24,7 |
| | 82° | -50° | 87,6 | 12,4 |
| | 122° | -30° | 75,8 | 24,2 |
| | 102° | -30° | 73,6 | 26,4 |
| | 82° | -30° | 86,6 | 13,4 |

Again the results where $\phi_{CN}$(syn) = 82° are substantially different and these may be disregarded for the same reasons as stated in the previous experiment. The above results are calculated quantitatively but due

to the multiple restrictions which have been imposed on the system they should only be regarded qualitatively. That is, this complex can be considered as mainly in the syn conformation but not totally, this being expected due to the large substituent at C-8.

Experimental data showing the differences in K values for the protons of the purine cyclic nucleotides being studied.

Equation 1.21 in section 1.4.6 can be shortened to give:

$$\frac{1}{f(T_{2p})_i} = K \frac{1}{r_i^6} \quad \ldots\ldots \quad 3.1$$

for a proton $H_i$, where $\tau_c$ is a component of the constant K. As $\tau_c$ is normally determined by the overall tumbling of the molecule it should be the same for all protons in the ligand.

In the Gd(III) broadening experiments the slopes in terms of $1/fT_{2p}$ for protons H-2 and H-8 were used in order to calculate the syn/anti ratios in the complex. The resultant K value corresponding to H-2 and H-8 was calculated. This value is shown in Table 3.27 together with the K values for the ribose protons, which are easily calculated by substituting their slopes in terms of $1/fT_{2p}$ and their fixed distances, r, from the Gd(III) on the phosphate, into equation 3.1.

TABLE 3.27.

K values for the protons in the Gd(III) broadening experiments.

| Complex | Proton | K x $10^{-7}$ |
|---|---|---|
| [a] cIMP - Gd(III) | H-2 | 12 |
| | H-8 | 12 |
| | H-1' | 10 |
| | H-2' | 4,6 |
| | H-3' | 2,6 |
| | H-5'u | 2,8 |
| [a] 6-chloropurine riboside 3',5' cyclic phosphate - Gd(III) | H-2 | 16 |
| | H-8 | 16 |
| | H-1' | 12 |
| | H-2' | 5,8 |
| | H-3' | 5,6 |
| | H-5'u | 4,8 |
| [b] 8-methylthio-adenosine 3',5' cyclic phosphate - Gd(III) | H-2 | 27 |
| | $CH_3$ | 27 |
| | H-1' | 24 |
| | H-3' | 10 |
| | H-5'u | 18 |

[a] Ribose conformation $^3_4T$

[b] Ribose conformation $_4T$

The relevance of the results shown above will be given in section 3.5.2.

3.5.2 Broadening techniques using Mn(II) with cIMP, 6-chloropurine riboside 3',5' cyclic phosphate and 8-methylthioadenosine 3',5' cyclic phosphate.

The broadening of the ligand proton resonances with Mn(II) enables the binding sites and the percentage times the metal occupies these sites, to be found for the above nucleotides provided that the syn/anti ratios calculated in the previous section 3.5.1 are assumed to remain the same in these systems. The ribose conformations found by other workers must also be assumed.

Since there are now multiple binding sites to be considered for the Mn(II) ion there must be at least an equal number of protons observed in each case to enable the computer programme to calculate the results. This means that some of the ribose proton data must be considered. In section 3.5.1 even though the ribose protons were not required their slope values in terms of $1/fT_{2p}$ were recorded. In addition, from these values their K values were calculated and compared with the K value found for the base protons. This data is shown in Table 3.27. The K values for H-1' are the same as the base proton values within the limits of experimental error. However, the other ribose protons have K values which give consistently low readings. This is effectively saying that the broadening of the ribose protons (except H-1') is too slow or that the broadening of the base protons and H-1' is too fast. The possible source for this deviation from what is expected is in the value of $\tau_c$, the dipolar correlation time, which is considered as a constant in equation 1.21 for all the protons. This correlation time

is determined by $\tau_r$ which is the rotational correlation time or 'tumbling' time for the molecule and one would expect it to be the same for all the protons. However, in all the molecules studied here, except 8-methylthioadenosine 3',5' cyclic phosphate, there is a ribose ring which is free to flip between the $^3T$ conformation and the $_4T$ conformation with little energy barrier. This flipping can, therefore, be very rapid and would move all the ribose protons with respect to the base except H-1'. This would effectively change the correlation times for these protons with respect to the base protons and H-1'. Syn/anti flipping would not give this effect since there is a large potential energy barrier between the two conformations thereby preventing rapid enough flipping to alter correlation times.

In the case of 8-methylthioadenosine 3',5' cyclic phosphate the K values for the ribose protons H-3' and H-5'u are only slightly lower than the value for the base protons and H-1'. This is probably due to the restricted flipping of the ribose ring in this molecule as described in section 3.5.1.

To calculate the populations of Mn(II) at the various postulated binding sites, it is necessary to provide theoretical data for binding wholly at each site. Clearly this must now take into account the two observed correlation times in the molecule. The theoretical values of $1/fT_{2p}$ are derived by measuring internuclear distances from the models which should then be weighted according to the differences in correlation times observed in the Gd(III) experiments. This correction is done more simply by adjusting the observed $1/fT_{2p}$ data for the ribose protons (except H-1') and is the method employed for the following experiments.

cIMP - Mn(II)

The assumptions made for the cIMP - Mn(II) complex are that the ligand is 96,5% of the time in an anti conformation and the remainder in the syn conformation. The ribose is considered to be in a $^3T$ conformation.

The spectrum of cIMP was shifted with Pr(III) and then Mn(II) added. The results of the Mn(II) titration with cIMP are shown in Fig. 3.31 in the form of a plot of $T_{2p}^{-1}$ vs. f. The values of the slopes of the plots in Fig. 3.31 are shown in Table 3.28, the H-3' and H-5'u values having been corrected.

TABLE 3.28

Slopes in terms of $1/fT_{2p}$, for the cIMP protons.

| Proton | Slope |
|---|---|
| H-2 | 120 |
| H-8 | 1328 |
| H-1' | 112 |
| H-3' | 1638[a] |
| H-5'u | 1457[a] |

a Value corrected for different $\tau_c$ value.

There are several potential binding sites for Mn(II) on cIMP and these are shown in Fig. 3.32.

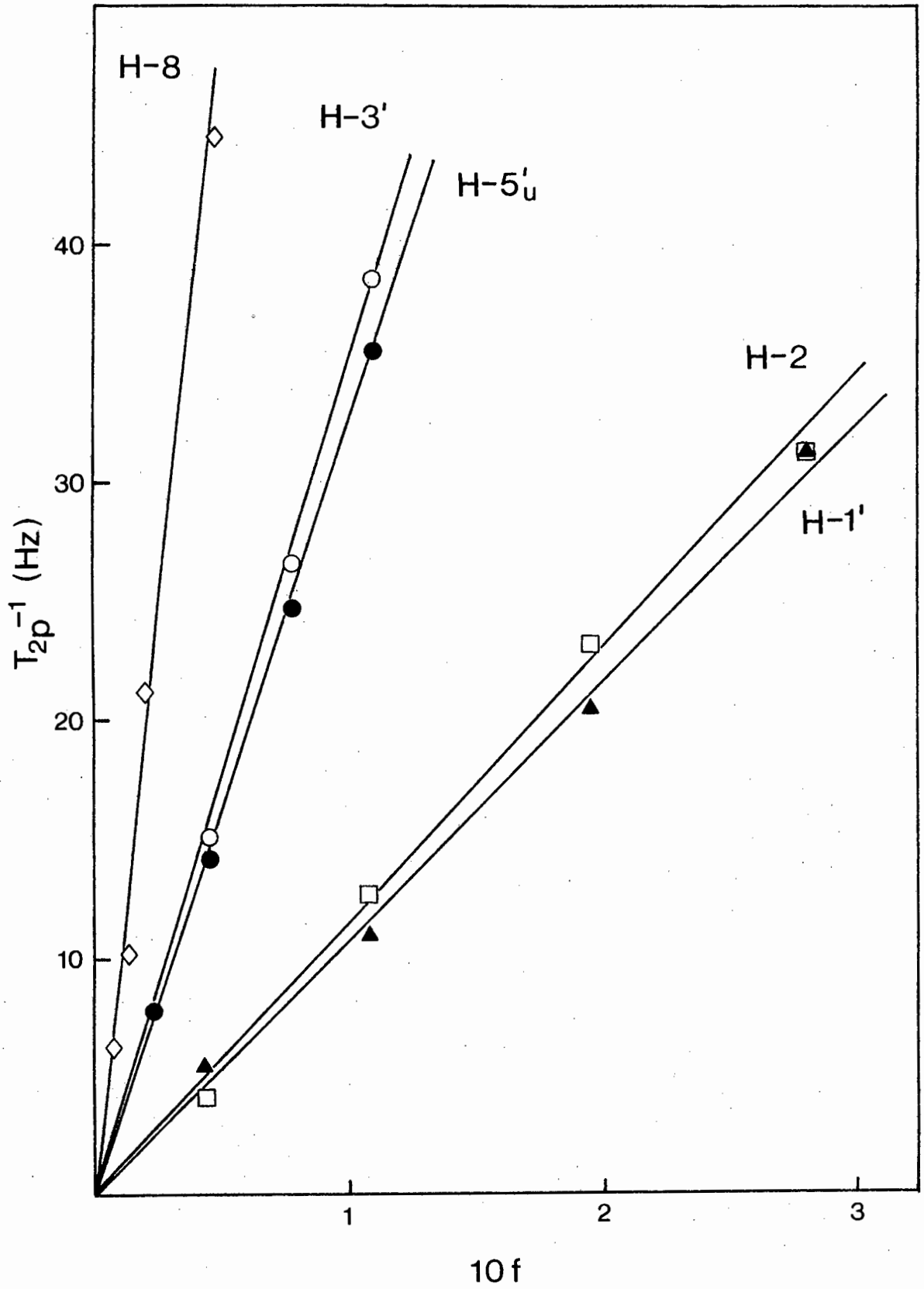


Fig. 3.31 Measured values of $T_{2p}$ for cIMP - Mn(II) as a function of f, pH 5,3, 23°C.

Fig. 3.32 Possible binding sites for Mn(II) on cIMP

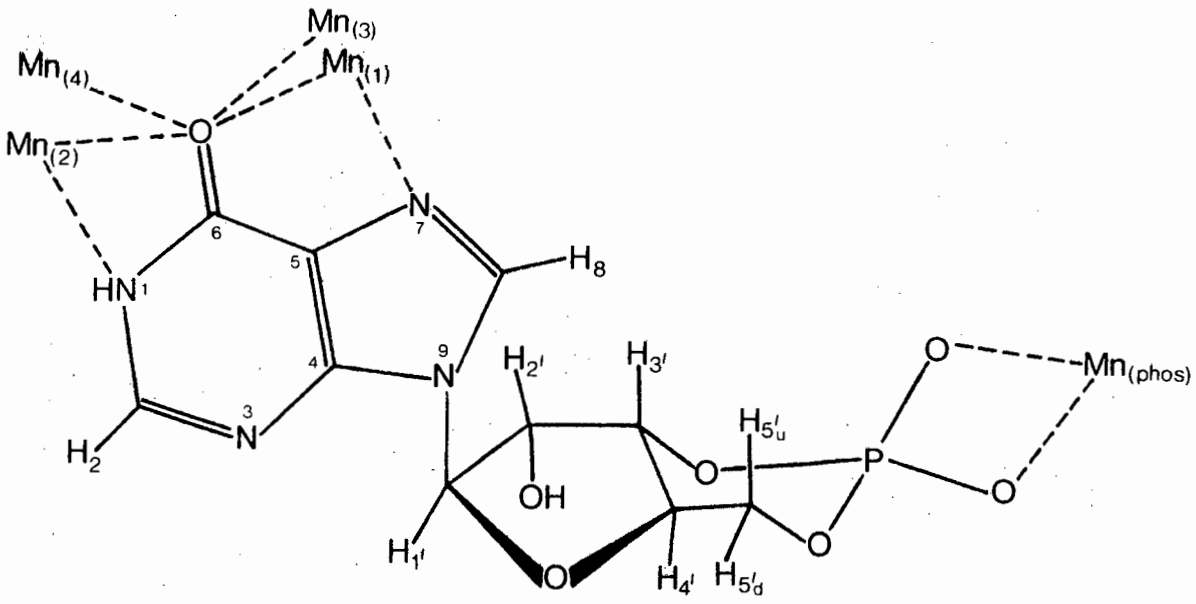


The sites $Mn_{(2)}$, (3), (4) are not considered as likely due to the results obtained from the binding of Mn(II) to 9-methylhypoxanthine and 2',3'-O-isopropylidene inosine in section 3.3.2. There only binding at site $Mn_{(1)}$ was found. However, the binding site $Mn_{(2)}$ was used as a potential site in the calculations here as an additional test. Distances from the metal at each binding site to the protons were measured on Dreiding models of the complex and a computer programme was used to find the best fit for the binding site and percentage binding time determinations. The results are reported in Table 3.29.

TABLE 3.29.

The experimentally determined binding sites and percentage binding times at each site for cIMP - Mn(II).

| Site | % binding time |
|---|---|
| $Mn_{(phos)}$ | 71 |
| $Mn_{(1)}$ | 29 |
| $Mn_{(2)}$ | 0 |

As expected there is no binding of Mn(II) in the vicinity of N-1 and O-6 (the $Mn_{(2)}$ site). The K values for all the five protons used to obtain the above results, agree very well indicating a good fit. The greater percentage of Mn(II) bound to the phosphate is as expected due to the favourable bidentate bonding to the two oxygens which forms a non-strained four membered ring.

6-chloropurine riboside 3',5' cyclic phosphate - Mn(II).

The assumptions made for the 6-chloropurine riboside 3',5' cyclic phosphate - Mn(II) complex are that the ligand is 65,4% of the time in an anti conformation and the remainder in the syn conformation. The ribose is considered to be in a $^3T$ conformation.

The ligand spectrum was shifted with Pr(III) and the resultant spectrum used for the Mn(II) titration, the results of which were plotted in the form of $T_{2p}^{-1}$ vs. f (Fig. 3.33). The slopes of the plots were measured and these are shown in Table 3.30 together with the slopes in terms of $1/fT_{2p}$ for the Gd(III) experiment. The ratios of

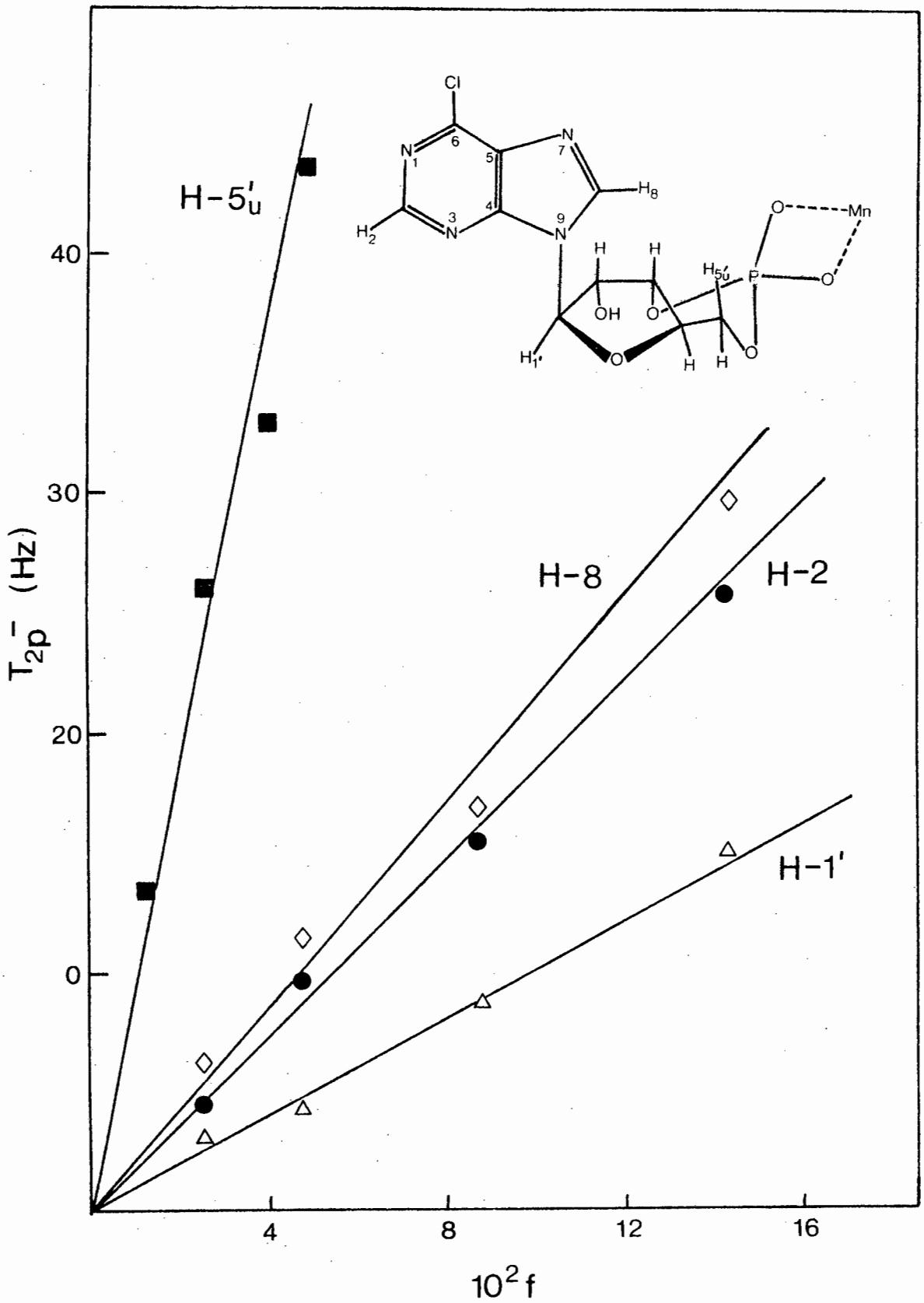


Fig. 3.33 Measured values of $T_{2p}$ for 6-chloropurine riboside 3',5' cyclic phosphate - Mn(II) as a function of f, pH, 1,7, 23°C.

the relative slope values are also given.

TABLE 3.30.

Comparison of the relative slopes in terms of $1/fT_{2p}$ for the Gd(III) and Mn(II) experiments with 6-chloropurine riboside 3',5' cyclic phosphate.

| | Gd(III) experiment | | Mn(II) experiment | |
|---|---|---|---|---|
| Proton | Slope | Slope ratios[a] | Slope | Slope ratios[a] |
| H-2 | 845 | 0,95 | 181 | 0,90 |
| H-8 | 885 | 1,00 | 211 | 1,05 |
| H-1' | 463 | 0,52 | 101 | 0,50 |
| H-5'u | 14800[b] | 16,72 | 3195[b] | 15,90 |

[a] Relative to H-8

[b] Corrected for different $\tau_c$ values.

The data shown in Table 3.30 implies that the binding sites for Mn(II) are the same as for Gd(III) assuming extremely little experimental error. This means that Mn(II) binds totally to the phosphate group, there being no base binding. This is not unexpected since, from the previous experiments involving binding of Mn(II) to the bases in section 3.3.2, the site in the vicinity of N-7 was found to be the most favourable. Binding here can be stabilized by either the oxygen substituents at C-6 or the nitrogen substituent at C-6 in the molecules considered so far. However, in this case chlorine is the C-6 substituent and since it does not bind Mn(II) the site in this vicinity is not as favourable as was previously the case.

8-methylthioadenosine 3',5' cyclic phosphate - Mn(II).

The assumptions made here are that the complex spends

approximately 75% of the time in a syn conformation and the remainder in an anti conformation. The ribose is still restricted to a $_4T$ conformation.

The results of the Mn(II) titration with the ligand were recorded in the form of plots of $T_{2p}^{-1}$ vs, f. The slopes of these plots are shown in Table 3.31.

TABLE 3.31.

Slopes in terms of $1/fT_{2p}$ for the 8-methylthioadenosine 3',5' cyclic phosphate protons.

| Proton | Slope |
|---|---|
| H-2 | 2395 |
| $CH_3$ | 312 |
| H-1' | 629 |

pH 5,4. $23^{o}C$.

Due to the large number of restrictions and assumptions made for this system, the results will only be treated qualitatively.

The slope values in Table 3.31 differ from those in the Gd(III) experiment Table 3.25 which indicates that the same base binding is present here. A comparison of the relative slope values for the two experiments is shown in Table 3.32.

TABLE 3.32

Comparison of relative slope values for the Gd(III) and Mn(II) experiments.

| Proton | Gd(III) Slope ratios[a] | Mn(II) Slope ratios[a] |
|---|---|---|
| H-2 | 1 | 1 |
| $CH_3$ | 0,21 | 0,13 |
| H-1' | 0,35 | 0,26 |

[a] Relative to H-2

Fig. 3.34 shows the possible binding sites for Mn(II) on the ligand.

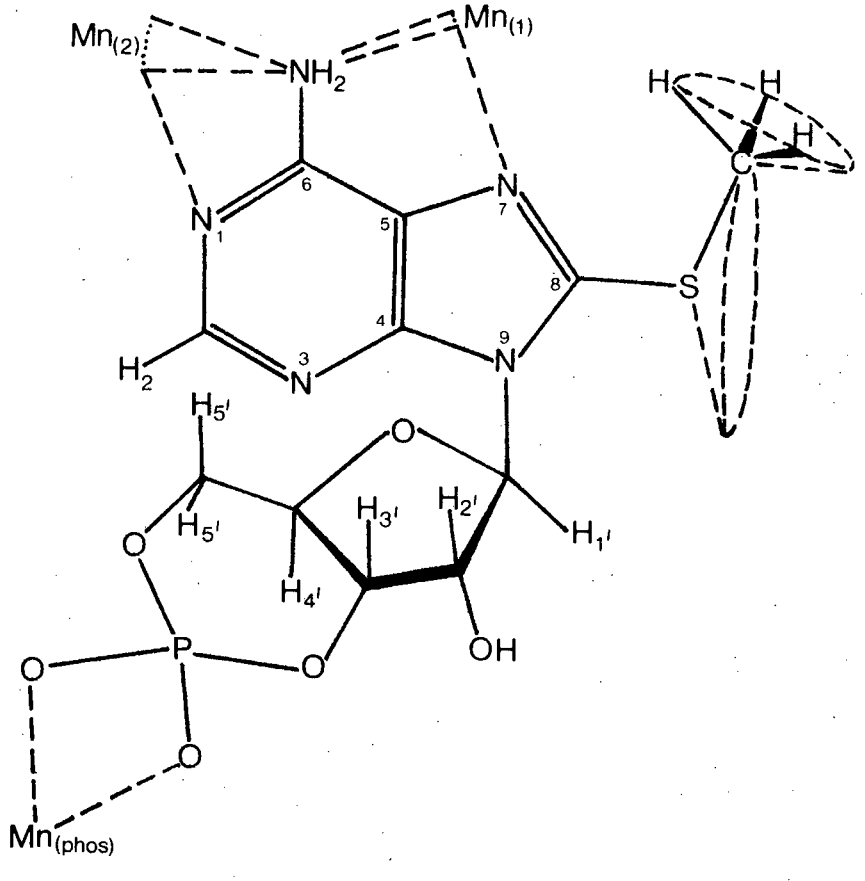


Fig. 3.34 Possible binding sites for Mn(II) on 8-methylthioadenosine 3',5' cyclic phosphate.

The $Mn_{(1)}$ site seems unlikely due to the steric hindrance of the -SMe group and since binding there would cause the slope for $CH_3$ to increase, the results obviously show no binding in that vicinity. The slope value for H-2 rises a little relative to the other protons. Since the $Mn_{(2)}$ site (either monodentate to N-1 or bidentate to (N-1) and (N-6)) is very close to H-2 only a small percentage of Mn(II) need bind there to give this alteration in the slope values, the dominant binding site, therefore, still being on the phosphate group.

### 3.5.3 General discussion

The results put forward in the previous sections 3.5.1 and 3.5.2 are the first quantitative determinations of these cyclic nucleotide conformations. Generally it seems that purine cyclic nucleotide complexes exist in an anti conformation for the greater part of their life times as seen for cIMP - Gd(III) ~96%, 6-chloropurine riboside 3',5' cyclic phosphate - Gd(III) ~65% and cAMP - Gd(III) ~60%[90]. However, why the percentages vary so much between these very similar molecules (they only differ in their substituents at C-6) is not easily explicable.

Again in this section 3.5 all measurements were made on models where the base and ribose rings were moved away from each other. Especially in these systems where a more bulky purine ring replaces a pyrimidine ring as base, this important parameter should be taken into account.

## 3.6 Experimental

The 1-methyl hypoxanthine and the cIMP were obtained from Sigma Chemical Co., 9-methyl hypoxanthine, 2',3'-O-isopropylidene inosine, and 1-methyl inosine from Cyclo Chemicals and all the remaining ligands from P-L Biochemicals, Inc. These ligands were used without further purification.

Analar $MnCl_2.6H_2O$ (1M, $1 \times 10^{-1}$ M and $1 \times 10^{-2}$ M) and $Gd(NO_3)_3.6H_2O$ (1M, $1 \times 10^{-1}$ M and $1 \times 10^{-2}$ M) solutions were prepared in $D_2O$ and adjusted to the relevant pH values for each experiment with NaOD or DCl. These solutions were the metal-ion sources for all the broadening experiments.

The lanthanide oxides (Ln = Pr, Dy and Ho) in $D_2O$ were treated with $HNO_3$ and evaporated to dryness. The $Ln(NO_3)_3.6H_2O$ formed was dissolved in $D_2O$ and evaporated to dryness under reduced pressure. This was repeated several times in order to substitute the $H_2O$ molecules with $D_2O$. Finally, saturated solutions were made up in $D_2O$ and altered to the pHs required for the shift experiments. It was not possible to raise their pH values much above pH 4-5 since the $Ln(OH)_3$ precipitated out.

The broadening metal-ion titrations were carried out on 0,04M solutions of the ligand in $D_2O$, small volumes of the metal-ion being added using a micro syringe. Experimentation using 0,015M ligand gave the same results as the 0,04M solutions, within experimental error, indicating that base stacking is not a major source of error.

The shifting metal-ion titrations were carried out on 0,02M solutions of the ligand in $D_2O$, DSS (3(trimethylsilyl)-propanesulphonic acid-Na salt)being added as an internal reference. The metal-ion solutions were added using a micro syringe.

The spectra were recorded on a Varian XL-100 spectrometer at a probe temperature of 23°C. Care was taken to avoid saturation effects and samples were kept in the probe for 5 minutes to attain thermal equilibrium before spectra were recorded. The pHs at which the various experiments were carried out are shown in Table 3.33.

TABLE 3.33

pHs at which experiments were carried out.

| Ligand | pH broadening experiment | | pH shifting experiment | |
|---|---|---|---|---|
| | Gd(III) | Mn(II) | Dy(III) | Ho(III) |
| 1-methyl hypoxanthine | - | 6,6 | - | - |
| 1-methyl inosine | - | 6,3 | - | - |
| 9-methyl hypoxanthine | - | 6,3 | - | - |
| 2',3'-O-isopropylidine inosine | - | 5,5 | - | - |
| cUMP | 5,3 | 5,1 | 5,5 | 5,6 |
| cCMP | 5,3 | 5,5 | 5,0 | - |
| cTMP | 6,0 | 6,2 | 5,4 | 6,0 |
| cIMP | 5,5 | 5,3 | - | - |
| 6-chloropurine riboside 3',5' cyclic phosphate | 1,7 | 1,7 | - | - |
| 8-methyl thioadenosine 3',5' cyclic phosphate | 5,3 | 5,4 | - | - |

The transverse relaxation times, $T_2$s, were estimated from the line widths ($\Delta\nu$) at half peak height.

$$T_2^{-1} = \pi\Delta\nu$$

Equation 1.24 in section 1.4.7 can be shortened as shown in section 3.5.1 to give

$$\frac{1}{f(T_{2p})_i} = K\frac{1}{r_i^6} \quad \ldots\ldots \quad 3.1$$

for a proton $H_i$, where f is the mole ratio of total metal ion to total ligand. Equation 3.1 can be adapted to give

$$\frac{1}{f(T_{2p})_i} = K\left(\frac{\tau_1}{(r_1)_i^6} + \frac{\tau_2}{(r_2)_i^6} + \cdots + \frac{\tau_n}{(r_n)_i^6}\right) \quad \ldots 3.2$$

for a proton $H_i$, where $\tau_n$ is the fraction of time spent by the metal at position $M_{(n)}$ and $r_n$ is the distance from the metal at $M_{(n)}$ to the proton $H_i$. In addition $\tau_1 + \tau_2 + \ldots\ldots \tau_n = 1$. This equation 3.2 is that which is solved by the computer programme. The various metal-proton distances plus the experimental slope values were fed into this programme, which, given a series of different starting values, found by reiteration a best fit for the fraction of time the metal ion spends at each binding site. The programme uses a SIMPLEX hill-climbing sub-routine.

In the Gd(III) experiments where the syn/anti ratios were found, equation 3.2 would be adapted to:

$$\frac{1}{f(T_{2p})_i} = K\left(\frac{\tau_{anti}}{(r_{anti})_i^6} + \frac{1-\tau_{anti}}{(r_{syn})_i^6}\right) \quad \ldots\ldots\ldots \quad 3.3$$

Here $\tau_{anti}$ is the fraction of time spent in the anti conformation and $r_{anti}$ and $r_{syn}$ are the distances from the Gd(III) in the anti and syn conformations to $H_i$ respectively.

The methyl protons average distance to the metal ion was calculated by measuring the distances from each of the three protons at a particular setting, to the metal ion and using the following equation

$$\frac{1}{r_{av}^{6}} = \frac{1}{3} \sum_{i=3}^{i=1} \frac{1}{r_i^{6}} \qquad \ldots\ldots\ldots \quad 3.4$$

For the SMe group multiple positions for the methyl were used due to rotation about the (C-8)-S bond and at each position the above methyl proton distances were measured and the $r_{av}$ found. The series of $r_{av}$s calculated were then averaged in the same way for the final distance value.

The models used for all the distance measurements were comprised of planar metal boards on to which were drawn the essentially planar base portion of the molecule and to which were attached Dreiding models of the ribose and phosphate ring structures. This structural set up eased the changing of torsion angles and conformations considerably. The base portions were drawn to scale from crystal structure data, the following structures being used cUMP[82] for itself, cytidine[93] for cCMP, thymidine[94] for cTMP, inosine[95] for cIMP and all the bases, and 5'-AMP[96] for 6-chloropurine riboside 3',5' cyclic phosphate and 8-methylthioadenosine 3',5' cyclic phosphate, since the cAMP crystal structure gives no detailed bond lengths and angles.

# PUBLICATIONS

1. "Copper (II) and Cobalt (II) Complexes of Thiamine Chloride Hydrochloride and some related Thiazoles".
G. V. FAZAKERLEY and J.C. RUSSELL. J. Inorg. Nucl. Chem., (1975) 37, 2377.

2. "Conformation of the Gadolinium Complexes of Adenosine 3',5' Cyclic Monophosphoric Acid and Inosine 3',5' Cyclic Monophosphoric Acid".
G. V. FAZAKERLEY, J. C. RUSSELL and M. A. WOLFE. J. Chem. Soc., Chem. Comm., (1975) 527.

## REFERENCES


1. R.R.WILLIAMS. Industrial and Engineering Chemistry, (1937) 29, 9, 980.
2. A.WHITE, P.HANDLER and E.L.Smith. "Principles of Biochemistry", 4th Edition, McGraw-Hill Book Co., Kogakusha Co., Ltd.
3. H.W.DOUGHERTY and P.I.POLLAK. "Medicinal Chemistry", Part II, Third Edition.
4. E.F.ROGERS. Ann. N.Y. Acad. Sci., (1962) 98, 412.
5. A.SCHELLENBERGER. Angew. Chem., (1967) 6, 1024.
6. R.J.WILLIAMS, R.E.EAKIN, E.BEERSTECHER, and W.SHIRE. "The Biochemistry of Vitamins", Reinhold Publishing Co., New York (1950) Page 686.
7. J.M.IACONO and B.C.JOHNSON. J. Am. Chem. Cos., (1957) 79, 6321.
8. F.W.LEVER and B.R.WOODY. Proc. Soc. Exptl. Biol. Med., (1964) 117(2) 359.
9. J.VAN EYS. Fed. Proc., (1960) 19, 26.
10. J.F.KUO and P.GREENGARD. Proc. Natl. Acad. Sci. USA., (1969) 64, 1349.
11. T.POSTERNAK and G.CEHOVIC. Ann.N.Y. Acad. Sci., (1971) 185, 42.
12. L.H.JEFFERSON, J.H.EXTON, R.W.BUTCHER, E.W.SUTHERLAND and C.R.PARK. J. Biol. Chem., (1968) 243, 1031.
13. E.W.SALZMAN and L.LEVINE. J. Clin. Invest., (1971) 50, 131.
14. E.W.SUTHERLAND, J.ØYE and R.W.BUTCHER. Recent Progress in Hormone Research, XXI. (1965) Page 623.
15. M.N.HUGHES. "The Inorganic Chemistry of Biological Processes". John Wiley & Sons.
16. D.R.WILLIAMS. Education in Chemistry, (1973) 10, 2.
17. B.L.VALLEE. Advances in Protein Chemistry, (1955) 10, 317.
18. K.KOBAYASHI. Vitamins, (1972) 45(5), 239.

19. A.MARZOTTO and L.GALZIGNA. 3rd National Congress of Inorganic Chemistry, Bressanone, Italy, Abstract C45.

20. W.T.KEETON. "Biological Science", 2nd Edition, W.W.Norton & Co., Inc., N.Y.

21. L. GALZIGNA. Biochem. Pharmacol., (1969) 18, 2485.

22. L. GALZIGNA. Int. J. Vit. Res., (1970) 40, 44.

23. A.MARZOTTO and L. GALZIGNA. Int. J. Vit. Res., (1971) 41, 401.

24. M.R.CAIRA, G.V.FAZAKERLEY, P.W.LINDER and L.R.NASSIMBENI. Chem. Comm., (1973) 900.

25. G.L.EICHHORN, N.A.BERGER, J.J.BUTZOW, P.CLARK, J.M.RIFKIND, Y.A.SHIN and E.TARIEN. Bioinorganic Chemistry, (1971) 135.

26. G.L.EICHHORN. Nature, (1962) 194, 474.

27. J.EMSLEY, J.FEENEY and L.SUTCLIFFE. "High Resolution Nuclear Magnetic Resonance Spectroscopy", Vols. I and II, Permagon Press, 1967.

28. J.A.POPLE, W.G.SCHNEIDER and H.J. BERNSTEIN. "High-Resolution Nuclear Magnetic Resonance", McGraw-Hill Book Co., Inc., New York, 1959.

29. R.A.DWEK. "Nuclear Megnetic Resonance in Biochemistry", Oxford University Press, 1973.

30. G.V.FAZAKERLEY and G.E.JACKSON. J. Chem. Soc., Perkin Trans. II, (1975) 567.

31. W.ESPERSEN, W.HUTTON, S.CHOW and R.MARTIN. J. Am. Chem. Soc., (1974) 96, 8111.

32. I.SOLOMON. Phys. Rev., (1955) 99, 559.

33. N.BLOEMBERGEN. J. Chem. Phys., (1957) 27, 572.

34. H.STERNLICHT, R.G.SHULMAN and E.W.ANDERSON. J. Chem. Phys., (1965) 43, 3123; (1965) 43, 3133.
R.SHULMAN, H.STERNLICHT and B.WYLUDA. J.Chem. Phys., (1965) 43, 3116.

35. T.J.SWIFT and R.E.CONNICK. J.Chem. Phys., (1962) 37, 307.

36. C.D.BARRY, J.A.GLASEL, R.J.P.WILLIAMS and A.V.XAVIER. J. Mol. Biol., (1974) 84, 491.

37. G.N.LaMAR, W.de W.HORROCKS JNR. and L.C.ALLEN. J. Chem. Phys., (1964) 41, 2126.

38. T.A.GLASSMAN, C. COOPER, L.W.HARRISON and T.J.SWIFT. Biochem., (1971) 10, 843.

39. A.A.GALLO, I.L.HANSEN, H.Z.SABLE and T.J.SWIFT. J. Biol. Chem. (1972) 247, 18, 5913.

40. W.D.WHITE and R.S.DRAGO. Inorg. Chem., (1971) 10, 12, 2727.

41. H.J.GRANDE, L.R.HOUGHTON and C.VEEGER. Ew. J. Biochem., (1973) (1973) 37, 563.

42. N.A.BERGER and G.L.EICHHORN. Biochem., (1971) 10, 1847.

43. G.L.EICHHORN and N.A.BERGER. "Jerusalem Symposia on Quantum Chemistry and Biochemistry. Vol IV, The Purines - Theory and experiment". E.D.Bergmann and P.Pullman Ed., Academic Press, Inc., New York, 1972, Page 314.

44. N.A.BERGER and G.L.EICHHORN. J.Am. Chem. Soc., (1971) 93, 7062.

45. H.FRITZSCHE. Biochim. Biophys. Acta, (1970) 224, 608.

46. G.KOTOWYCZ and O.SUZUKI. Biochem, (1973) 12, 18, 3434.

47. D.K.LAVALLEE and A.H.ZELTMANN. J. Am. Chem. Soc., (1974) 96 : 17 5552.

48. K.WATENPAUGH, J.DOW and L.H.JENSEN. Science, (1968) 159, 206.

49. P.T.TALBERT, J.A.WEAVER and P.HAMBRIGHT. J. Inorg. Nucl. Chem., (1974) 32, 2147.

50. A.MARZOTTO, M.NICOLINI, A.SIGNOR and L.GALZIGNA. Atti. Accad. Peloritana Pericolanti, Cl. Sci. Fis., Mat. Natur., (1970) 50, 79.

51. J.A.WEAVER, P.HAMBRIGHT, P.T.TALBERT, E.KANG and A.N.THORPE. Inorg. Chem. (1970) 9(2), 268.

52. D.E.BILLING and A.E.UNDERHILL. J. Inorg. Nucl. Chem., (1968) 30, 2147.

53. I.P.EVANS and G.WILKINSON. J. Chem. Co., Dalton Trans., (1974) 9, 946.

54. M.R.CAIRA and L.R.NASSIMBENI. Acta Cryst., (1974) B30, 2332.

55. M.M.THACKERAY and L.R.NASSIMBENI. Acta Cryst., (1974) B30, 2469.

56. D.M.L.GOODGAME and F.A.COTTON. J. Chem. Soc., (1961, 2298.

57. A.SABATINE and L.SACCONE. J. Am. Chem. Soc., (1964) 86, 17.

58. F.A.COTTON and G.WILKINSON. "Advanced Inorganic Chemistry". A Comprehensive Text, 3rd Edit. Interscience, New York (1971).

59. F.A.COTTON, D.M.L.GOODGAME and M.GOODGAME. J. Am. Chem. Soc., (1961) 83, 4690.

60. R.L.CARLIN. "Transition Metal Chemistry". Volume 1. E.Arnold, London (1965).

61. A.B.P.LEVER, J.LEWIS and R.S.NYHOLM. J. Chem. Soc., (1963) Part 2, 2552.

62. A.B.P.LEVER and E.MANTOVANI. Inorg. Chim. Acta. (1971) 5 : 3, 429.

63. D.J.RAYER, V.H.SCHIEVELBEIN, A.R.KALYANARAMAN and J.A.BERTRAND. Inorg. Chim. Acta (1972) 6 : 2, 307.

64. W.J.EILBECK, F.HOLMES and A.E.UNDERHILL. J. Chem. Soc., (1967) 5, 757.

65. P.W.HUNTER and G.A.WEBB. J. Chem. Soc. Dalton Trans. (1973) 1, 26.

66. J.D.DUNITZ. Acta Cryst. (1957) 10, 307.

67. I.S.AHUJA, D.H.BROWN, R.H.NUTTALL and D.W.A.SHARP. J. Inorg. Nucl. Chem., (1965) 27, 1625.

68. E.J.DUFF, M.N.HUGHES and K.J.RUTT. J. Chem. Soc., (1968) 10, Part 3A 2354.

69. M.N.HUGHES and K.J.RUTT. J. Chem. Soc., (1970) 18, 3015A.

70. M.N.HUGHES and K.J.RUTT. Inorg.Chem. (1971) 10, 2, 414.

71. R.J.H.CLARK. Spectro. Chim. Act., (1965) 21, 955.

72. R.R.WILLIAMS, R.E.WATERMAN, J.C.KERESZTESY and E.R.BUCHMAN. J. Am. Chem. Soc., (1935) 57, 536.

73. W.E.C.WACKER and B.L.VALLEE. J. Biol. Chem., (1959) 234, 3257.

74. J.DONOHUE and K.N.TRUEBLOOD. J. Mol. Biol., (1960) 2, 363.

75. M.SUNDARALINGHAM and J.ABOLA. J. Am. Chem Soc., (1972) 94 : 14, 5070.

76. G.KOTOWYCZ and K.HAYAMIZU. Biochemistry, (1973) 12, 3, 517.

77. H.STERNLICHT, D.E.JONES and K.KUSTIN. J. Am. Chem. Soc., (1968) 90, 7110.

78. M.MAEDA, M.SANEYOSHI and Y.KAWAZOE. Chem. Pharm. Bull. (1971) 19, (8) 1641.

79. A.V.E.HASCHMEYER and A.RICH. J. Mol. Biol. (1965) 13, 930.

80. M.P.SCHWEIZER and R.K.ROBINS, in "The Jerusalem Symposia on Quantum Chemistry and Biochemistry V - Conformation of Biological Molecules and Polymers". Edit. E.D.Bergmann and P.Pullman. Academic Press Inc., New York (1972) Page 329.

81. N.YATHINDRA and M.SUNDARALINGHAM. Biochem. and Biophys. Research Com., (1974) 56, 1, 119.

82. A.SARAN, H.BERTHOD and B.PULLMAN. Biochim. and Biophys. Acta, (1973) 331, 154.

83. C.L.COULTER. Acta Cryst. (1969) B25, 2055

84. M.KAINOSHO and K.AJISAKA. J. Am. Chem., Soc., (1975) 97 : 23, 6839.

85. B.J.BLACKBURN, R.D.LAPPER and I.C.P.SMITH. ibid. (1973) 95 : 9 2873.

86. G.E.HAWKES, D.LEIBFRITZ, D.W.ROBERTS and J.D.ROBERTS. ibid. (1973) 95, 1659.

87. R.M.WING, J.J.UEBEL and K.K.ANDERSON. ibid. (1973) 95, 6046.

88. C.D.BARRY, J.A.GLASEL, A.C.T.NORTH, R.J.P.WILLIAMS and A.V.XAVIER. Nature (London) (1971) 232, 236.

89. W.A.KLEE and S.H.MUDD. Biochemistry, (1967) 6 : 988.

90. G.V.FAZAKERLEY, J.C.RUSSELL and M.A.WOLFE. J. Chem. Soc., Chem. Somm., (1975) 527.

91. M.SUNDARALINGHAM. University of Wisconsin-Madison, College of Agricultural and Life Sciences (1975). Private communication.

92. C.M.DOBSON, R.J.P.WILLIAMS and A.V.XAVIER. J. Chem. Soc., Dalton (1974) 1762.

93. S.FURBERG, C.S.PETERSEN and C.ROMMING. Acta Cryst., (1965) 18, 313.

94. D.W.YOUNG, P.TOLLIN and H.R.WILSON. ibid, (1969) B25, 1423.

95. A.R.I.MUNNS and P.TOLLIN. ibid., (1970) 26(B), 1101.

96. J.KRAUT and L.H.JENSEN. ibid., (1963) 16, 79.

97. J.A.ANDERSON, G.P.P.KUNTZ, H.H.EVANS and T.J.SWIFT. Biochemistry (1971) 10, 4368.